ELECTRONIC ENGINEERING

VOL. 30 No. 364

JUNE 1958

Commentary

UNTIL recently, the only method of recording television programmes for subsequent reproduction has been to use the film camera to photograph the scenes as produced on a cathode-ray tube.

Several methods of making such telerecordings have been used by the BBC but, at the best, they have not been entirely satisfactory and they all suffer from certain limitations. The film has to be developed and processed before it can be played back and this involves an inevitable delay which, under some circumstances, can impose severe restrictions as to its use.

However, with the introduction of magnetic tape for sound recording and reproduction it was a logical step to attempt to use tape for the recording of television signals and successful results in this direction were achieved in America several years ago, particularly by the Ampex Corporation who have marketed a commercial version of their development.

The Research Department of the BBC has now produced, with considerable ingenuity and skill, a magnetic tape recorder for television programmes which it has recently demonstrated. Known as VERA, this Vision Electronic Recording Apparatus has been under development in the Research Department of the BBC for the comparatively short period of two years. Yet it is by no means an experimental apparatus hurriedly assembled merely to investigate the possibilities of magnetic tape recording, but a thoroughly well-engineered piece of equipment and one which, to judge from the results achieved, appears to approach the ultimate.

The information contained in the existing 405 line system requires a band of frequencies some 300 times as wide as that required for high quality sound recording but considerations of mechanical strength of the tape among other things preclude an increase of tape speed by this amount. In VERA, however, the television signal spectrum is divided into two and each part is recorded separately. The lower part of the band is recorded on one magnetic track using frequency modulation, while the higher frequencies are recorded on a second track. The accompanying sound is recorded on a third track, again using frequency modulation. The reproducing heads are independent of the recording heads and, among the advantages claimed by the BBC for VERA, is that this allows continuous monitoring of the picture recorded on the tape while recording is actually in progress.

Having now passed out of the laboratory stage, VERA is being put into regular service at the BBC Television Studios where it will add enormously to the programme facilities for it is immeasurably superior to the existing film methods and it is likely to supersede all other methods of telerecording.

It is at present a rather bulky piece of studio equipment and can record only those events as seen by the studio cameras but, as development proceeds, and as experience is gained in its use, it should be possible to extend its activities beyond the studio. It might be an advantage, for example, to develop a mobile version to record those outside events which so often occur at times which do not coincide with the main viewing periods, leaving the film camera to record the less important news items and interviews where the quality of reproduction is not an essential requirement.

In congratulating the Research Department of the BBC on the introduction of VERA one is, however, left wondering why the BBC in the first instance felt it necessary to embark on this project and why industry had no suitable equipment to offer.

However, having now brought VERA to its present stage, it is now the intention of the BBC, with no manufacturing facilities of its own, to hand over the design to industry for further development and exploitation.

A Multiple Beam Oscilloscope

for the Study of High Voltage Transient Discharges

By K. G. Beauchamp*, C.G.I.A., A.M.Brit.I.R.E.

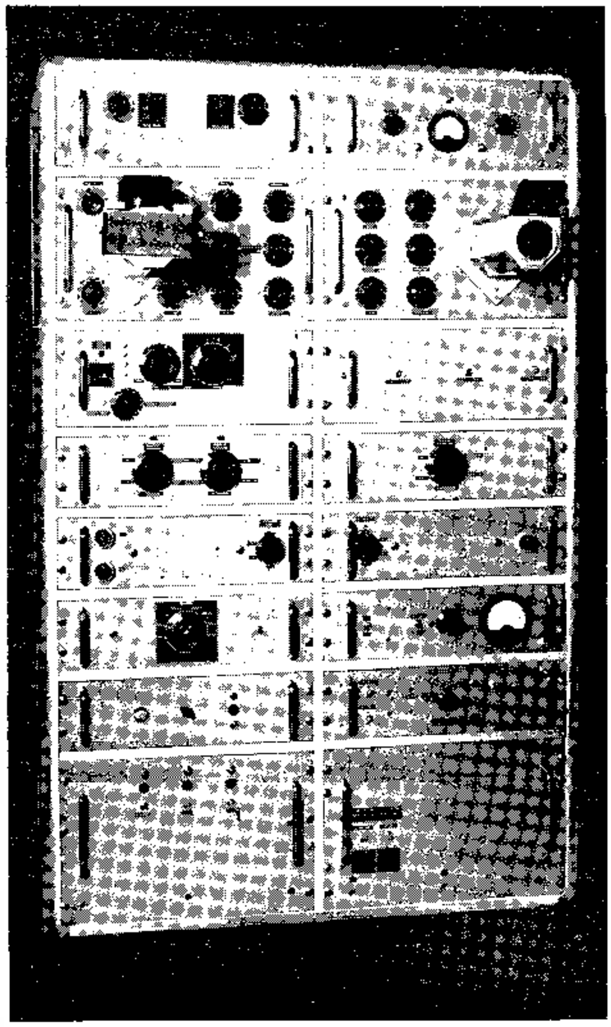

The complete design of a multiple-beam oscilloscope is described, showing how, by means of trace-expansion and a selective brightening system, the detailed study of transient discharge phenomena is facilitated. Means are also described to separate the effects of corona and main discharge in the oscilloscope display.

IN order to facilitate the study of high-voltage discharges between points having a potential difference of 0·5 to 1MV, it became necessary to construct a special oscilloscope adapted to this type of work. The first and major requirement was to record as much information as possible during the progress of a single transient discharge, a requirement arising out of the varied nature of these discharges, no two of which are exactly similar in duration or nature of the current build-up.

As very often the rapid variations of current in the discharge path are of interest in relation to the total discharge waveform, some form of trace-expansion was called for, and a method of correlating the expanded section with the complete waveform. Finally, a method was required for electrical display of the corona discharge or 'streamers' occurring slightly before the main discharge.

It was considered that these requirements would best be met by incorporating two tubes into the oscilloscope, a double-beam tube displaying the complete discharge waveform on one trace and a calibrating waveform on the other, corresponding to the sections chosen for expansion on a second single-beam tube. This latter tube was to be scanned with a triangular deflecting waveform, having a sweep duration of 1μsec in each direction; separation of the multiple traces produced being provided by the relatively gradual rising nature of the current discharge waveform being studied, and also by the use of a selective brightening circuit arranged to supply a pulse to the tube grid corresponding in time to the portion of the main discharge selected for expansion.

To assist measurement of the recorded phenomena, time and amplitude calibration was provided, and an internal pulse generator for triggering the sweep circuit, etc., in the absence of a discharge signal.

Owing to the high field strength within which the oscilloscope was required to be used, stringent precautions were necessary to prevent inductive pick-up from triggering the time-base and causing interaction with the signal desired to be measured. These included mains surge suppressors and filters, and also the use of trigger circuits which remain insensitive to subsequent input signals after being initially fired.

General Arrangements

A block schematic diagram of the complete oscilloscope is shown in Fig. 1. It will be seen that selection switches are provided to enable the required input signal to be applied to the appropriate deflexion plates. As the input to the oscilloscope may be as high as 30kV, oil-filled attenuators were necessary in order to reduce the signal amplitude to a desired level.

In order to make the complete equipment as flexible as possible, the oscilloscope was designed as a series of individually screened units, mounted in a double rack construction (see above), thus enabling servicing of an individual unit to be undergone away from the oscilloscope, and allowing subsequent modifications to be carried out later to meet any special requirements.

Cathode-Ray Tubes Used

The tubes chosen for the equipment were 20th Century types S6AB-20-3 and D6AB-20-3. These are single and double-beam tubes respectively, having a blue phosphor backed by a thin aluminium film. Three post-deflexion

* *Associated Electrical Industries Ltd.*

acceleration (p.d.a.) ring electrodes are incorporated, and in the case of the double-beam tube, entirely separate electrode systems provided.

The tubes are operated with the third anode A_3, earthy and negative and positive e.h.t. supplies applied to the cathode and p.d.a. electrodes respectively. The negative supply is variable over the range 6 to 10kV and enables the deflexion sensitivity to be varied. Positive potentials of 3, 6 and 10kV are applied to the three p.d.a. electrodes. Both positive and negative potentials are monitored by means of a meter incorporated in the e.h.t. voltage control panel.

With a total accelerating potential of 20kV, the c.r.t. beam spot size obtained was 0·25 to 0·3mm, giving a useful screen diameter of 4 to 500 spot widths. The brilliance of the trace when using the highest sweep speed of 5 × 10[3] spot/widths/sec, enables transients having rise times of 10mμsec to be clearly photographed.

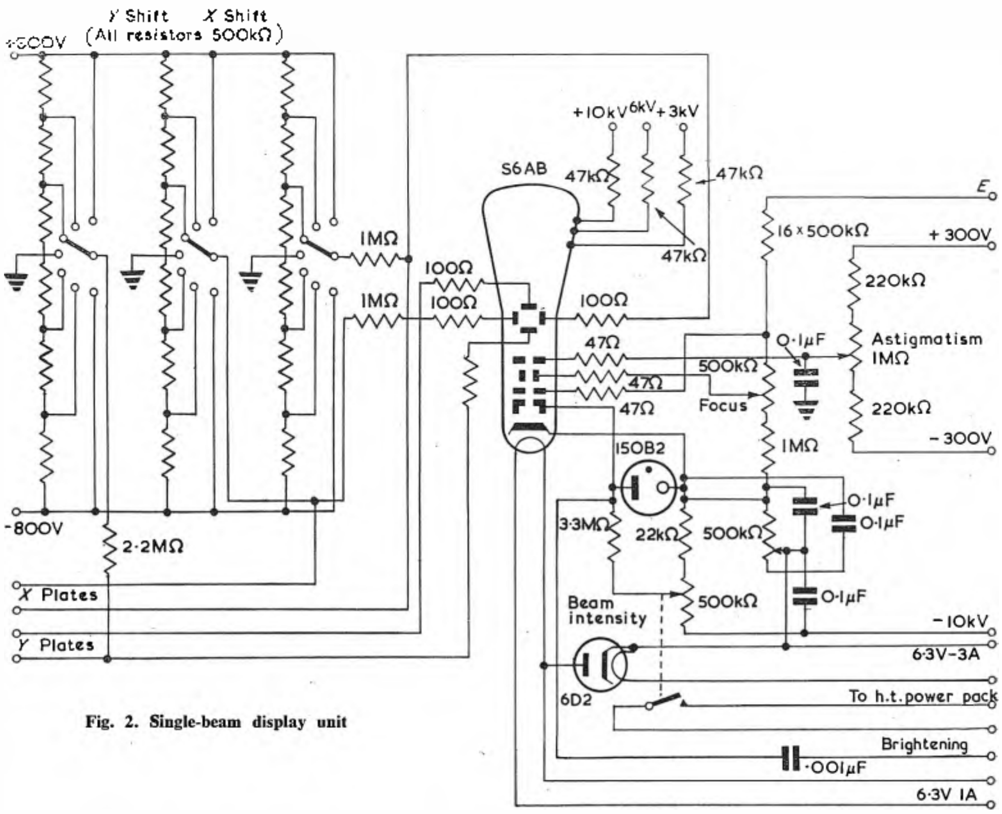

Fig. 2. Single-beam display unit

Display Units

The tubes were mounted in adjacent panels, provision having been made to remove them from their mountings without the necessity to withdraw the complete panels from the rack. Mumetal screens were fitted to shield the electron beams from extraneous fields, and the entire tube assemblies incorporated in light-tight and screened compartments.

Circuit arrangements for the display units are given in Figs. 2 and 3. Controls fitted to the front panel include astigmatism and brightening intensity. The brightening of the trace was achieved by switching the grid of the tube to a variable bias potential with a square-wave of the required duration. This bias potential was tied to that of the intensity control bias, so that the latter could set the general level of illumination. Protective neons were connected across the grid - cathode path to guard against positive voltage surges, and all three beam intensity controls were fitted with mechanical interlock switches in order that the e.h.t. may not be applied unless the controls are set in their minimum positions. This precaution was essential if damage to the phosphor was to be avoided, as when oscilloscope recording

Fig. 1. Block diagram of complete equipment

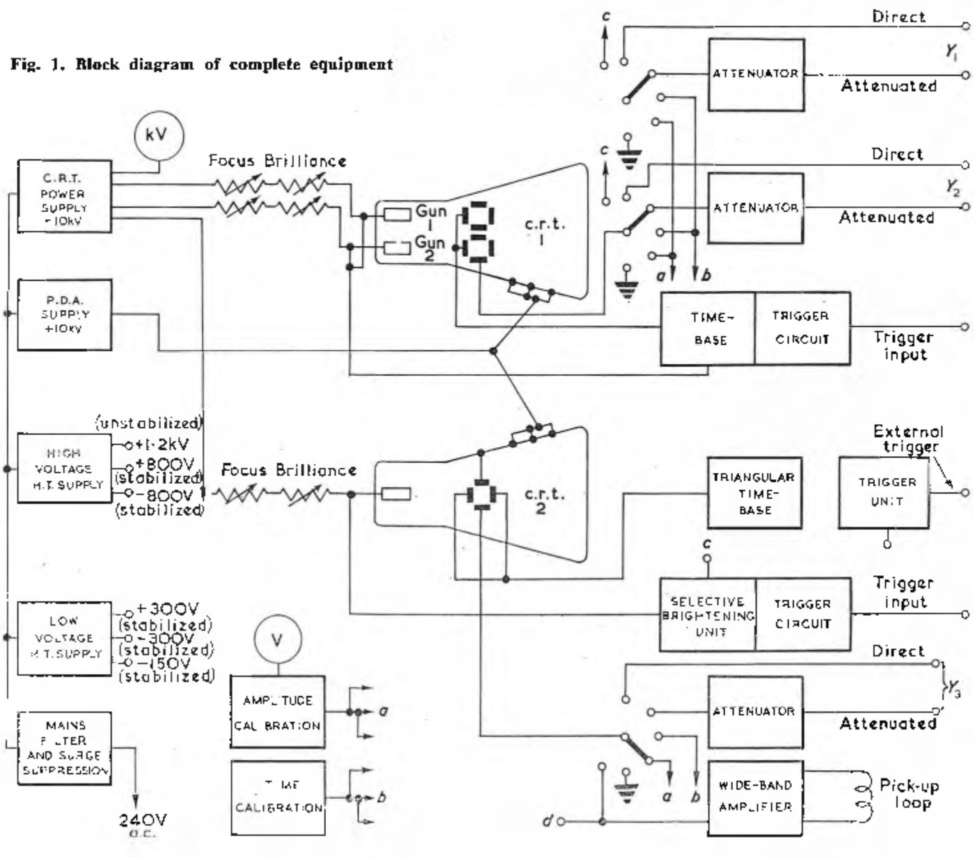

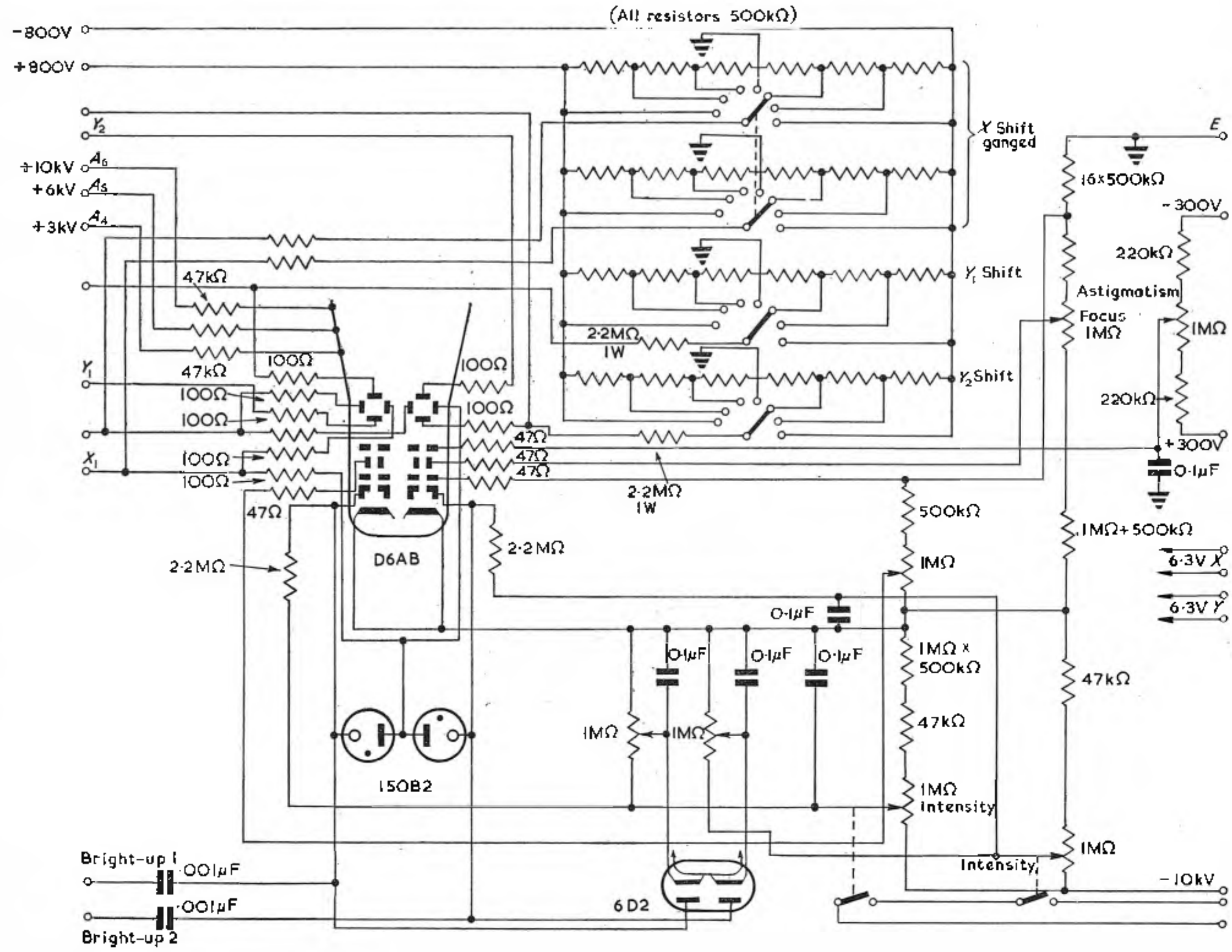

Fig. 3. Double-beam display unit

cameras are fitted, the operator has only a limited visibility of the tube screens.

Lewis and Wells[1] have shown that resonances of the deflector plate capacitances and lead inductances can seriously modify the displayed transient at very fast writing speeds. In order to damp these resonances, resistors are connected close to the tubes between two Y plates and signal input terminals.

Triggered Time-Base

Of the two types of triggered time-bases generally chosen for oscilloscope work, viz: the Bootstrap and Sanatron arrangements, the former is to be preferred in this application in order to avoid the high screen grid dissipation inherent with the Sanatron circuit and also to enable one plate of the charging capacitors to be permanently earthed.

The X plate sensitivity of the D6AB-20-3 tube is given as 1 300mm/V/V_{a6}, i.e. for 160mm deflexion, a potential of 2·4kV is required. In order to ease the requirements of the h.t. supply, and at the same time avoid deflexion defocusing, push-pull deflexion was used.

The complete trigger and sweep circuit is shown in Fig. 4. V_1 is a thyratron trigger circuit initiated by a positive pulse of >2V in amplitude. This produces a large positive wavefront across the cathode resistor and is conveyed, via diode V_{2b}, to a fast bistable multivibrator V_4 and V_5.The anode time-constant of V_1 is such that a second initiation is not possible for approximately a millisecond, until C_1 is charged to near h.t. line potential.

The discharge of C_1 through V_1 is also used to initiate a second multivibrator V_{12} and V_{13}, which serves to show, by means of a relay in the anode of V_{12}, when the time-base has been initiated. Further contacts on the relay provide a short-circuit at the trigger input terminals to prevent any unwanted triggering after V_1 has returned to its stable condition.

The multivibrator $V_{4\text{-}5}$ is normally stable with V_5 cut-off and V_4 in the conducting state. Upon initiation, the anode potential of V_5 falls rapidly, and the negative excursion is transferred to the switch valve V_6, which is normally heavily conducting with its anode 'bottomed' at about +50V. When V_6 is cut off, its anode rises to +1·2kV as capacitor C is charged via R and V_7, the product CR determining the timing period. This change in capacitor potential is also communicated to a cathode-follower V_8, which performs the Bootstrap action of liniarizing the potential across C.

The instantaneous potential across C can be expressed as:

$$e_c = (E/RC)\left\{t - \frac{(1-G)}{RC}\cdot t^2/2\cdot 1 + \frac{(1-G)^2}{(RC)^2}\cdot t^3/3\cdot 1 - \ldots\right\}$$

where G = gain of an amplifier inserted between the output at C and the top end of the charging resistor R.

If $G = 1$ (approximately the case with a cathode-follower), then e_c will be a linear function of time t.

The rising cathode potential of V_8 is transferred also via a biased diode V_{10} to a secondary-emission trigger valve[1] V_{11} conduction of which occurs towards the end of the linear rise and the negative pulse so produced is used to return V_{45} back to its second stable state.

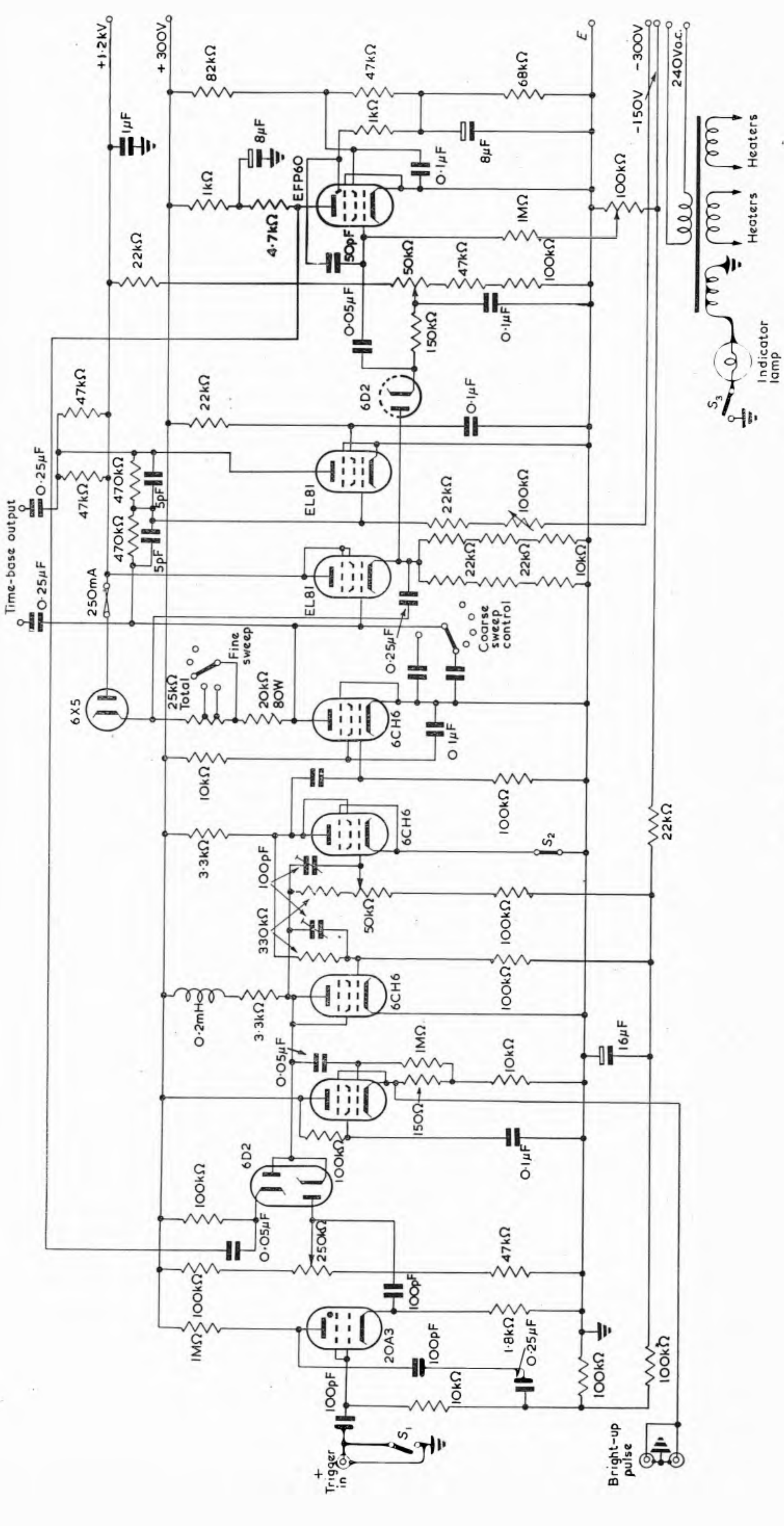

Fig. 4. Triggered time-base

The timing range between 1μsec and 3msec is covered in 10 steps by adjustment of capacitor values. Fine adjustment is by variation of part of charging resistor R_1, also in 10 steps. At the fastest sweep speed, the circuit stray capacitance sets a limit to the minimum sweep period obtainable. With this oscilloscope, the limit is reached at 1μsec when C consists entirely of stray capacitance of about 50pF. In order to charge this capacitance in 1μsec, a current of 60mA is required for a charging potential of 1·2kV.

The minimum charging resistor is thus 20kΩ, and must be capable of dissipating 72W when V_6 is in the 'bottomed' state. Arrangements were made, therefore, to keep the heat dissipated from affecting other components by suitable mounting of this, and other resistors comprising the total charging resistance.

A brightening pulse was taken from the anode of V_4 via a cathode-follower V_5 in order to reduce the effects of stray capacitance in the brightening circuit from affecting the shape of the pulse. The rise-time of the square-wave so produced was kept within 0·1μsec in this way.

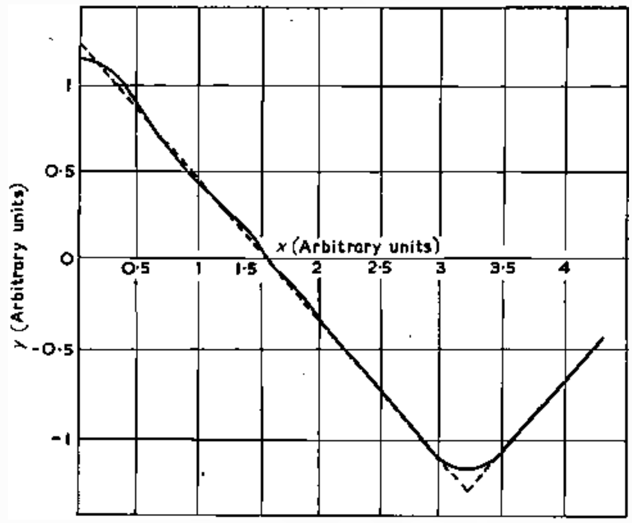

Fig. 5. Triangular-wave synthesis

Triangular-Wave Time-Base

As previously mentioned, a constant velocity trace was required for the single-beam tube in both transverse directions. Calculations showed that a maximum amplitude of about 2·5kV peak-to-peak was needed to be reached in 1μsec for each screen traversal and symmetrical deflexion was necessary to avoid deflexion defocusing. This continuous triangular waveform could be obtained by the use of conventional sweep circuits, suitably arranged, or alternatively, an amplification technique employed. In either case, the bandwidths involved would lead to a number of high-dissipation valves being used if the shape of the scanning waveform was to be preserved. Consequently, it was decided to attempt a synthesis method using sinusoidal class-C oscillators, with which the amplitude required could easily be obtained and symmetrical deflexion achieved from an isolated transformer winding.

Fourier analysis for a triangular wave gives the following expression

$$y = (8/\pi^2) \cdot E \left\{ \cos x + 1/9 \cdot \cos 3x + 1/25 \cdot \cos 5x \dots + 1/n^2 \cdot \cos nx \right\}.$$

where E is the peak amplitude of the fundamental frequency component. A plot of this expression involving the first three terms only is given in Fig. 5, where it is seen that the composite waveform falls short of the required triangle by less than 6 per cent at the peaks only, and such a synthesis seems eminently suitable for the purpose required.

In order to maintain correct phase relationships between the harmonic generators, a series of frequency multiplying stages were used, controlled initially by a 0·5Mc/s, fundamental frequency oscillator. The complete circuit is shown in Fig. 6, where V_1 is the 0·5Mc/s oscillator, while V_2 and V_3 are the third and fifth harmonic generators respectively. The magnitude of the harmonic components is controlled by adjusting the grid drive to V_2 and V_3 and the phase by the anode circuit tuning.

Fig. 6. Triangular-wave time-base

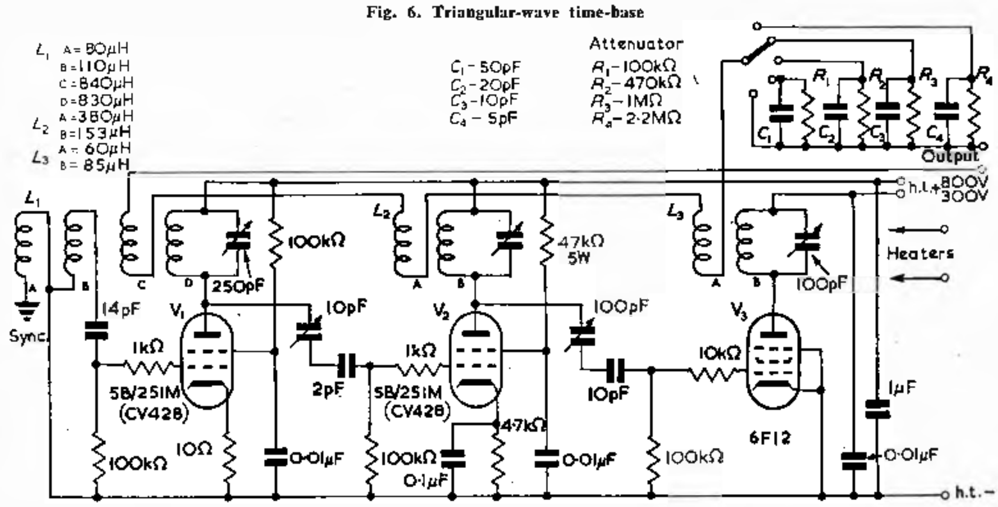

Selective Brightening Unit

The duration of the brightening potential applied to the grid of the single-beam tube was required to be variable and its commencement subject to an adjustable delay relative to the initiation of the triggered time-base. This enables a selected portion of the total discharge waveform to be displayed in much greater detail, and its position indicated by means of a timing waveform in the other tube.

Two similar monostable multivibrators are used (Fig. 7) to give an adjustable delay and pulse width, and are preceded by a thyratron trigger circuit, similar to that used in Fig. 4. The square wave produced by the first (delay) multivibrator is differentiated, and the negative pulse so produced is used to initiate a second (pulse width) multivibrator via a stacked cathode-follower. A delayed output pulse is obtained, which is applied via a cathode-follower V_{12} to the grid of the single-beam tube. An amplified output is also available via V_{13} for calibration display on the other tube.

Coarse adjustment of pulse delay and width is obtained by variation of capacitor valve C, forming with a fixed resistor R, a timing circuit for controlling the period of conduction for the first multivibrator valve (i.e. V_8 and V_9). A fine control is obtained by adjustment of the grid potential to this valve, and a linear variation of pulse width with potentiometer setting is secured over a range of 10:1. This enables the range between 5μsec and 2msec to be covered using three capacitor values.

The initial level of the grid potential for the normally

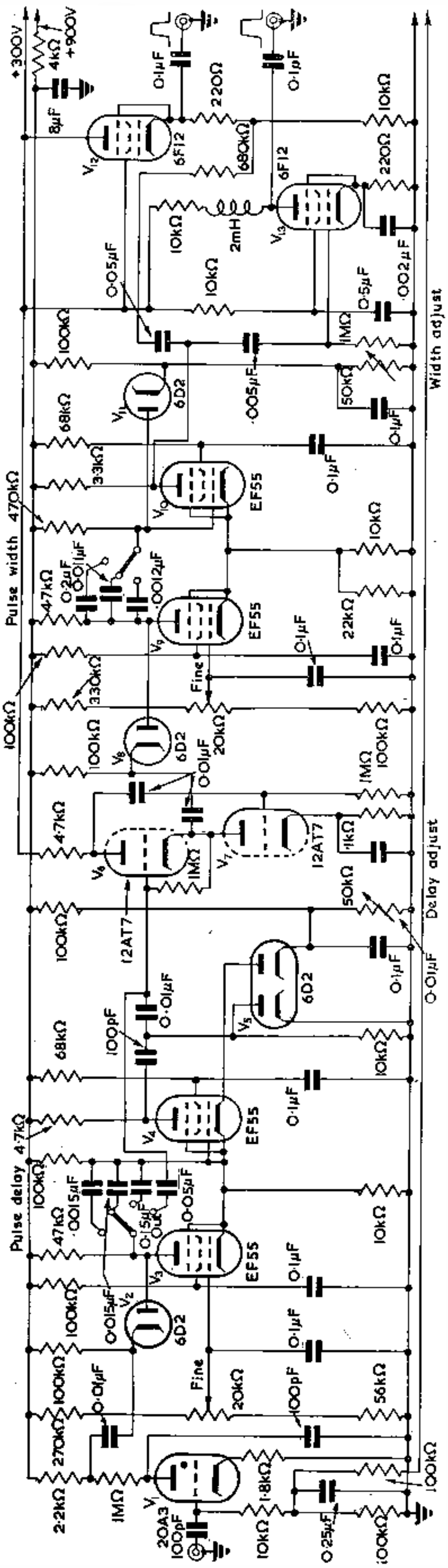

Fig. 7. Selective brightening circuit

conducting valve is set via a diode to a point on a potential divider connected across the h.t. supply. This potentiometer (designated 'delay adjust' or 'width adjust') enables the calibration to be set up initially.

Wide-Band Amplifier and Inductive Pick-Up Method of Display

A second function of the oscilloscope is as a detector of electromagnetic radiation associated with the current discharge, and in particular, to locate in time, and measure the relative amplitudes of the corona discharges or 'streamers' preceding the main discharge. It was essential that the detector differentiated this from the electrostatic field set up by the build-up and discharge of the potential energy of the main discharge, and to enable this to be realized, a small loop aerial was used.

The ferrite rod aerial[2] is ideally suitable for this purpose. It can be shown that the ratio of e.m.f.'s induced in a frame (e_f) and rod (e_R) aerials are given by

$$e_R/e_f = \frac{\mu_1 Q_R \,.\, a_R \,.\, n_R}{Q_f \,.\, a_f \,.\, n_f}$$

where μ_1 is the effective permeability of the rod to an external field. (This is rather less than μ_0, normally given as the permeability where an external field is concerned.) Q, a, and n refer to the Q-factor area, and number of turns for the rod and frame aerials designated by the suffix R and f respectively.

Comparing the potentials induced in a ferrite rod aerial of dimensions 9/16in diameter by 8in to that of a frame aerial of sides 20cm in length, it will be seen that, unless a large number of turns is used for the frame aerial, then the rod will give a considerable improvement in signal pick-up. In addition, the rod aerial will have a more balanced stray capacitance to earth, and due to its smaller physical dimensions, greater immunity to electrostatic pick-up.

Examination of the characteristics of the electromagnetic radiation indicated that a bandwidth of a few megacycles per second would be required in the amplifier following the pick-up loop.

A negative feedback amplifier was constructed whereby the gain was controlled by alteration of the feedback constants to assure the widest possible bandwidth at any given gain setting (Fig. 8).

Four gain positions were provided viz:

Position	Gain	Bandwidth
1	10	10Mc/s
2	20	8 ,,
3	40	6 ,,
4	80	4 ,,

A greater gain was subsequently found desirable for certain conditions, and to provide this a long-tailed pair stage was included to give an additional gain of 10, and at the same time to provide a balanced output to the deflector plates. In this case, however, the bandwidth was limited to 4Mc/s.

The signal induced in the loop aerial is directly related to the rate of change of current in the discharge gap. A direct measure of the value of this current could be obtained by including an integrating network in the amplifier, preferably by modification to the feedback circuit. In use, however, the differentiated signal proved of greater value in the time location of discharge events.

Calibration Units

A variable d.c. shift potential was provided for amplitude measurements and the magnitude of shift indicated on a

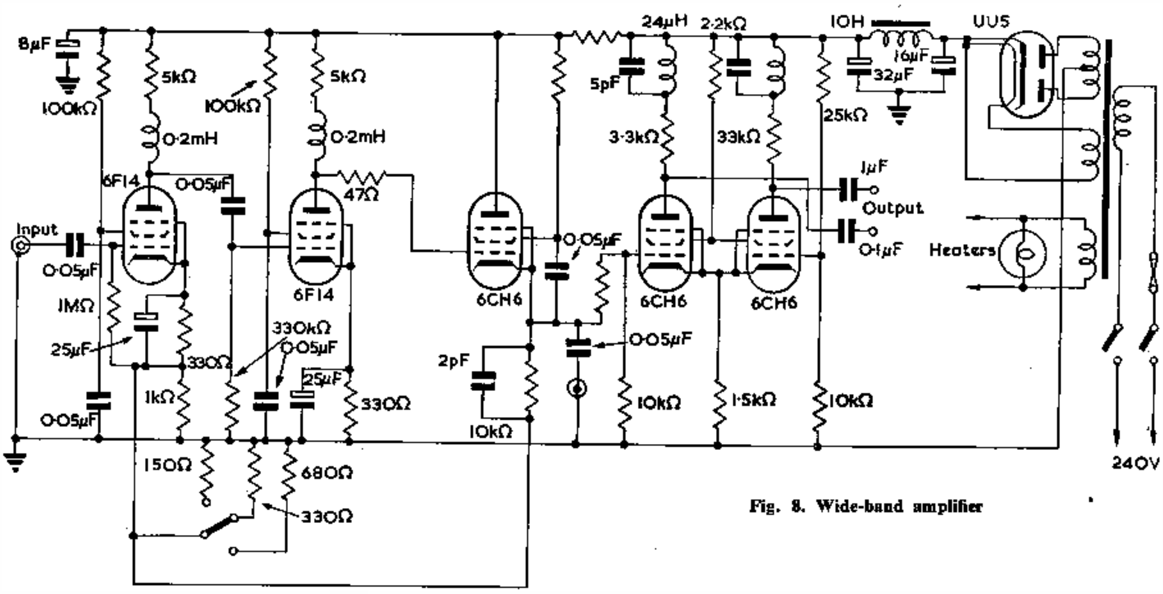

Fig. 8. Wide-band amplifier

meter. Time measurements were made using a sinusoidal oscillator giving eight frequencies in the range 10kc/s to 25Mc/s. A turret tuner was used, and provision made for adjustment of oscillation amplitude. Alternative Hartley or Colpitts oscillator connexions are made dependent on frequency and physical construction of the coil used. Ferrite cores were used for the two lowest frequency ranges.

Maximum amplitude of oscillations available was 200V peak-to-peak, provided a deflexion of some 1·5cm on the double-beam tube. A certain amount of cross-modulation was experienced between the two beam deflexion plates when using the highest frequency calibration wave. Where the detail observed is small enough for this to be significant, a double exposure method can be used for recording purposes, and a separate 'off' switch is provided for this purpose.

Internal Pulse Generator

A completely self-contained pulse generator was incorporated to enable the oscilloscope to be adjusted in the absence of a discharge signal, and may be seen in Fig. 9 to constitute an astable multivibrator V_{12}, having a choice of three repetition frequencies, namely 8, 24, and 120 pulse/minute, which are used to trigger a monostable circuit $V_{4\cdot5}$ via a diode V_3. This provides a narrow positive pulse of 5μsec duration and 140V amplitude. A negative pulse generator V_5 is also included and gives a pulse of similar amplitude, but of 1μsec duration. Provision is made for external triggering.

Power Supplies

The e.h.t. unit can be seen at the base of the double-rack construction, and consists of a positive and negative 10kV supply with provision for varying the negative potential from 6 to 10kV and for monitoring both outputs. Safety interlocks are included to prevent the e.h.t. potentials from being applied to the tubes, unless the beam intensity controls are initially set to their minimum positions.

A second power supply unit provides stabilized h.t. and also heater supplies (Fig. 10) for the remainder of the equipment, except for the pulse generator and wide-band amplifier which have their own self-contained supplies.

Two separate stabilized supplies are provided:

800V at 100mA

300V at 250mA

and an unstabilized supply of

1·2kV at 75mA.

The basic stabilizing circuit is shown in Fig. 11.

Cascode stabilizing control circuits are used, modified to provide an additional bleed current through the lower valve. Attree[3] has shown that the gain for a cascode circuit approximates to $A = g_m, R_a$, where g_m, refers to this valve. Now as g_m is directly proportional to anode current over the range 10 to 1 000μA, it is possible by including a bleed resistance in shunt with the grid input amplifier (lower

Fig. 9. Trigger pulse generator

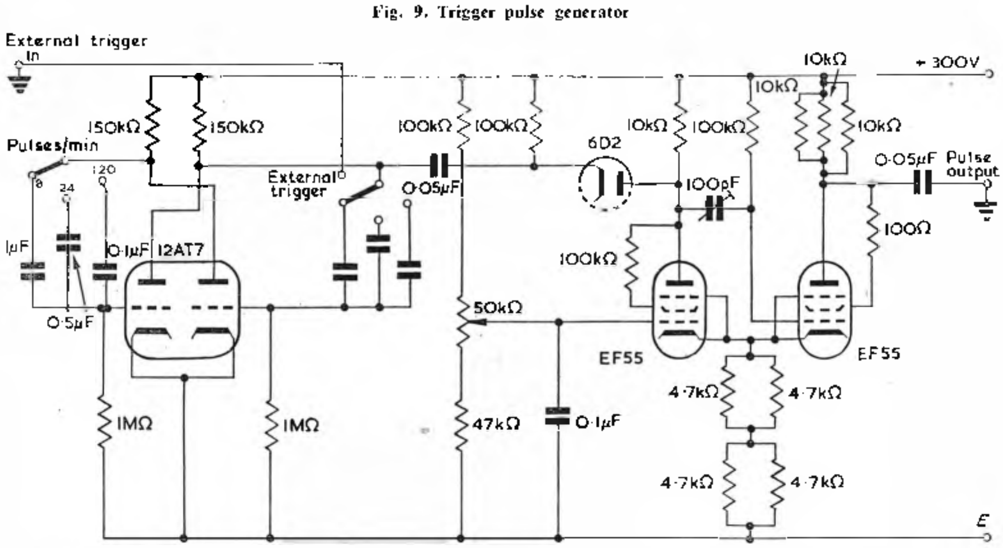

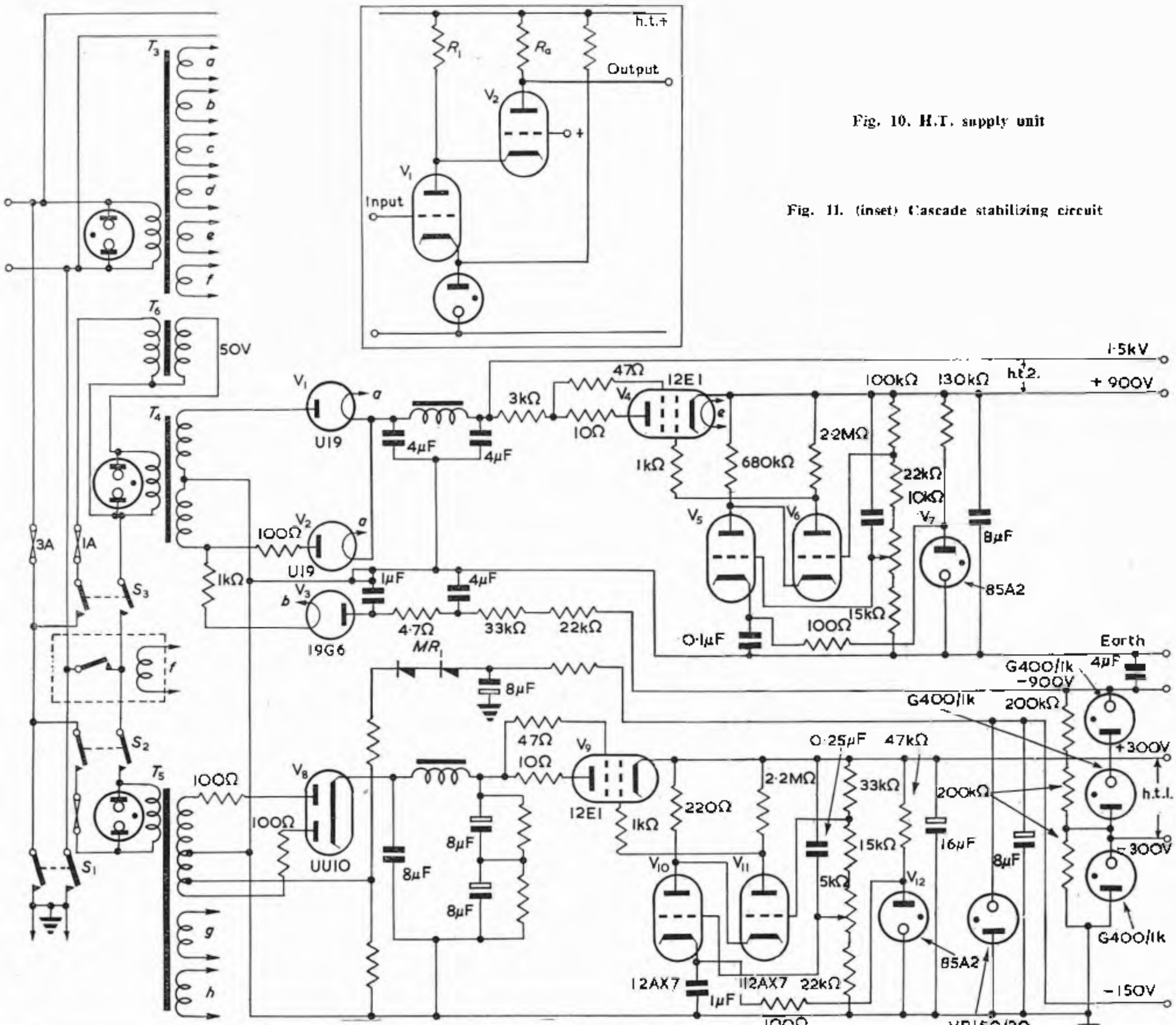

Fig. 10. H.T. supply unit

Fig. 11. (inset) Cascade stabilizing circuit

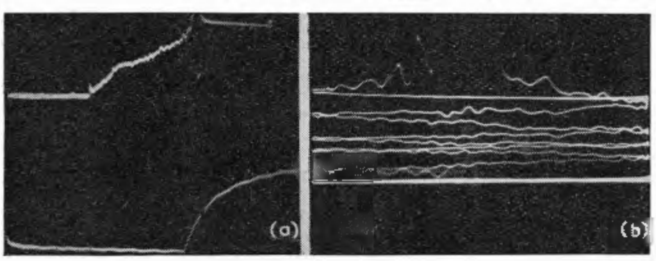

Fig. 12. Spark discharge current waveforms

valve) to secure a high value of g_m, and hence a large gain. This overcomes a disadvantage of the single pentode stabilising amplifier, where a low value of g_m is obtained due to the necessity to include a large value resistor in its anode circuit.

An output impedance of 3 to 4Ω was measured and a stabilization ratio $\left\{\frac{\text{change of output potential}}{\text{change of input potential}}\right\}$ of 170.

Neon stabilized supplies of −150, −300 and −800V were also included in this unit.

In order to avoid the effects of high voltage mains surges occasioned by the signal discharge, Metrosil elements were fitted between each incoming mains terminal and earth; to remove the smaller surges not reduced by the Metrosil elements, a balanced low-pass filter having a cut-off frequency of 20kc/s was included.

Performance

Fig. 12 illustrates the type of display obtained with the oscilloscope. The first photograph (a) shows the discharge current waveform developed across a small resistor inserted at the base of the gap electrodes, and is compared with the lower trace which gives the duration of the brightening pulse applied to the signal-beam tube.

The same signal is also applied to the Y plates of this tube, shown at (b), and shows a trace expansion of some ten times as the beam traverses the screen linearly in both directions, an upward deflection being secured by the gradually increasing amplitude of the applied signal.

Acknowledgments

The author would like to thank Dr. T. E. Allibone, F.R.S., Director of the Research Laboratory, Associated Electrical Industries, for permission to publish this article.

REFERENCES

1. Lewis, I. A. D., Wells, F. H. Millimicrosecond Pulse Techniques. (Pergamon Press, 1954).
2. Everden, W. A. Ferrite Rod Aerials. *Wireless World*, 60, 440, (1954).
3. Attree, V. H. A Cascode Amplifier Degenerative Stabilizer. *Electronic Engng.*, 27, 174, (1955).

The Synchro Resolver as a Shaft Position Transducer

By M. B. Wood*

The article is a report of an investigation of the potentialities of the modern synchro resolver as an initial transducer in an analogue to digital convertor for quantizing shaft position.

The synchro is used as part of a phase shifting unit operating upon a 400c/s sinusoidal input. Marker pulses are generated at the instant of zero crossover of the output, and are gated into a time period counter to indicate the difference in time-phase between a reference channel and a measuring channel. A linearity of better than ±0·1 per cent was achieved in the relationship between shaft position and time modulated pulse position.

THE modern synchro resolver can be used as a precision shaft position transducer of comparatively low cost, and has several advantages as against the resistive elements which are generally used for this purpose.

The system described here (see Fig. 1) is one of analogue to digital conversion, in which the relative angular position of a shaft is represented in digital form at the output. Such a conversion may, of course, readily be achieved by using coded commutator digitizers, but in many cases the shaft whose position is to be quantized cannot supply enough torque to drive the digitizer. This system in which synchros are used as the initial transducers might be suitable for such applications.

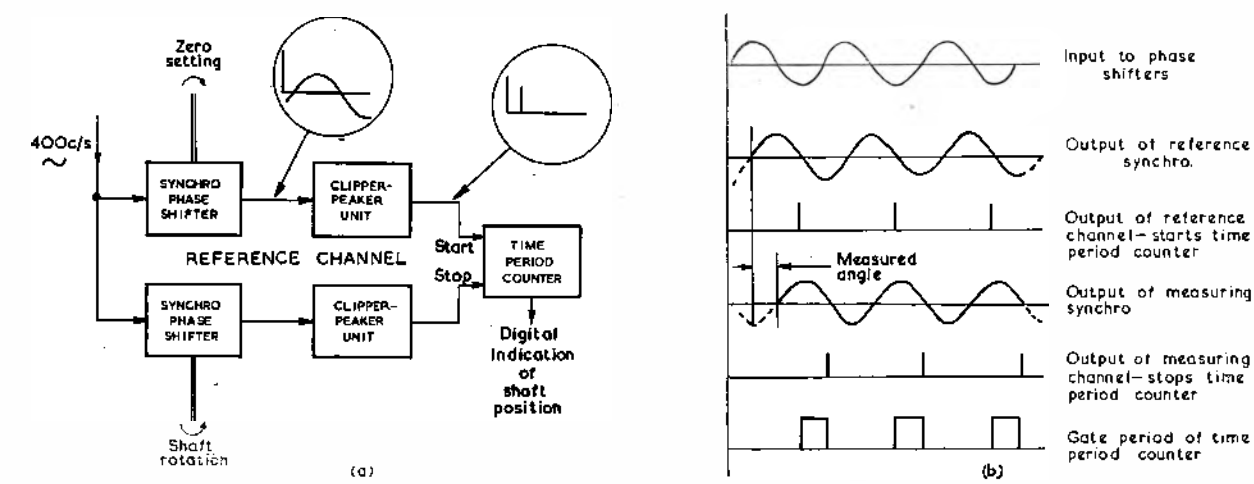

Fig. 1. Block diagram and waveforms of the complete digitizing system

Synchro resolvers are used as phase shifting elements operating upon a common 400c/s input signal. The output obtained from the phase shifting unit is shifted in phase relative to the input by an angle corresponding to the angular position of the resolver shaft. This output signal is subsequently clipped and amplified and a marker pulse is generated by triggering a thyratron at the instant of zero crossover of the sinusoid.

One channel is used as a zero reference, and its output pulses are used to start a time period counter. The pulses from a second channel are used to stop the counter, and the time indicated by the counter is then proportional to the phase difference of the two channels and hence to their relative input shaft positions.

By suitable use of gate and control circuits it would be possible to multiplex a number of channels in sequence into one counter, with consequent economy of equipment.

In this instance 400c/s was used, giving a period of 2·5msec for one cycle. If the counter is reset every alternate period, then the total time for one conversion is 5msec.

Time marker pulses from linear sweep generators have previously been used in a similar manner, but the generation of an accurate marker pulse from a sinusoidal waveform is more simple, since the slope of a sinusoidal waveform at zero crossover is π times as great as that of a linear sweep of equal peak-to-peak amplitude and period.

At the start of this project it was not known that Sisson had previously used a synchro control transformer in a similar system[1].

The Resolver in a Phase Shifting Unit

The resolver has been used as a phase shifting element in two distinct ways[2,3]. The resolver has two separate stator windings which are mechanically arranged within the instrument to produce fields which are in quadrature within the air-gap.

If the stator windings are excited by two equal currents which are in quadrature, then a rotating field of constant amplitude will be produced within the air-gap, and the stationary rotor winding will have induced in it a voltage of constant amplitude, but of phase corresponding to the position of the rotor relative to the stator. Unfortunately the method necessitates the adjustment of the amplitude and phase of one of the stator currents, and it is easily shown[4] that in an ideal resolver an unbalance of only 1 per cent in the magnitude of the currents in the two

* *Aircraft Research Association Ltd.*

stator windings will produce a phase error of more than 17min in the rotor currents. This method was not used at A.R.A. and will not be considered further.

In the second method the rotor is excited from a single-phase supply of constant frequency. The two stators are connected in series with an *RC* series circuit as shown in Fig. 2, in which $R\omega C = 1$, where $\omega/2\pi$ is the frequency of the rotor signal. The values of the resistor and capacitor are chosen sufficiently high to prevent appreciable loading of the synchro and minimize the effect of the stator impedances. The order of impedance chosen was 0·5MΩ, which gives a reasonable value for the capacitors at 400c/s.

If a single-phase current $i = I_o \sin \omega t$ is applied to the rotor, e.m.f's e_1 and e_2 are induced in the stators.

$$e_1 = KI_o \cos \omega t \cos \theta$$

$$e_2 = KI_o \cos \omega t \sin \theta$$

where θ is the rotor angle.

When the synchro is connected as shown in Fig. 2 to the series *RC* circuit, the phases of e_1 and e_2 are shifted by

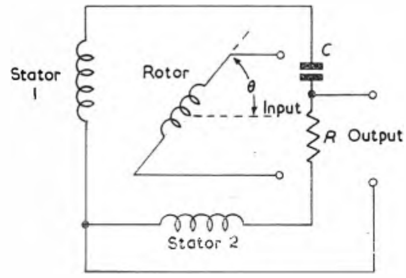

Fig. 2. The resolver connected as a phase shifting unit ($R\omega C = 1$)

$+(\pi/4)$ and $-(\pi/4)$ respectively and added, to yield an output.

$$E_{out} = KI_o/\sqrt{2} \;\sin(\omega t + \theta + (\pi/4))$$

which is of constant amplitude shifted in phase by angle θ, the rotor angle[3].

In passing it must be mentioned that, at the cost of increased complexity of equipment, a greater accuracy can be achieved with active filters, incorporating operational amplifiers, than is possible with passive filter techniques. Accuracies of the order $\pm 0{\cdot}02$ per cent have been achieved by this means in one computer[5,6].

Some Advantages of Synchros as Transducers

Apart from the very real functional advantage of a sinusoidal output waveform mentioned previously, synchros in general have several valuable features. They are manufactured to close mechanical limits which permits easy replacement of units in production equipment. Both the inertia and friction torques are extremely low, the breakaway torque of a typical synchro being quoted as 0·5oz.in. The life expectancy is high, 1 000 hours at 200 rev/min (i.e. 12×10^6 revolutions) was quoted by one manufacturer and a greater life can be expected at lower speeds.

Possible Sources of Error in the Phase Shifting Unit

The circuits which follow the phase shifting unit in this system are designed to generate a marker pulse at the instant of zero crossover of the output sinusoid. In this section the accuracy of the unit is considered in relation to this restricted requirement. Factors which distort the waveform, other than at the instant of zero crossover, are not considered. Some of the principal causes of error are discussed below.

Non-equality of the Transformation Ratio

The transformation ratios of the two stators with reference to the rotor as the primary, would be equal in an ideal synchro resolver, but in practice there is a discrepancy between the two. Assume that

$$e_1 = K_1 e_r \cos \theta$$

$$e_2 = K_2 e_r \sin \theta$$

where e_1, e_2 are the stator voltages induced by a rotor voltage e_r at a rotor angle θ. K_1, K_2 are the transformation ratios.

Then $K_1 e_2 / K_2 e_1 = \tan \theta$

but referring to Fig. 3

$$\tan \alpha = e_2/e_1$$

where α is the phase-angle of the output.

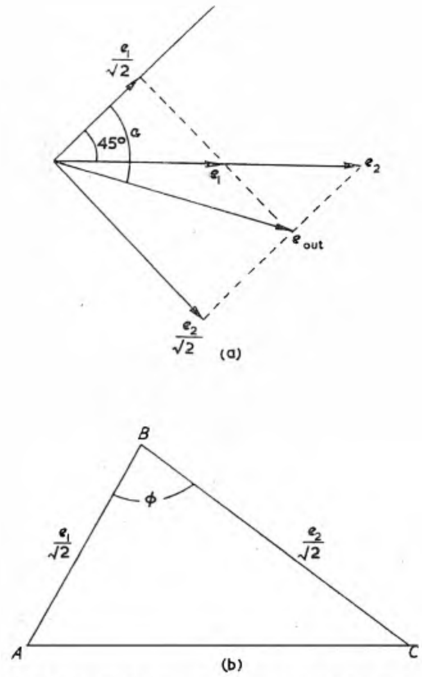

Fig. 3. Vector diagrams of the phase shifting unit

Tan α and tan θ differ by $(K_2 - K_1)/K_2$, and the error will be greatest when $d(\tan\theta)/d\theta$ is a minimum, i.e. when $\theta = 0$. In the resolver which was used the maximum difference between the transformation ratios is 0·2 per cent which would produce a maximum error of 7′ in the phase of the output sinusoid.

Inequality of Phase Shift Between Rotor and Stators

There is a small phase shift between the rotor and the stators because of the magnetizing current drawn by the rotor. If this phase shift were constant and equal for the two stators, it could be eliminated in the initial alignment of the system. In practice there is a slight difference between the two phase shifts which causes the two stator voltages to be slightly out of phase.

Consider the case when one stator voltage is zero. The phase shift of the second stator can be eliminated in the initial adjustment of the stator phasing. As the rotor is turned the error caused by the difference in phase shift will increase through the first quadrant reaching a maximum after 90° rotation. The error will here be equal to the difference between the two phase shifts, because the first stator will now yield zero output. Through the second quadrant the error will decrease to zero at 180° rotation, and the effect will be repeated in the same sense through the other two quadrants. The error is therefore cyclic of period π and of a maximum value of plus or minus half the difference between the phase shifts.

Typical values for the phase shift difference are a maximum of 10′ arc and an average value of 2′ of arc. The average error from this cause would therefore be $\pm 1'$ of arc.

Non-quadrature of the Two Windings

The effect of physical departure from quadrature between the stator windings is that whereas the outputs from an ideal resolver would be

$$e_1 = Ke_r \cos\theta$$
$$e_2 = Ke_r \sin\theta$$

the outputs are in practice

$$e_1 = Ke_r \cos(\theta + \phi)$$
$$e_2 = Ke_r \sin\theta$$

where ϕ is a small constant angle which may be either positive or negative.

Referring to Fig. 3,

$$\tan\alpha = (e_2/e_1) = \frac{Ke_r \sin\theta}{Ke_r \cos(\theta+\phi)}$$
$$= \frac{\sin\theta}{\cos\theta\cos\phi - \sin\theta\sin\phi}$$
$$= \frac{1}{\cot\theta\cos\phi - \sin\phi}$$

but ϕ is very small, and hence

$$\tan\alpha = \frac{1}{\cot\theta\cos\phi} \text{ approximately} = \frac{\tan\theta}{\cos\phi}$$

The error will be greatest when $d(\tan\theta)/d\theta$ is a minimum, i.e., when $\theta = 0$, π etc., and since in practice ϕ is about 4′ of arc giving $\cos\phi = 1{\cdot}00000$ the error can be ignored.

Error Due to Stator Impedance

The circuit of the resolver stators and the phase shift network can be redrawn as in Fig. 4, in which

$$Z_1 = r + j\omega L + R$$
$$Z_2 = r + j\omega L + 1/j\omega C$$

(The stator impedance is of the form $r + j\omega L$).

For simplicity consider the case when Z_1 and Z_2 are made equal in magnitude.

Then

$$(r+R)^2 + \omega^2L^2 = r^2 + (\omega L - (1/\omega C))^2$$
$$\therefore R = -r \pm \sqrt{[r^2 + (1/\omega^2C^2) - (2L/C)]}$$

In the synchro used $r + j\omega L = (0{\cdot}7 + j\,3{\cdot}0)\mathrm{k}\Omega$ and $1/\omega C$ was 400kΩ which gives $R = 402{\cdot}1\mathrm{k}\Omega$.

Referring to Fig. 5,

$$\tan\gamma = \frac{\omega L}{R + r} = 3/402{\cdot}8, \text{ hence } \gamma = 26'$$

and

$$\tan\beta = \frac{r}{(1/\omega C) - \omega L} = 0{\cdot}7/397, \text{ hence } \beta = 6'$$

Hence $\phi = 45°\ 10'$, since $Z_1 = Z_2$, and the result is a cyclic error of $\pm 10'$ of period π.

Theoretically the error could be reduced by increasing the values of the impedances in the phase shifting network, but in practice there was no advantage in this approach because there is no simple way of setting up the networks to give the increased accuracy.

The usual method of adjusting the network is to apply a signal to the rotor input and display the output of the phase shifting unit on an oscilloscope[4]. The RC network is then adjusted until there is negligible modulation of the amplitude of the output when the rotor is turned to different positions.

(The same method can incidentally be used for setting up the quadrature phase current in the alternative method).

The method results in a constant magnitude for the output vector, and it can easily be shown that this produces quadrature between the two stator components after they have been phase shifted.

Referring to Fig. 3(a), in which vector AC is the resultant of AB and BC, which are separated by angle ψ.

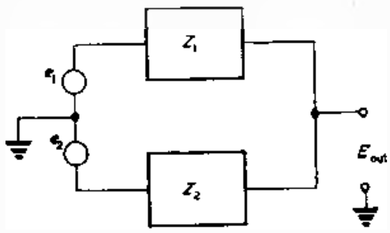

Fig. 4. Illustrating the effect of stator impedance

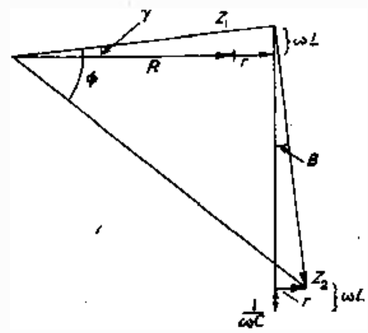

Fig. 5. Vector diagram showing the effect of stator impedance

$$AC^2 = AB^2 + BC^2 + 2AB\,.\,BC\cos\psi$$

But if in the phase shifting unit R and $1/\omega C$ are approximately equal, then $AB = (e_1/\sqrt{2})$ and $BC = (e_2/\sqrt{2})$ and $AC = e_{out}$.

The r.h.s. of the equation becomes

$$e_{in}^2\cos^2\theta + e_{in}^2\sin^2\theta + 2e_{in}^2\sin\theta\cos\theta\cos\psi$$
$$= e_{in}^2\,(1 + 2\sin\theta\cos\theta\cos\psi.)$$

but the l.h.s. $= e_{out}$, which is made constant by the adjustment, and therefore $\cos\psi = 0$ giving $\psi = 90°$ or $270°$.

In practice the presence of a small harmonic component in the output is sufficient to so distort the waveform that measurement of the peak-to-peak amplitude is not an accurate method of determining the amplitude of the 400c/s component. While other elegant methods of aligning the phase shift circuit can be envisaged, the method described does have the advantage of speed and simplicity.

Errors in the Supply to the Rotors

Ideally the supply to the rotors should be a pure sinusoid of constant frequency; constancy of amplitude is not necessary. Harmonics in the supply are very troublesome and filtering of the input would normally be desirable. Drift in the frequency has two effects. The first is that the impedance of the capacitor in the RC circuit changes and the relationship $R\omega C = 1$ is no longer satisfied, and secondly the relationship between the angular increment in shaft position and the time shift of the output pulse from the channel is changed, with a consequent change in the calibration.

Both these troubles can be overcome if the rotor supply is derived by frequency division from a crystal controlled source of clock pulses which are used in the time period measuring equipment.

If the synchro were used simply as a phase shifting device, the driving signal could conveniently be obtained from a valve maintained fork supply. There are several high quality forks commercially available which would prove suitable for this purpose.

DEPARTURE FROM TRUE SINUSOIDAL RELATIONSHIP BETWEEN ROTOR AND STATOR

Although in an ideal resolver the stator voltage would be a true sinusoidal function of the rotor angle, in practice a typical limit of error on this relationship is $\pm 0{\cdot}2$ per cent of peak output.

The outputs of the stators therefore become

$$e_1 = E\,(a + \sin\theta)$$
$$e_2 = E\,(b + \cos\theta)$$

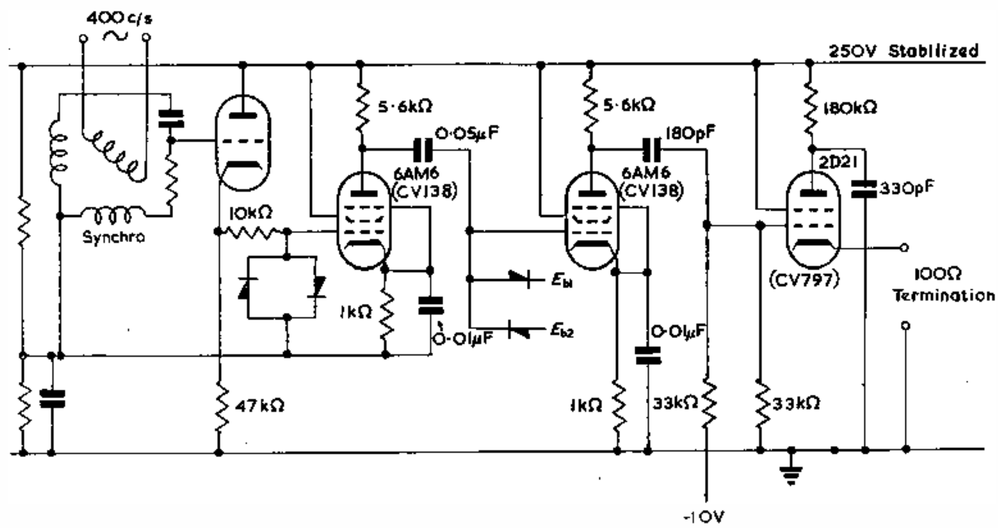

Fig. 6. The clipper-peaker circuit

where a and b are small components of error. The angle of phase shift of the output α, will be given by

$$\tan\alpha = (e_1/e_2) = \frac{a + \sin\theta}{b + \cos\theta}$$

The error in phase shift is the difference between α and θ.

$$\theta - \alpha = \theta - \tan^{-1}\frac{(\sin\theta + a)}{(\cos\theta + b)}$$

$$\therefore \frac{d(\theta - \alpha)}{d\theta} = 1 - \frac{(\cos\theta + b)\cos\theta + (a + \sin\theta)\sin\theta}{\left(1 + \dfrac{(\sin\theta + a)^2}{(\cos\theta + b)^2}\right)(\cos\theta + b)^2}$$

$$= 1 - \frac{(b + \cos\theta)\cos\theta + (a + \sin\theta)\sin\theta}{(b + \cos\theta)^2 + (a + \sin\theta)^2}$$

$$= \frac{b\cos\theta + b^2 + a\sin\theta + a^2}{1 + 2b\cos\theta + b^2 + 2a\sin\theta + a^2}$$

Neglecting terms in a^2 and b^2, since a and b are both small,

$$\frac{d(\theta - \alpha)}{d\theta} = \frac{b\cos\theta + a\sin\theta}{1 + 2b\cos\theta + 2a\sin\theta}$$

Equating to zero, for maximum or minimum error

$$a\sin\theta + b\cos\theta = 0$$

or

$$\tan\theta = (-b/a)$$

Unfortunately for the purposes of analysis, the factors a and b are not simple constant errors. They may be a combination of noise and distortion. If the errors are equal for the two windings and at their limit values the error will be a maximum or a minimum, depending on the sign of a and b, at $\theta = (\pi/4)$ $(3\pi/4)$ etc. In this case the maximum error will be $\pi/4 - \tan^{-1}(1{\cdot}002)/(0{\cdot}998)$

$$= \pi/4 - 45^\circ\,7' = 7' \text{ of arc.}$$

In the case when $\theta = 0$ or $\pi/2$ etc., the maximum error will be $\tan^{-1} a$ or $\tan^{-1} b$ and since $a = b = {\cdot}002$, the maximum error at this angle is about 7′ of arc.

In fact of course, since $\pm\,{\cdot}002$ is the limit of error on the relationship, the synchros are likely to produce a much smaller error than these figures would suggest.

ANTICIPATED ERROR

The largest single source of error is likely to be that caused by the stator impedances. The errors caused by defects in the synchro will generally be smaller than the figures given above, since in all cases the rejection limits were considered and any one synchro is unlikely to be deficient in all respects.

Errors caused by the supply not being an ideal sinusoid of constant frequency can be reduced to a minimum by using one of the several synchro power supplies which are now commercially available.

If a departure from linearity of $\pm 0{\cdot}1$ per cent can be accepted in the analogue to digital conversion, then the error in phase shift which can be allowed is $\pm\dfrac{360 \times 60}{100}$ $= \pm 21{\cdot}6'$ of arc, ignoring for the moment any errors in the gate generation.

Experimental Investigation

EQUIPMENT

Two clipper-peaker circuits (Fig. 6) were built, which generate a marker pulse at the zero crossover point of the sinusoidal output from the phase shifting unit.

Two size 15 resolvers were mounted with their rotors mechanically coupled in such a fashion that one of the stators could be phased relative to the other. The two synchros were each provided with an *RC* network and cathode-follower, the outputs from which were fed to the clipper-peaker units. The stator windings were so connected

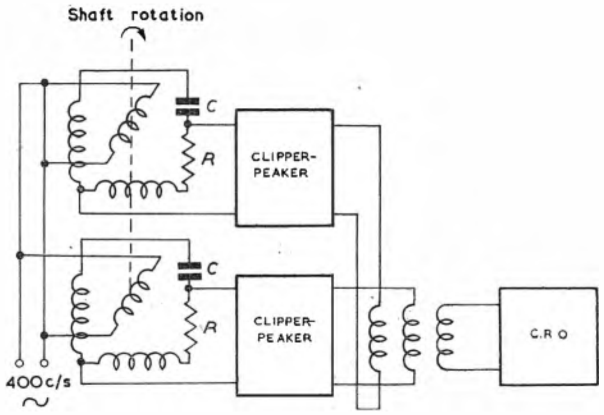

Fig. 7. Block diagram of the error measuring circuit

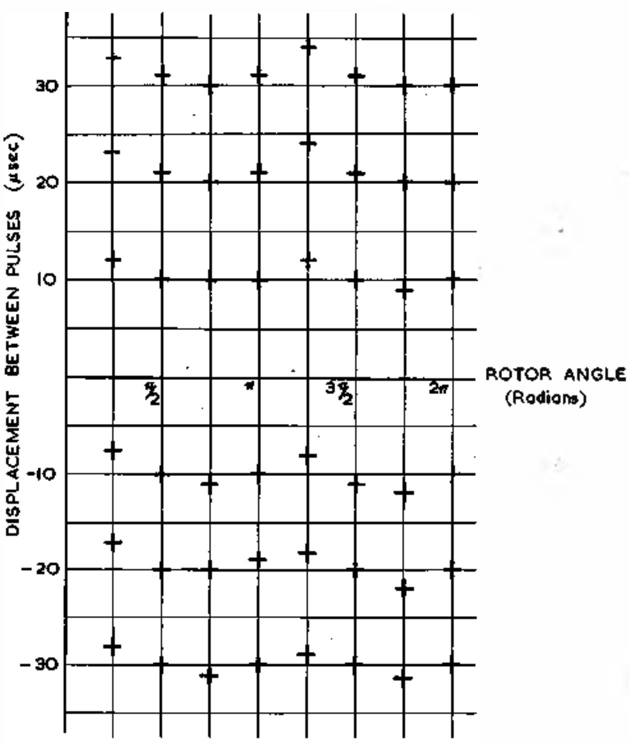

Fig. 8. A typical error distribution

that when the coupled rotors were turned both channels shifted in the same direction in the time domain.

The outputs from the two channels were mixed on a three winding pulse transformer, the third winding being connected to the oscilloscope (Fig. 7).

Details of Test Results

The observed jitter between the two channels was under $0{\cdot}5\mu$sec total and did not vary with time.

To determine the error in the time modulated output pulses the two pulse trains were displaced by a fixed amount in the range from 2μsec to 400μsec.

The coupled rotors were then slowly turned and the change in displacement between the pulse trains was measured with an oscilloscope. The total variation observed was 5μsec maximum.

The frequency of operation was 400c/s, giving a full scale shift of 2·5msec and the error of $\pm 2{\cdot}5\mu$sec in the position of the pulse therefore corresponds to an error of $\pm 0{\cdot}1$ per cent full scale. However, this is a combination of the errors of two complete channels, whereas in fact only one channel would be changing in practice, the other being a fixed reference channel. The maximum displacement used, 400μsec, was determined by the measuring facilities of the oscilloscope, but it corresponds to a phase displacement of approximately 60°.

The experiment was repeated on the two following days with the same result, and in other experiments the outputs from the phase shifting units were fed into the alternate clippers, and one stator of each phase shifter was reversed, but the same result was again obtained.

In an attempt to discover the nature of the errors, the displacement of the two pulse trains was measured at different positions of the rotors relative to the stators. The experimental error in the plotted results, Fig. 8, is probably $0{\cdot}5\mu$sec. The results were repeatable over a period of several days.

Conclusions

The error in displacement, which corresponds to a phase-angle change of $\pm 21'$ of arc for the two channel set-up, appears to be composed of two components. The smaller is of period 2π and the larger of period π, but no clue was obtained as to the causes.

It is known, however, that the signal used in this work for driving the rotors was of poor quality with appreciable harmonic content. No filters were used, because the accuracy required ($\pm 0{\cdot}1$ per cent full scale) was obtained without them.

Excellent power supplies operating at 400c/s and 1kc/s are now commercially available, and the use of a time period counter or chronometer would greatly facilitate any future investigation.

Recommendations for Future Work

The resolver phase shifter method offers a convenient method of transducing shaft position, and with suitable equipment it should prove reasonably easy to achieve a linearity of $\pm 0{\cdot}05$ per cent. The use of the operational amplifier technique appears to be very promising but very little has as yet been published about it.

The synchro should be considered wherever low inertia and friction torque are needed in a transducer of small physical size.

Acknowledgments

The author's thanks are due to the Chief Executive Aircraft Research Association Ltd, for permission to publish the information in this article, and to Mr. A. Tiffany for much advice and encouragement throughout the project.

REFERENCES

1. Sisson, R. L., Susskind, A. K. Devices for Conversion Between Analogue Quantities and Binary Pulse Coded Numbers. Report R-176. (Servomechanisms Laboratory. M.I.T. March, 1950).
2. Millman, J., Taub, H. Pulse and Digital Circuits. p. 497 (McGraw Hill, 1957.)
3. Chance, B. Waveforms. 498 (MIT Radiation Laboratory Series McGraw Hill, 1949.)
4. Schachter, J. Phase Error of a Two Phase Resolver. *Proc. Inst. Radio Engrs. 45*, 1018 (1957).
5. Robinson, A. S. An Electronic Analogue Computing Technique for the Solution of Trigonometric Problems. *IRE Trans. EC-4*, 95 (Sept., 1955).
6. Shumard, C. C. Design of High-pass, Low-pass and Band-pass Filters Using RC Filters and Direct Current Amplifiers with Feedback. *RCA Rev. 11*, 534 (1950).
7. Chance, B. Waveforms. 495 (MIT Radiation Laboratory Series McGraw Hill, 1949).

A Method for Sharpening the Output Waveform of Junction Transistor Multivibrator Circuits

By A. E. Jackets*, B.Sc.(Eng.)

The transistor multivibrator circuit provides a simple means of generating rectangular waveforms. The design of such circuits was discussed in a previous article[1] and it was shown that the output waveforms are marred by the recharging of the coupling capacitors. This article, an extension of the previous work, presents a method of designing the circuit to reduce this recharging time and thus sharpen the output waveform at the collector of one transistor. However, this improvement in waveform is only obtained at the expense of the other output waveform.

IN many multivibrator circuits it is necessary that the transition between states be as rapid as possible. A good example is the use of a multivibrator to drive d.c. convertor circuits, where slow switching speeds result in increased power dissipation in the output transistors, with a consequent loss of efficiency.

The transition from off to on for most multivibrator circuits is quite rapid, usually of the order of 1µsec. This rapid transition is mainly due to the large pulse available to switch the transistor and the regenerative action of the circuit. However, the transition period from on to off is largely determined by the recharging time of the coupling capacitors and the slow transition which results may be seen from the oscillogram of the collector voltage waveform in Fig. 5(a). A design procedure is discussed in this article to reduce this transition period by minimizing the recharging time of a coupling capacitor. This can be achieved by making the circuit asymmetrical. Thus, in one half of the multivibrator, the values of the components are reduced, and in the other half they are increased. The effect is to improve the waveform at one collector at the expense of the other. There is a limit to the extent of this improvement which will be discussed later.

This design procedure is only suitable for applications which require one output.

Principles of Operation of a Transistor Multivibrator

Fig. 1 shows the basic circuit of the mulivibrator. Feinberg, in his analysis of the equivalent thermionic valve circuit, has shown that the operation of the circuit may be represented by an equivalent diagram using a switch[2,3,4]. The equivalent diagram of the transistor multivibrator circuit is shown in Fig. 2 and is simpler than that for thermionic valve circuits; this is because the transistor may be assumed to be a perfect switch in many cases.

Referring to the equivalent diagram of Fig. 2, the components correspond to the circuit in Fig. 1, and the diodes D_1 and D_2 represent the emitter-base diodes of the transistors. In practice, the values of the components often allow the forward resistance of these diodes to be neglected and the reverse resistance to be considered infinite; thus the diodes may be considered perfect.

The switch in position A indicates that transistor X_1 is on and transistor X_2 is off. In position B these states are reversed and X_1 is off while X_2 is on. Consider the switch in position A; capacitor C_1 is then charged to a voltage of approximately V_{cc} via R_{L2} and D_1, which is biased in the forward direction and thus has a low resistance. When the switch moves to position B, C_1 is placed in parallel with D_1 and the charge on C_1 biases D_1 in the reverse direction; X_1 is thus switched off. C_1 then discharges through resistor R_1 and the battery V_{bb}, until the voltage across D_1 falls to zero; the reverse resistance of D_1 is very high and may be neglected. D_1 then conducts, switches X_1 on, and returns the switch to position A.

Thus the time t_1 for which the switch is in position B is governed by the time required for the voltage across C_1

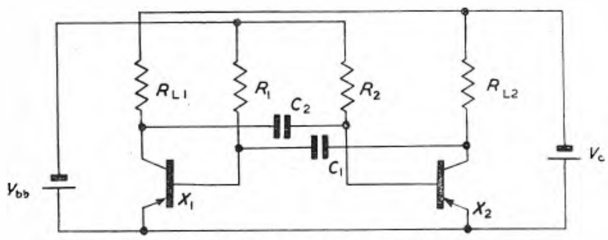

Fig. 1. The circuit of the multivibrator

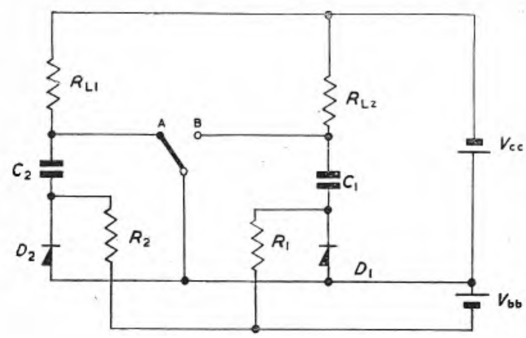

Fig. 2. The equivalent multivibrator diagram

to decay to zero. The value of t_1 is given by the expression.

$$t_1 = C_1R_1 \ln \left[\frac{V_{cc} + V_{bb}}{V_{bb}}\right] \quad \text{.......... (1)}$$

$$= C_1R_1 \ln [1 + k] \quad \text{................ (2)}$$

where $k = (V_{cc}/V_{bb})$.

Similarly, the time t_2 for which the switch is in position A (the period for which X_2 is off) is given by

$$t_2 = C_2R_2 \ln \left[\frac{V_{cc} + V_{bb}}{V_{bb}}\right] \quad \text{.......... (3)}$$

$$= C_2R_2 \ln [1 + k] \quad \text{................ (4)}$$

Hence T, the period of the multivibrator, is given by

$$T = t_1 + t_2 = (C_1R_1 + C_2R_2) \ln \ [1 + k].$$

Formulae (1), (2), (3) and (4) neglect the effects of I_{co} and collector 'bottoming' voltage which are usually small.

To obtain rectangular waveforms each transistor must be biased so that it is 'bottomed' when in the on state. Referring to Fig. 1, the condition for X_1 to 'bottom',

* *The General Electric Co. Ltd., Wembley*

neglecting the effect of I_{co}, is

$$i_b \geqslant (i_c/\alpha_{e1}')$$

$$\text{or } (V_{bb}/R_1) \geqslant (V_{cc}/R_{L1}\,\alpha_{e1}')$$

$$\text{i.e. } \alpha_{e1}' \geqslant (kR_1/R_{L1}) \quad \ldots\ldots\ldots\ldots\ (5)$$

Similarly, the condition for X_2 to 'bottom' is

$$\alpha_{e2}' \geqslant (kR_2/R_{L2}) \quad \ldots\ldots\ldots\ldots\ (6)$$

The Sharpness of the Collector Waveforms

Fig. 3 shows the waveforms of the typical multivibrator with $t_2 < t_1$. The sharpness of the transition of X_1 from on to off is limited by the time taken to charge the capacitor C_2 via the resistor R_{L1}. Similarly the transition of X_2 from on to off is limited by capacitor C_1 and resistor R_{L2}. An indication of the sharpness of the collector waveforms is given by the ratio (T/CR_L) where T is the period of the multivibrator.

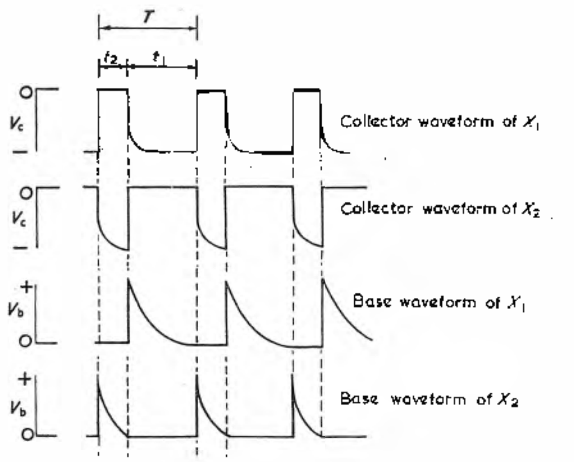

Fig. 3. The base and collector waveforms

For the collector waveform of X_1

$$\frac{T}{C_2R_{L1}} = \frac{t_1 + t_2}{C_2R_{L1}} = \frac{t_2\,(1 + (t_1/t_2))}{C_2R_{L1}}$$

Substituting for t_2 in this expression

$$\frac{T}{C_2R_{L1}} = (1 + (t_1/t_2))\,\frac{R_2}{R_{L1}}\,\ln(1 + k)$$

To obtain the sharpest transition from on to off, T/C_2R_{L1} must be as high as possible. R_{L1} thus requires to be as low as possible and from expression (5) the minimum value of R_{L1} is

$$R_{L1}|_{\min} = (kR_1/\alpha_{e1}')$$

This corresponds to the maximum value of T/C_2R_{L1} which becomes

$$\left.\frac{T}{C_2R_{L1}}\right|_{\max} = (1 + (t_1/t_2))\,\frac{R_2}{R_1}\,\alpha_{e1}'\,\frac{\ln(1 + k)}{k} \quad \ldots\ldots\ (7)$$

Similarly for the collector waveform of X_2

$$\left.\frac{T}{C_1R_{L2}}\right|_{\max} = (1 + (t_2/t_1))\,\frac{R_1}{R_2}\,\alpha_{e2}'\,\frac{\ln(1 + k)}{k} \quad \ldots\ldots\ (8)$$

The variation of the expression $\ln(1 + k)/k$ with k has been calculated and the results presented in Fig. 4. It will be seen that the expression has a maximum value of unity when $k = 0$, i.e. $V_{bb} \gg V_{cc}$. When a single battery is used for V_{bb} and V_{cc}, $k = 1$ and then $\ln(1 + k)/k$ is equal to 0·69. Thus although some improvement in waveform may be obtained by using a low value of k the improvement is slight and in most practical cases it is usual to let k equal unity.

However, a great improvement may be made in the waveform of X_1 by making R_2/R_1 as high as possible. It will be noticed that although this increases T/C_2R_{L1}, and hence the sharpness of the collector waveform of X_1, the value of T/C_1R_{L2} is reduced. This improvement in the waveform of X_1 is thus only obtained at the expense of the collector waveform of X_2.

The Maximum Value of R_2/R_1

To find the maximum value of R_2/R_1 consider the collector waveform of X_2. It will be seen from Fig. 3 that t_2 must be sufficiently large to allow C_1 to charge to a voltage nearly equal to V_{cc}. If this does not happen it is impractical to predict the periods and waveforms. As the time for C_1 to charge to V_{cc} volts is infinite, it is convenient to assume that C_2 reaches a potential AV_{cc} where A is slightly less than unity. Thus assume that

$$R_{L2}C_1 < t_2\,.\,B \quad \ldots\ldots\ldots\ldots\ (9)$$

where B is a constant, the value of which ensures that C_1 is charged to AV_{cc}.

From equations (9) and (4)

$$(C_1/C_2) < B\,.\,(R_2/R_{L2})\,.\ln(1 + k) \quad \ldots\ldots\ (10)$$

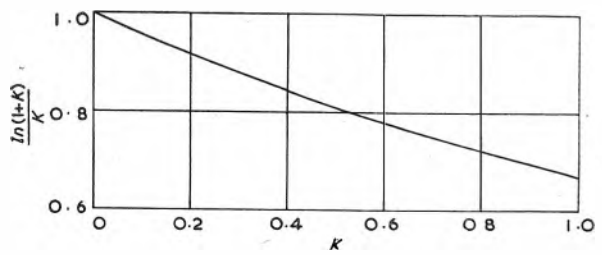

Fig. 4. The variation of $\ln(1+K)/K$ with K

Now, from equations (1) and (3)

$$(C_1/C_2) = (t_1/t_2)\,.\,(R_2/R_1) \quad \ldots\ldots\ldots\ (11)$$

Also, from equations (10) and (11)

$$(R_2/R_1) < B\,(R_2/R_{L2})\,.\,(t_2/t_1)\ln(1 + k)$$

But, from equation (6), the maximum value of R_2/R_{L2} is α_{e2}'/k.

Hence, the maximum value of R_2/R_1 is given by

$$\left.\frac{R_2}{R_1}\right|_{\max} = (t_2/t_1)\,B\,\alpha_{e2}'\,\frac{\ln(1 + k)}{k} \quad \ldots\ldots\ldots\ (12)$$

If $B = \frac{1}{3}$, C will be charged to $0{\cdot}95V_{cc}$. In practice, when designing, this value of B can be used when determining the maximum value of R_2/R_1.

The maximum value of T/C_2R_{L1} may now be obtained from expressions (7) and (12) and becomes

$$\left.\frac{T}{C_2R_{L1}}\right|_{\max} = (1 + (t_2/t_1))\,\alpha_{e1}'\,\alpha_{e2}'\,.\,B\left[\frac{\ln(1 + k)}{k}\right]^2$$

For the sharpest waveforms one therefore requires high gain transistors. A low value of k will also improve the waveform but this is not always practical.

Fig. 5 shows the output waveforms of a 360c/s multivibrator using the circuit of Fig. 1, in which R_2/R_1 was varied, while maintaining C_1R_1 and C_2R_2 equal and constant to prevent the frequency changing. GET4 transistors were used for these tests, and a single supply voltage employed ($V_{cc} = V_{bb}$).

The improvement in the output waveform of X_1 as R_2/R_1 is increased is readily seen and so is the deterioration in the X_2 waveform. The lower output voltage of X_2 when $R_2/R_1 = 10$ is due to the fact that C_1 did not have time to fully charge up to V_{cc} volts.

Fig. 6 shows the effect of varying R_2/R_1 as in Fig. 5 but the multivibrator frequency was increased to 10kc/s in this case.

The Effect of Temperature

A transistor is in the off state when the base is held positive with respect to the emitter by the charge on the coupling capacitor. Under these conditions the input impedance is high, the only current flowing in the base circuit of the transistor being the combined collector and emitter leakage currents. Ebers and Moll[5] have shown that the

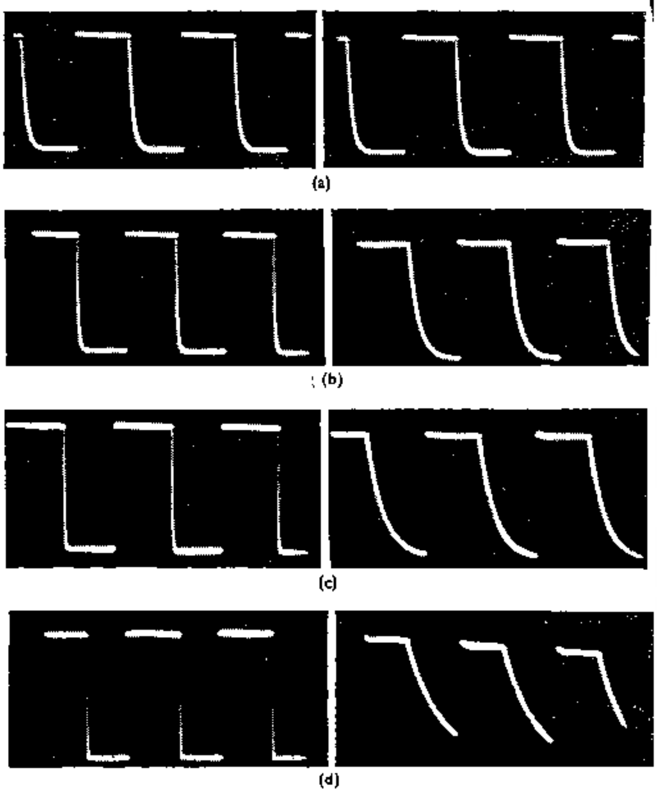

Fig. 5. Multivibrator output waveforms (1)
(X_1 left, X_2 right. Frequency 360c/s, V_{cc} = 9V)

(*a*) *Symmetrical circuit* $(R_2/R_1)=1$ $R_{L_1}=R_{L_2}=1\text{k}\Omega$, $C_1=C_2=0{\cdot}1\mu F$, $R_1=R_2=22\text{k}\Omega$. (*b*) *Asymmetrical circuit* $(R_2/R_1)=2$ $R_{L_1}=1\text{k}\Omega$, $R_{L_2}=2{\cdot}2\text{k}\Omega$, $R_1=22\text{k}\Omega$, $R_2=47\text{k}\Omega$, $C_1=0{\cdot}1\mu F$, $C_2=0{\cdot}05\mu F$. (*c*) *Asymmetrical circuit* $(R_2/R_1)=5$ $R_{L_1}=1\text{k}\Omega$, $R_{L_2}=4{\cdot}7\text{k}\Omega$, $R_1=22\text{k}\Omega$, $R_2=100\text{k}\Omega$, $C_1=0{\cdot}1\mu F$, $C_2=0{\cdot}025\mu F$. (*d*) *Asymmetrical circuit* $(R_2/R_1)=10$ $R_{L_1}=1\text{k}\Omega$, $R_{L_2}=10\text{k}\Omega$, $R_1=22\text{k}\Omega$, $R_2=220\text{k}\Omega$, $C_1=0{\cdot}1\mu F$, $C_2=0{\cdot}001\mu F$.

sum of the collector and emitter leakage currents is approximately I_{co}. This current is small at low ambient temperatures (typically 4μA at 20°C), but it increases with temperature, approximately doubling for every 10°C rise in temperature. As I_{co} is reasonably independent of the voltage applied across the collector-base junction this transistor parameter may be included when the discharge time of the coupling capacitors is calculated. Thus equations (1) and (3), modified to include I_{co}, become

$$t_1 = C_1R_1 \ln \left[\frac{V_{cc} + V_{bb} + I_{co}R_2}{V_{bb} + I_{co}R_2}\right] \quad \ldots\ldots\ldots (13)$$

$$t_2 = C_2R_2 \ln \left[\frac{V_{cc} + V_{bb} + I_{co}R_2}{V_{bb} + I_{co}R_2}\right] \quad \ldots\ldots\ldots (14)$$

As the terms $I_{co}R_1$ and $I_{co}R_2$ are small at ambient temperatures, they may often be neglected when designing multivibrator circuits for low temperature operation. However, at higher temperatures these terms must be considered due to the increased value of I_{co}.

When designing circuits for operation at elevated temperatures it is necessary to use low values for R_1 and R_2 and also if possible to use a high value of V_{bb} in order to maintain the periods t_1 and t_2 reasonably constant as the temperature is increased. The maximum deviation of t_1 and t_2 due to temperature may be computed by substituting values for I_{co} in equations (13) and (14) at the lower and higher temperatures.

Frequency Limitations

The upper frequency limit for the design of multivibrators as described in this article is governed largely by a small loss of charge on the coupling capacitors, which

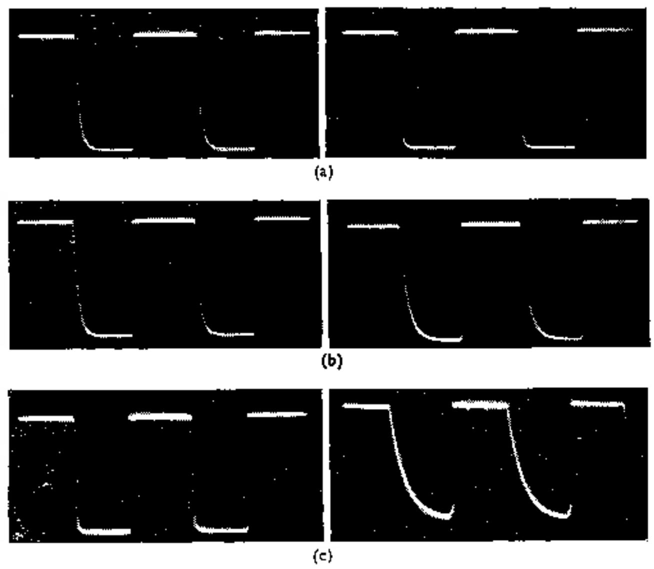

Fig. 6. Multivibrator output waveforms (2)
(X_1 left, X_2 right. Frequency 10·5kc/s, V_{cc} = 9V)

(*a*) *Symmetrical circuit* $(R_2/R_1)=1$ $R_{L_1}=R_{L_2}=560\Omega$, $C_1=C_2=0{\cdot}005\mu F$, $R_1=R_2=15\text{k}\Omega$. (*b*) *Asymmetrical circuit* $(R_2/R_1)\simeq 2$ $R_{L_1}=560\Omega$, $R_{L_2}=1\text{k}\Omega$, $R_1=15\text{k}\Omega$, $R_2=30\text{k}\Omega$, $C_1=0{\cdot}005\mu F$, $C_2={\cdot}0025\mu F$. (*c*) *Asymmetrical circuit* $(R_2/R_1)=5$ $R_{L_1}=560\Omega$, $R_{L_2}=2{\cdot}2\text{k}\Omega$, $R_1=15\text{k}\Omega$, $R_2=75\text{k}\Omega$, $C_1=0{\cdot}005\mu F$, $C_2=0{\cdot}001\mu\text{F}$.

occurs when the coupling capacitor is switched across the initially low input impedance of the transistor, and provides the energy to turn the transistor off. This causes the voltage of the charged coupling capacitors to fall considerably below the usual value of V_{bb} before the exponential timing discharge occurs, and thus the calculated values for t_1 and t_2 are larger than those obtained in practice when t_1 and t_2 are small.

The Design of Multivibrators to Generate a Sharp Waveform

For simplicity it is usually desirable to operate the circuit from a single supply. The voltage of this supply may be determined from the peak-to-peak voltage of the required waveform since, for practical purposes, the peak-to-peak output voltage is equal to the supply voltage. However, for predictable performance, it is necessary that the supply voltage should be large compared with the 'bottoming' voltage of the transistors.

Assuming the supply voltage to be fixed, the first step is to choose a suitable value of R_{L1}. This value is required to be as low as possible consistent with power requirements and the peak collector current rating of the transistors.

Having chosen R_{L1}, and knowing the value of α_{e1}' R_1 may be calculated from expression (5). To ensure that the transistors fully bottom, a value of R_1, about 20 per cent lower than calculated, is generally used.

Knowing t_1, t_2, α_{e2}' and k, the maximum value of R_2/R_1 is then found from expression (12); B is taken as $\frac{1}{3}$. As R_1 has been determined this ratio fixes the value of R_2. R_{L2} may then be calculated from expression (6), the practical value being made about 20 per cent higher than this value. It now remains to find C_1 and C_2, and these are found from expressions (1) and (3).

If it is desired to operate the circuit at elevated temperatures, the values obtained for R_1 and R_2 using the above procedure may be sufficiently high to cause t_1 and t_2 to become temperature dependent. In this case it is preferable to first determine the maximum value of R_2 so that the change of $\ln\left[\dfrac{V_{cc}+V_{bb}+I_{co}R_2}{V_{bb}+I_{co}R_2}\right]$ with temperature is within the desired limits. From R_2, the value of R_{L2} may be determined using equation (6), and the ratio R_2/R_1 calculated from equation (12). Since R_2 is known this ratio fixes the value of R_1. It is important to realize that a low value of R_1 will result in excessive base current and this may be a limitation to the minimum value of R_1 which may be employed. Similarly, a low value of R_{L1} calculated from equation (5) may result in excessive collector current. Thus in practice it may be necessary to use higher values of R_1 and R_{L1} than those calculated above, although this results in an increased on to off transition in the collector waveform of X_1. The design is completed by calculating C_1 and C_2 from equations (1) and (3).

Conclusions

Multivibrator circuits form a simple means of generating rectangular waveforms at lower frequencies, the circuits being readily designable. The off to on transition of the output waveform is usually rapid ($\approx 1\mu$sec) but the on to off transition is slowed by the charging of the coupling capacitors. The latter transition can be speeded to some extent by using a higher supply voltage for the base than for the collector, but this transition may be considerably improved if some deterioration can be tolerated in the other output waveform; this is achieved by a particular choice of component values.

The on to off transition may also be improved by using transistors of higher current gain (α_e'); however, it is important to note that this improvement is only obtained if the circuit components are also modified to take advantage of this higher gain. The effect of temperature upon the circuit performance may be predicted, and the circuit designed to minimize these effects.

REFERENCES

1. JACKETS, A. E. Multivibrator Circuits Using Junction Transistors. *Electronic Engng. 28*, 184 (1956).
2. FEINBERG, R. On the Performance of the Push-Pull Relaxation Oscillator. *Phil. Mag. 29*, Series 7, 268 (1948).
3. FEINBERG, R. Symmetrical Multivibrators. *Wireless Engr. 26*, 153 (1949).
4. FEINBERG, R. Asymmetrical Multivibrators. *Wireless Engr. 26*, 325 (1949).
5. EBERS, J., MOLL, J. Large Signal Behaviour of Junction Transistors. *Proc. Instn. Radio Engrs. 42*, 1773 (1954).

The Measurement of High Value Resistances

By J. K. Wood*, M.Sc., Ph.D.

It is frequently required to calibrate a high resistance, and some procedures leading to this end are described. Standard laboratory equipment is used, since special apparatus is only an economic proposition when such calibrations are routine. Some of the sources of error and methods of reducing them are described.

WITH the increasing use of very high resistances in high voltage measurement circuits, electrometer circuits, and other high impedance measuring circuits, it is important that the methods of determining absolute resistance in the range tens of megohms and upwards be examined as to their suitability. Methods available all show some undesirable characteristic, except perhaps over a limited range, and the purpose of the present article is to describe the author's experience with some of them. The methods considered are:

(1) Capacitor discharge and ballistic galvanometer method.

(2) Capacitor discharge and electrostatic voltmeter methods.

(3) Bridge and other methods.

In the present instance the aim was the calibration of high voltage measuring resistances, composed of a large number of units of a few megohms each in series. Consequently the error due to humidity and absorbed moisture on the surface of the units was relatively small compared with the error in resistance value of a single unit of up to $10^{14}\Omega$ under similar conditions. The former may be used in any warm dry room, but the latter must be used in a sealed container incorporating a drying agent such as silica gel, and surrounding the electrometer valve or other circuit with which it is associated. The experiments described were all carried out with the former type of resistance, but the results are applicable to the latter.

Experimental Methods

CAPACITOR DISCHARGE AND BALLISTIC GALVANOMETER METHOD

The circuit is shown in Fig. 1(a). The standard capacitor C is charged to a constant voltage E provided by a standard cell, firstly through a resistor R and then directly. This protects the standard cell from current surges which impair its accuracy. Next, the capacitor is isolated for a known period of time, during which it discharges through the unknown resistance X. Finally, the capacitor discharges through the ballistic galvanometer G. The sequence of events is indicated by the numbers 1 to 4 on the switch S.

After a time t has elapsed from the isolation of the capacitor from the charging circuit, the voltage V across

* *Pilkington Bros. Ltd., formerly University of Manchester.*

the capacitor is given by

$$V = Ee^{-t/CX} \quad \ldots\ldots\ldots\ldots\ldots\ldots \quad (1)$$

or

$$\ln V = \ln E - (t/CX)$$

Since

$$V = q/c \text{ and } d = kq,$$

$$\ln d = \ln d_0 - (t/CX) \quad \ldots\ldots\ldots\ldots\ldots \quad (2)$$

where q is the charge on the capacitor at any time, d is the deflexion due to the passage of the charge q, and d_0 is the deflexion due to the passage of the charge CE, through the galvanometer circuit.

Several readings of deflexion are taken after different discharge times, and $\ln d$ is plotted against t. The slope is $-1/CX$, and as C is known, X is readily obtained.

A further test with X removed determines the equivalent

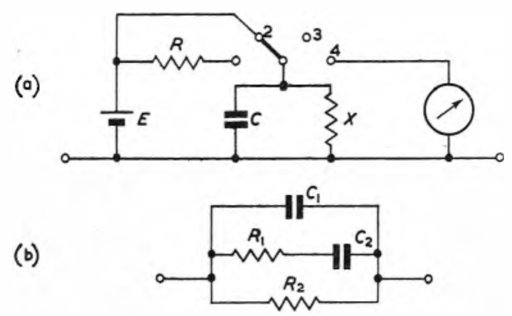

Fig. 1. (a) Ballistic high resistance measuring circuit
(b) Capacitor equivalent circuit

shunt leakage resistance L. If this is not negligible, the true value of X is determined by the equation.

$$X = (LX'/L - X') \quad \ldots\ldots\ldots\ldots\ldots \quad (3)$$

where X' is the apparent value of the resistance X.

One of the pitfalls of this method lies in the standard capacitor. This must be left to charge for at least a minute to reduce 'soaking' effects. If the voltage source is disconnected before this, the charge on the capacitor tends to redistribute itself, so that the potential appearing at its terminals falls. The equivalent circuit is approximately as shown in Fig. 1(b). R_2 represents the shunt leakage of the capacitor, and R_1C_2 accounts approximately for the 'soaking' effect. The time-constant R_1C_2 appears to vary with applied voltage as well as between capacitors.

On discharge, however, the effect cannot be compensated. The longer the period of the ballistic galvanometer the better, but the effect must be borne in mind when estimating the accuracy of the results. For the same reason the capacitor must be kept short-circuited when not in use, especially after use at higher voltages, so that it is completely discharged before use at these low voltages. A 1μF standard mica capacitor tested yielded a steady deflexion of 1mm with a moderately sensitive galvanometer after use at 100V and in spite of being short-circuited for four hours.

Another factor which must be considered is the accuracy of time measurement. Using an ordinary stop watch to time the period of isolation, a minimum of about 50sec is required to achieve an error less than 1 per cent. A mechanical or electrical timing unit associated with a well insulated relay may be used with advantage. Contact bounce must be avoided or loss of linearity will occur by high frequency oscillatory discharges and sparking if the circuit is inductive. Accuracy is improved by measuring each point a number of times, though the improvement does not justify the time taken beyond six to ten readings.

With 1·0, 0·1 and 0·01μF standard capacitors, voltage sources up to the order of 10V for the smaller capacitors, and a sensitive galvanometer, resistors from about 10^8 to $10^{11}\Omega$ can be measured with an error of about 0·1 per cent. Higher voltages are not satisfactory because of greater errors in the ballistic galvanometer circuit and the possibility of sparking at the switch contacts.

A typical decay plot is shown in Fig. 2. Each point represents the mean of four readings, and the slope of the line is 0·01003. As a 1·000μF capacitor was used, the resistance is thus 99·7MΩ.

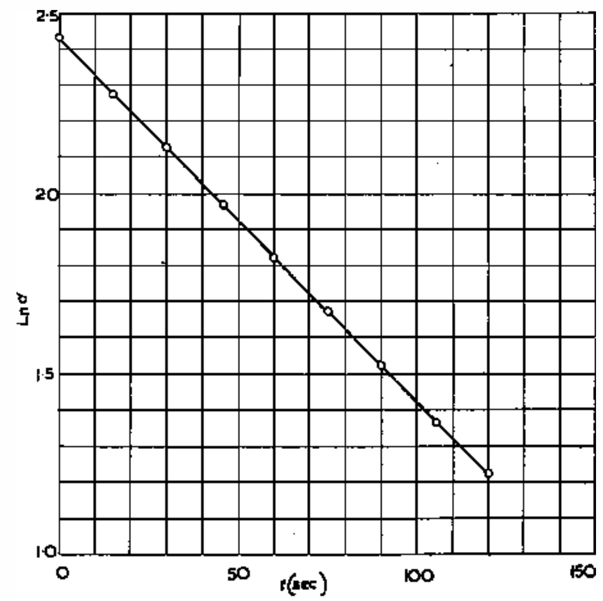

Fig. 2. Determination of high resistance

The slope of the line can be determined by the method of least squares, making t the independent variable. The slope b is given by the relation

$$b = \frac{\Sigma(y - y')(x - x')}{\Sigma(x - x')^2} = \frac{\Sigma xy - \Sigma x \Sigma y/n}{\Sigma x^2 - (\Sigma x)^2/n} \quad \ldots\ldots \quad (4)$$

where $x = t$ and $y = \ln d$, there being n pairs of readings. x' and y' are the average values of x and y. The latter form is the practical form of the relation. The standard deviation of b is given by

$$\sigma_b = \sqrt{\left[\left(\frac{1}{n-2}\right)\left(\frac{\Sigma y^2 - (\Sigma y)^2/n}{\Sigma x^2 - (\Sigma x)^2/n} - b^2\right)\right]} \quad \ldots (5)$$

There is approximately 2/3 probability that the true value of $-1/CX$ lies within the experimentally determined range $b \pm \sigma_b$. Thus, using the thirty-six pairs of results from which Fig. 2 was plotted,

$$b = 0{\cdot}0100243$$

$$\sigma_b = 0{\cdot}0000105$$

Hence,

$$X = 99{\cdot}75 \pm 0{\cdot}1\text{M}\Omega$$

Three points arise when using the mathematical approach.

(1) The calculated error is the random error, and does not include any calibration or other systematic errors, for which due allowance must be made in the measured quantities.

(2) Calculations should be to as many significant figures

as possible, since in work on near-straight lines, differences of large numbers reduce accuracy.

(3) A large random error may indicate the need for more readings, or possibly a miscalibration. A limit is set to the accuracy obtainable by the experimental method and instruments used, and the random error can only be reduced to a similar but larger value.

Capacitor Discharge and Electrostatic Voltmeter Methods

A circuit is given in Fig. 3(a). Since an electrostatic voltmeter is used, the applied voltage is of the order of hundreds of volts. The capacitor is charged as before, and during discharge corresponding values of voltage and time are noted. $t = 0$ is assumed at the first noted voltage.

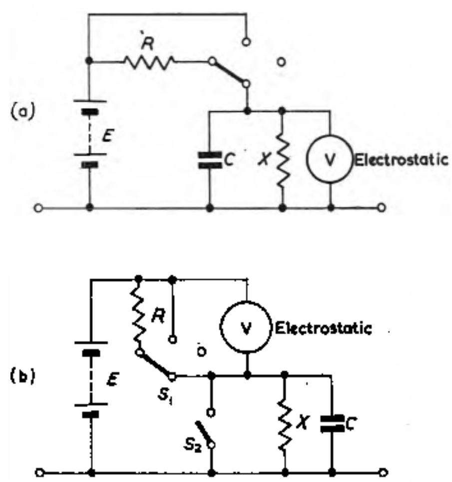

Fig. 3. Electrostatic methods of high resistance measurement

Several runs of results may be taken, and average points plotted if voltage readings are always taken at the same values of t, keeping $V_t = 0$ constant. Further runs with X disconnected are taken to determine the leakage resistance, and the same procedure (plotting $\ln V$ versus t) is used as in the ballistic method. Since there are no sudden discharges, the inaccuracies due to 'soaking' are less than in the ballistic method.

The limitations of the method are mainly due to the mechanics of the voltmeter. The electrostatic force on the movement is a function of the applied voltage and the deflexion. Viscous damping is usually provided, so that the equation of motion can be written as:

$$I\,(d^2d/dt^2) + K_1\,(dd/dt) + K_2 d - K_3 f(V(t),d) = 0 \quad \ldots (6)$$

where d is the deflexion in radians, I the inertia of the movement, $V(t)$ the applied voltage, and $K_2 d$ represents the torsion of the suspension. K_1, K_2 and K_3 are constants.

In the steady state, i.e. ($V(t)$ = const.; $t \to \infty$,

$$K_2 d = K_3 f(V,d) \quad \ldots\ldots\ldots\ldots\ldots\ldots (7)$$

or

$$d = \phi(V)$$

Which is the law governing the calibration of the voltmeter.

In the present instance, however, $V(t)$ is defined by

$$V(t) = E\ (t \leqslant 0)$$
$$\ldots\ldots\ldots\ldots (8)$$
$$V(t) = E e^{-t/CX}\ (t > 0)$$

The solution is approximately of the form

$$d = \phi(V(t)) + K_4\,(d/dt)\,(V(t)) + K_5\,e^{-K_6 t}\sin K_7 t \quad \ldots (9)$$

If CX is large, the last two terms disappear, but when CX is small they can be troublesome.

Using the same 100MΩ resistor and 1·000μF standard capacitor as previously and a sub-standard electrostatic voltmeter, the voltage was measured at two second intervals for 40sec. The results of five runs were averaged, and the expected voltages (derived from the known values of X and E) subtracted from them. This difference between observed and expected readings is plotted in Fig. 4, and shows clearly the initial damped oscillations (the third term in equation (9)) and the voltage lag due to viscous damping (the second term in equation (9)).

Thus the lower limit of usefulness of the method is set at about $10^9\Omega$, using a 1μF standard capacitor. The upper limit is set by the leakage resistance of the apparatus, the time available for the discharge, and the size of the capacitor used.

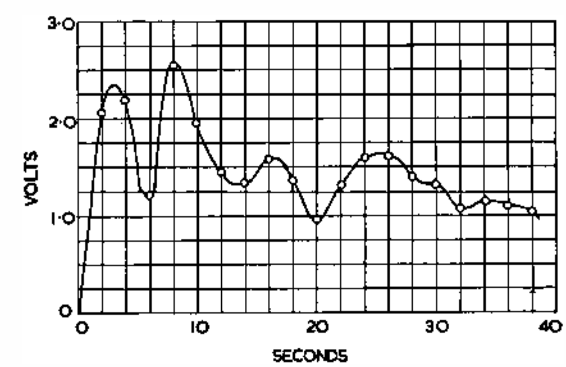

Fig. 4. Dynamic error of electrostatic voltmeter

To increase the upper limit of resistance measurement within a reasonable discharge time smaller capacitors may be used. In this case the capacitance of the electrostatic voltmeter, which is not constant, must be considered. If, over the proposed range of measurement, the capacitance of the voltmeter varies from C_1 to C_2, the correction applied to the standard capacitor C is assumed to be $(C_1 + C_2)/2$.

To limit the total variation of capacity to $\pm$ p per cent, then

$$C + \frac{C_1 + C_2}{2} = \frac{100}{p}\cdot\frac{C_1 - C_2}{2} \quad \ldots\ldots\ldots (10)$$

or

$$C = \left(\frac{100 - p}{2p}\right) C_1 - \left(\frac{100 + p}{2p}\right) C_2$$

$$\simeq (100/2p)\,(C_1 - C_2) \text{ Since } p \text{ is small} \quad \ldots\ldots (11)$$

This can place quite severe restrictions on the size of C, and for large value resistors there is an advantage in using a higher voltage with a smaller capacitance, since an electrostatic voltmeter designed for higher voltages usually has a smaller total capacitance, and a smaller capacitance variation. Since the highest value resistors are usually single units, with which high voltages are not permissible, the upper limit of the method is probably about $10^{12}\Omega$.

An inverted circuit arrangement used by the author reduces the lower limit of measurement by electrostatic voltmeter methods. The circuit is shown in Fig. 3(b). When the capacitor is fully charged, the voltmeter registers zero; as it discharges the pointer begins to move almost imperceptibly because of the extremely cramped scale. Readings of voltage at fixed time intervals are taken as the pointer moves across the calibrated part of the scale. The final reading to measure E is taken with the capacitor short-circuited.

The advantages of the system are:

(1) The maximum pointer acceleration is reduced by orders of magnitude, since the initial acceleration is rendered negligible by the cramped voltmeter scale.

(2) The maximum velocity is reduced by a factor of about 5, since the rate of discharge is considerably reduced by the time the pointer reaches the widest part of the scale.

(3) The smallest voltages across the standard capacitor are read from the widest part of the scale, thus improving accuracy.

Thus the last term in equation (9) disappears, and the second term is considerably reduced.

The method requires a constant voltage source of the order of 100V. A dry battery is quite suitable if the laboratory ambient temperature is reasonably constant during the period of the test.

There are two possible leakage resistances; across the voltmeter and across the capacitor. By removing X and observing the rate of change of voltage across the fully discharged capacitor, and by determining the leakage of the same instruments by the electrostatic voltmeter method previously described, two leakage resistances can be found; the leakage of the voltmeter and S_1, and the leakage of the capacitor and S_2. In the same way as previously, it may be necessary to correct for the capacitance of the voltmeter. However, if the method is restricted to extending the use of an electrostatic voltmeter to the measurement of lower resistances, the above corrections can be neglected since the leakage resistance and standard capacitance will be large compared to X and the voltmeter capacitance.

The variables are $\ln(E - V)$ and t, where V is the indicated voltage. Results are dealt with in the same way as already described for the ballistic galvanometer method. The overall range covered by the two circuit arrangements is of the order of 10^8 to $10^{12}\Omega$.

Bridge and Other Methods

Only d.c. bridge circuits are permissible, since a high resistance has quite a long time-constant with its self capacitance. A 500MΩ (nominal) resistor built for high voltage measurement had a frequency response which was 6dB down at 10c/s, and higher resistors such as are met in ionization chamber circuits often have a time-constant of tens of seconds when connected to the chamber.

Using a Wheatstone bridge, resistances up to $10^7\Omega$ are determined with the usual 11, 111Ω variable resistance, and standards of $10^6\Omega$ and $10^5\Omega$.

A sensitive galvanometer enables accuracies better than $\pm 0{\cdot}1$ per cent to be obtained. Higher voltages also improve the discrimination, most of the potential drop occurring across the standard and the unknown. Care must be taken to avoid heating these components.

Where high voltage measuring resistors are to be calibrated, two courses are open. Either the unknown may be compared with a known similar resistor, using very high voltages (10^4 to 10^5V), or the resistance of each unit of the unknown may be determined separately, and the results added. In either case, each unit is stressed to something like its normal working voltage during measurement, thus eliminating the effect of the small amount of non-linearity usually to be found in these resistors when used at low voltages. The former method also includes the effect of any residual corona discharges which may be present at junctions between the units in spite of precautions taken to prevent them. Resistances up to about $10^9\Omega$ are covered by these methods.

Another method of resistance measurement applicable to small units with low working voltages is to compare the current passed by the resistor from a constant voltage source, with the current passed by a known resistor from the same voltage source. Various methods of detection are possible. A sub-standard microammeter enables comparisons up to $10^7\Omega$ with voltages of the order of 100V or less. Using a valve as a null detector with a known grid leak taken to a known variable bias voltage source (calibrated potentiometer), the resistance can be determined in terms of the voltage applied to the unknown resistance. Using a high input impedance triode, resistances up to $10^9\Omega$ can be measured, and using an electrometer triode or tetrode in a dessicator, the range is extended to about 10^{13} or possibly $10^{14}\Omega$, depending on the valve used. Electronic methods based on the discharge of a capacitor through the resistor are also used[1].

All the methods described in this section require the use of resistors which, with the exception of the lower value resistors in the bridge circuits, must be calibrated by one of the other methods which applied to high value resistors. The null method is useful in that it can extend the range of resistance measurement by up to a factor of 100 when one of the other methods is used to calibrate the reference resistor. None of these methods is amenable to statistical methods of error determination.

Conclusion

Some of the difficulties met in the accurate determination of high resistance have been mentioned, and as a comparison the same 100MΩ (nominal) resistor was measured by several different methods. The results are given in Table 1.

TABLE I

Resistances at 20°C

Nominal resistance	100MΩ
Measured by the ballistic galvanometer method	$99{\cdot}75 \pm 0{\cdot}1M\Omega$
Measured by the electrostatic voltmeter method	$110{\cdot}4$MΩ*
Measured by the inverted electrostatic voltmeter method	$100{\cdot}5 \pm 0{\cdot}2M\Omega$
Measured by the bridge method ..	$99{\cdot}6 \pm 0{\cdot}2$MΩ

* *Exhibits large error due to the oscillation and viscous damping of the electrostatic voltmeter.*

The value by the ballistic galvanometer method may be low due to the capacitor 'soaking' effect, while that by the bridge method will be slightly lower than the others as a result of the non-linearity of resistance with voltage exhibited to a small extent by this type of resistor.

Acknowledgments

The author would like to thank Professor F. C. Williams for facilities provided, and the Department of Scientific and Industrial Research for a maintenance grant over a period during which this work was carried out.

REFERENCE

1. France, G. High Value Resistors and Their Measurement. *Electronic Engng.* *29*, 24 (1957).

'VERA'

A New Equipment for Recording Television Signals on Magnetic Tape

THE Research Department of the BBC has designed and recently installed a magnetic tape equipment for the recording and reproducing of television and the accompanying sound signals.

This Vision Electronic Recording Apparatus (VERA) has been designed to record the vision and sound signals of television programmes for subsequent reproduction at any time after the recording has been made. A photograph of one machine is shown in Fig. 1. The channels which are to be put into service consist of two such machines which can be controlled from a central control desk. The machine employs half-inch magnetic tape and a reel (20½in diameter) such as those shown in Fig. 1 will accommodate 15min of programme. Continuous recording is possible by the use of two machines and the control desk. The tape speed employed in the present model is 200in/sec and the magnetic tape used may be a normal thin-base sound recording tape of good quality.

The machine employs a three-track system of recording, two of the tracks being devoted to the storing of the video signal and one to the storing of the sound signal. Separate recording and reproducing head-stacks are employed, each stack containing three identical heads separated from each other by copper screens and aligned to the accuracy required in the manufacturing process. Continuous monitoring of the recorded signal during the process of recording may be carried out.

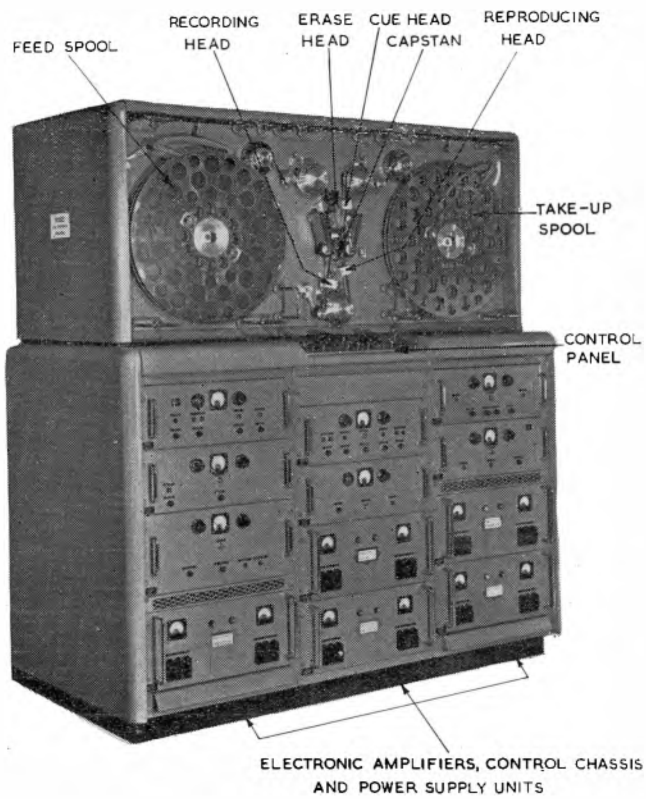

Fig. 1. A complete recording-reproducing machine

In the tape transport system embodied in the machine most of the power required to drive the tape is supplied by the spooling motors which are arranged to move the tape past the heads at a speed just below the chosen recording speed of 200in/sec and close to the constant tension required, even when the drive motor is not engaged. This result is obtained by varying the power fed to the spooling motors in accordance with (a) their torque/speed characteristic and (b) the amount of tape on the reels at any particular moment, the latter determining the speed of rotation required of the reels. When the drive is engaged the drive motor is, therefore, required to supply only a limited amount of power to bring the tape speed up to 200in/sec. The drive is engaged by lowering two rubber idlers on to a common capstan so that a loop of tape is formed, largely isolated from transient effects in the reels by these idlers and other mechanical filtering elements. Inside this loop lie the recording and reproducing head stacks. The erasing head is placed at a convenient point which lies outside the loop and precedes the recording head. A 'Velodyne' system of speed control and correction of the driving capstan is employed. During recording periods the servo driving motor is made synchronous with the mains frequency while on reproduction the output of the machine is frame-synchronized to station synchronization signals. The machine is fitted with the usual facilities for braking and for spooling the tape backwards or forwards at a variable speed when the drive system is not engaged.

A block schematic diagram showing the connexions of the principal electronic units embodied in the machine is shown in Fig. 2. For storing the video signal the two video tracks are associated, on the recording side, with a band-splitting system in which the video signal is divided into two frequency bands of approximately 0 to 100kc/s and 100kc/s to 3Mc/s. The 0 to 100kc/s video band is made to frequency-modulate a carrier and this frequency-modulated carrier is recorded on one track. The low-frequency content of the video signal is thereby transferred to a frequency band corresponding to shorter wavelengths so that both the low-frequency and the long-wavelength difficulties inherent in the conventional magnetic-recording system are avoided. In addition, the amplitude-limiting facilities normally associated with the reception of frequency-modulated signals may be incorporated in the reproducing chain to eliminate undesired amplitude fluctuations and overcome almost all 'drop-out' difficulties, even when employing thin-base sound recording tape not specifically manufactured for video or instrumentation purposes. The higher vision band, from

100kc/s upwards, is recorded simultaneously on the second video track in a conventional manner.

On reproduction the output from the frequency-modulated video track is limited, demodulated, and added to the output from the higher-frequency track to reform the composite television waveform. Before transmission to line the synchronization information, including line and frame synchronizing signals and suppression periods, is extracted, reconstituted and added back into the video signal.

It is, of course, obvious that the higher-frequency video band, which employs a conventional recording-reproducing system, will be subject to the same unwanted amplitude-modulation which is being eliminated by the frequency-modulation system of the lower frequency video band. It is, however, an important finding that in practice this does not appear of major importance, for as long as the synchronization signals and the main brightness structure of the picture, represented by the 0 to 100kc/s band of the video signal, are maintained intact, reasonable variations in the higher-frequency band do not noticeably degrade the subjective result.

All the low-frequency and long-wavelength difficulties which, in the case of the lower video frequency, are overcome by the use of the carrier system, will also be manifest in the sound channel if a conventional recording of the sound signal is attempted under the higher tape-speed conditions dictated by the video-signal requirements. The difficulties are, however, overcome by an identical technique to that employed to store the lower video frequencies. Accordingly the sound signal is, before recording, made to frequency-modulate another carrier which is recorded on the third track. On reproduction the carrier is limited and demodulated to provide a sound signal of high fidelity exactly synchronous in time with the video information reproduced from the other two tracks.

As in other forms of picture or sound recording, a requirement will arise in the use of magnetic vision recorders for the editing of programme previously recorded. Simple editing, in the form of replaying extracts from a previously recorded programme, may be achieved by starting the machine at any predetermined point in the recording. This facility is available because the machine is equipped with the usual facilities for spooling the tape backwards and forwards to find a desired point in the recording. The method may be extended, as in magnetic sound-recording practice, by cutting and joining extracts from various recordings or different parts of the same recording. Individual frames cannot, however, be examined in a 'gate', as in optical film editing, for the tape must be reproduced at the correct speed before a picture can be reproduced on a monitor. A cueing arrangement for the 'marking' of editing points has, therefore, been provided. The method adopted is to provide an extra cueing head, lying outside the isolated tape loop, which is fed through a separate recording amplifier from a 30kc/s oscillator. When the tape is being normally reproduced and the observer wishes to mark some particular point for subsequent cutting or starting he presses a 'cue' key on the control panel of the machine which causes a 30kc/s burst of signal to be recorded on the sound track of the tape. At this frequency it will not appear in subsequent normal reproduction since it lies well below the frequency-modulated carrier signals which carry the sound programme and any interference effects it might otherwise have will be removed by the limiting process which precedes detection of the television sound signal. However, when the tape is being slowly transported past the reproducing head, using the spooling speed control, at a fraction of the normal speed, the cue signal will produce an audible note in the loudspeaker or headphone system so that the point previously marked is found. The cutting and joining of tapes is accurately and quickly carried out by the use of a splicing device provided and the resultant joint provides no visible disturbance in the picture.

The equipment has been developed by a team under the leadership of R. E. Axon, O.B.E., Ph.D., A.M.I.E.E., based at the BBC's Research Departments at Nightingale Square, Balham, and Kingswood Warren, Surrey.

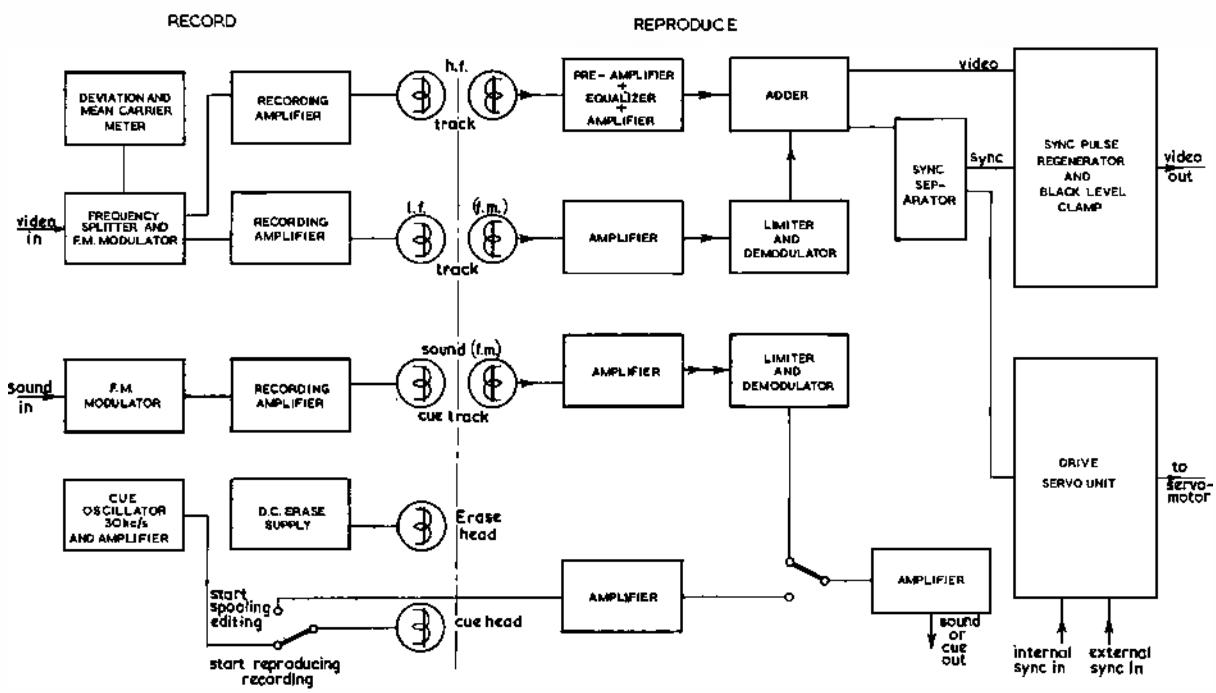

Fig. 2. Arrangement of principal electronic units

A Survey of
Delay Lines for Digital Pattern Storage

By S. Morleigh*, A.M.I.E.E., A.M.Brit.I.R.E.

Due to the increasing use of automatic digital computers for business and scientific purposes the importance of satisfactory devices for the delay or storage of digital information is becoming more pronounced.

In the present article an investigation is made of electromagnetic and ultrasonic delay lines as these may be used over a wide range of delay times. Wire type acoustic delay lines using magnetostrictive transducers, acoustic lines using (a) liquids and (b) solids as delay media, and also both the continuous and lumped-parameter types of electromagnetic delay line are examined.

THE basic requirements of any storage system (Fig. 1) for digit pulse trains are a delaying device, a detector, and a gate which can be used for recycling the detected output back through the delay medium or for allowing fresh data to reach the input.

The main limitation to the operation of the system is when the pulse shape arriving at the detector input has deteriorated so much due to the effects of attenuation and distortion caused by the delay medium that the information can no longer be extracted. The detector usually consists of a threshold device followed by an amplifier, to compensate for losses in the system, and a regenerating unit used to standardize and retime the delayed output pulses so that they may be recycled and stored for as long as required.

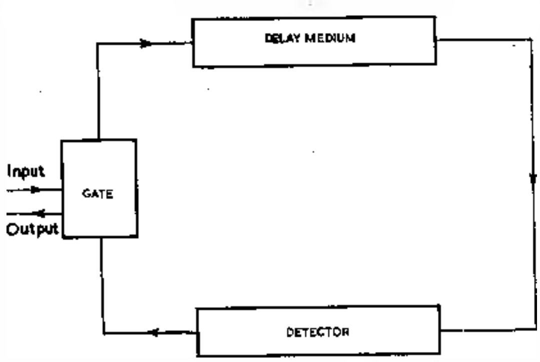

Fig. 1. Basic delay system

In most storage systems the time delay is obtained by passing energy in the form of pulses through a medium the path length of which is determined by the necessary storage time. The actual capacity of a given system is dependent upon the total delay time D and the time interval t between the leading edges of successive digit pulses. Thus if n is the total number of digits which can be stored, then $n = D/t$.

Digit patterns representing numbers or words are usually stored in binary form, 'ones' being indicated by positive pulses of a particular duration and spacing, while 'zeros' are indicated by the absence of pulses.

The type of delay device to be used in a particular case depends upon such factors as the required delay time, available space, simplicity of construction, and the cost per binary digit. From these considerations electromagnetic delay lines (electrical waves) are the most suitable for time delays of up to a few microseconds, while acoustic delay lines (using materials such as nickel wire, mercury or quartz as media for sonic waves) are suitable for delays of up to several milliseconds.

With an acoustic storage device (Fig. 2) it is necessary to convert the data to be stored, which enters the system in the form of electrical signals, into sonic pulses for transmission along the delay medium and then back into an electrical waveform after traversing the required path length. Both of these tasks can be accomplished by means of electromechanical transducers which will be subsequently described in the sections devoted to acoustic delay lines.

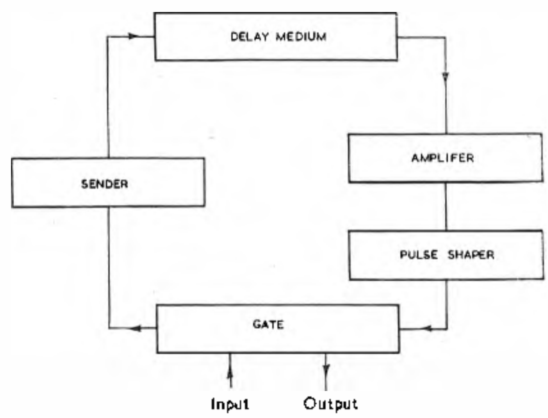

Fig. 2. Acoustic delay unit simplified schematic diagram

It will be appreciated that in a comprehensive survey of this nature insufficient space is available for rigorous mathematical treatment of the various subjects involved, but adequate references have been supplied.

Comparison of Delay Lines

Before examining each type of line in detail it may be of interest at this stage to compare the essential features of the different systems.

The main requirements of a delay system can be enumerated as follows:

(1) Information content must be recoverable when required.

(2) Delay time should be relatively independent of temperature.

(3) Physical dimensions should be reasonable and construction simple.

(4) Cost of the overall system must be low.

Liquid Delay Lines

Mercury is the most suitable of liquids as a delay medium. Due to its high mechanical impedance it can be readily matched with a quartz crystal to give a high value of

* *Formerly Powers-Samas Accounting Machines Ltd.*

power transfer. Bandwidths of several megacycles per second can be handled, so that pulses less than 0·5μsec in width may be transmitted. With liquid delay lines shear wave propagation is eliminated. Path length in mercury is approximately 4·8ft for 1msec delay. Attenuation due to the acoustic medium is about 13dB/msec at 10Mc/s. In addition to this, due mainly to the piezo-electric transducers, there is a loss of roughly 50dB between input and output voltages.

This system has been proved to be very reliable as some mercury delay lines have been in use for many years without requiring attention.

Disadvantages are:

(a) Difficult to handle. Inconveniently large and heavy.

(b) Shock mounting is essential.

(c) Design of suitable input and output systems is complicated, making alignment difficult.

(d) These lines are much more susceptible than solid lines to temperature variations, e.g. the temperature coefficient of velocity of mercury is about -340 parts in $10^6/°C$, while that for nickel is about 140 parts in $10^6/°C$.

(e) Mercury is costly.

Solid Delay Lines

This type of delay line has certain advantages, and other major disadvantages, over those in which mercury is employed as the delay medium.

The main advantages are:

(a) Lower relative temperature coefficient of linear expansion.

(b) Greater bandwidth obtainable.

(c) Attenuation of the sonic wave due to the acoustic medium for solids varies approximately proportionally to the frequency, while for liquids it varies in proportion to the frequency squared.

(d) Less susceptible to extraneous disturbances.

(e) A more compact type of line can be constructed.

Disadvantages are:

(a) Precautions must be taken against multiple mode propagation.

(b) Attenuation per unit delay is generally higher than that for other types of acoustic delay line.

(c) The velocity of acoustic waves in solid media is roughly three times that in mercury or water.

The most satisfactory results have been obtained when using magnesium alloys or fused quartz as the delay medium.

Wire Type Delay Lines

These lines are comparatively easy to construct, and they can be readily adjusted to give the desired delay. The materials used are cheap, as nickel wire and ribbon of sufficient purity are readily obtainable. They are very compact, can be easily made transportable, and can be made almost independent of variations in temperature. The delay can be made variable by suitable positioning of transducers.

Losses are mainly due to the electromechanical coupling. Insertion loss (output measured against input) due to the latter is usually of the order 55dB, although wire type delay lines can be constructed for considerably lower losses, while attenuation of the acoustic wave due to nickel is approximately 6dB/msec.

With these lines acoustic pulses may be propagated in either the longitudinal or torsional mode. Using nickel wire as the delay medium the path length is approximately 16ft for 1msec delay using longitudinal waves, 9·6ft for 1msec delay using torsional waves. From this it can be seen that the torsional mode offers considerable economy in length of line.

A disadvantage of the torsional mode of propagation is the difficulty in designing suitable transducers.

A disadvantage of wire type delay lines for pulse inputs is that the bandwidth handled cannot be much greater than 1Mc/s.

Electromagnetic Delay Lines

These lines are relatively simple to design and construct for comparatively small time delays. They may be used for a variety of purposes with digital computers, radar systems and many other types of electronic equipment.

Both types of electromagnetic delay line are considerably bulkier than the equivalent acoustic lines for a given delay time. The continuous-parameter type is the more expensive as it requires specially designed cables, while the simplest forms of lumped-parameter lines can be constructed from standard radio components.

From considerations of design and bandwidth the continuous-parameter lines tend to become the less efficient of the two for storage of more than a few pulses. Losses due to input and output coupling are much lower than those for equivalent acoustic lines.

The main factor limiting storage capacity appears to be dissipation in the inductive elements.

Disadvantages are:

(1) Large volume per unit delay.

(2) Limited storage capacity.

(3) Appreciable attenuation and dispersion of signal.

Acoustic Delay Lines: The Ratio of Wavelength to Path Cross-Section, and its Effect on Bandwidth

There are three modes of propagation for acoustic waves: longitudinal, torsional and shear. The choice of mode for a particular delay line is governed by such factors as the nature of the delay medium, the path length required, the effective acoustic wavelength of the pulses to be transmitted, and the dispersion which can be tolerated.

Electromechanical transducers for use with longitudinal waves are easy to produce, and this mode can be used provided that the cross-section of the path is either much larger or much smaller than the wavelengths to be propagated. At path widths comparable to the wavelengths the acoustic wave suffers considerable intermode distortion due to the Poisson coupling of longitudinal and transverse strains. Thus delay lines using the longitudinal mode of propagation can be subdivided into wide and narrow types. Torsional waves are relatively difficult to propagate, and this restricts their use to the narrow class of delay line, although they have, however, the advantage of zero dispersion due to intermode coupling. On the other hand, shear waves are restricted to the wide class of delay line in order to keep distortion to a minimum.

Acoustic lines of the wide class can be designed to handle bandwidths of several megacycles per second. This class includes lines using mercury, quartz, glass, invar, magnesium alloys, or various types of steel as delay media, with piezo-electric crystals as transducers. These crystals can be cut very thin so as to allow transmission of very short waves, the smallest wavelength passed being dependent upon the length of the transducer. Wire type delay lines, which use pure nickel, nickel iron alloys, R31 steel, or even ferrite tube as delay media, are essentially of the narrow class. Due to the transducer length, the upper bandwidth of these lines is in the region of 1Mc/s, but, however, when longitudinal propagation is required they have the advantage of being able to use magnetostrictive transducers which are easy to design. With torsional waves the problem of suitable transducer design becomes more difficult and various alternatives have been tried. These will be described in a later section.

Liquid Delay Lines

Among the most important considerations associated with ultrasonic delay lines are those affecting the choice of transmission medium and the type of electromechanical transducer. Properties of the delay medium to be initially examined are:

(1) The sonic wave should have a low transmission velocity along the acoustic path.

(2) Attenuation of the wave due to the medium should be small.

(3) Delay time should be relatively independent of temperature.

Delay media which have been used in experimental lines include gases, liquids and solids. Air is probably the most natural acoustic medium as the velocity of sound through (dry) air at 20°C is approximately $3{\cdot}31 \times 10^4$cm/sec at standard pressure. The transmission of ultrasonic pulses through the atmosphere has been carried out for many purposes including sound ranging and altitude determination. The frequency band used for these purposes has been of the order 10 to 30kc/s, while the ultrasonic energy has been produced by compressed air whistles. Unfortunately, air, in common with other gases, has many disadvantages when used as a medium for pulse propagation. Bandwidth is considerably restricted, the acoustic path has a high attenuation factor and the variation of delay time with temperature is appreciable. For wide-band systems it is essential to use either liquid or solid delay media.

The transmission of ultrasonic pulses through water has been carried out for depth determination, submarine signalling and location of shoals of fish. In liquid delay lines the acoustic waves are kept to a fixed path by containing the fluid within a pipe. The piezo-electric crystal is the most suitable form of transducer at high frequencies, and X-cut quartz crystals are extensively used for propagation of longitudinal waves. The losses due to the crystal are lowest at its resonant frequency, and because of this it is usual to use the electrical signals to modulate a high frequency carrier at this frequency. For efficient transfer of energy between electrical and sonic forms the effective mechanical impedance of the delay medium should be closely matched to that of the transducer. Also any material in close contact with a quartz crystal increases the damping, thus effectively increasing bandwidth, this effect being greatest for materials of high mechanical impedance. The equivalent circuit of a quartz crystal is shown in Fig. 3.

Mason[2] has illustrated that with water as the acoustic medium the bandwidth of the sonic waves is roughly 10 per cent of the mid-frequency. The mechanical impedance of mercury ($19{\cdot}8$kΩ/cm^2) is much higher than that of water, so that wider bandwidths can be obtained, and it can be easily matched with quartz (15kΩ/cm^2), the reflection coefficient being about 12 per cent. The velocity of sound in mercury is about $1{\cdot}45 \times 10^5$cm/sec at 25°C (similar to that of water) and the temperature coefficient of velocity is about -340 parts in 10^6/°C, very much lower than that of most liquids. Another factor emphasizing the advantages of mercury over other liquids as a transmission medium is its low attenuation of sound waves. Due to these considerations mercury delay lines have been widely used, but nevertheless for applications requiring only narrow bandwidths water is sometimes employed as a delay medium. In this case, however, some means of temperature compensation is usually necessary even for comparatively short lines. This problem can be solved by using a mixture of water and ethylene glycol, as these have temperature coefficients of opposite sign, and with particular proportions of these fluids[5] a very low coefficient may be obtained.

CONSIDERATIONS AFFECTING DESIGN OF MERCURY DELAY LINES

An important characteristic of the transducer is the relationship of the resonant frequency to the physical dimensions of the crystal. An X-cut quartz crystal vibrates

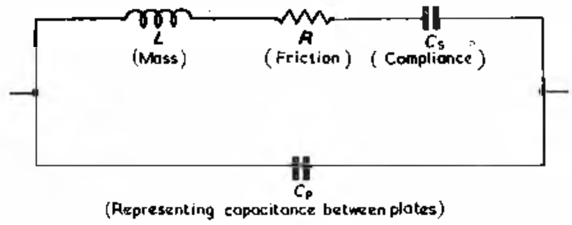

Fig. 3. Equivalent circuit of a quartz crystal

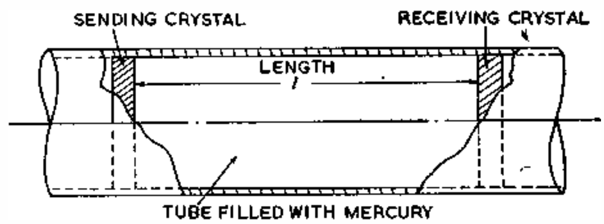

Fig. 4. Mercury delay line

longitudinally in its thickness dimension at the fundamental frequency, and it can be shown that

$$f_r \simeq (2{\cdot}86/d) \text{ Mc/s}$$

where f_r = resonant frequency

and d = thickness in mm

An additional factor causing attenuation of the ultrasonic wave in mercury delay lines is the bad mechanical contact between the mercury and the inner wall of the containing tube (usually steel). Attenuation due to this source increases with reduction of tube diameter. A detailed examination[6] of the mercury line shows that there is a close analogy between the distortion introduced to an acoustic signal in its passage through the transmission medium and that caused by a bandpass filter (see Fig. 4).

In the design of a particular line, the path length, the desired bandwidth and the choice of carrier frequency play an important part. Bandwidth is clearly dependent upon the fundamental frequency, so that for satisfactory results this should be at least 10Mc/s. Attenuation of the sonic wave due to mercury increases, however, as the square of the frequency, and this tends to impose an upper limit on the carrier frequency.

When the sonic pulse arrives at the receiving transducer, part of it is reflected back along the line causing corresponding distortion. In long delay lines these subsidiary echoes are not significant as they are considerably reduced by attenuation along the delay path. The quartz/mercury reflection coefficient is small, so that the amount of energy reflected is mainly dependent on the degree of matching between the crystal and its backing material; hence with short lines it is necessary to absorb most of this energy in the backing. Materials used for backing include mercury and lead, although the use of an end cell in this manner reduces the signal level[5].

Close alignment between the transmitting and receiving crystals is important in order to avoid beam spread. Provided that the crystal is several wavelengths in diameter, and nearly equal to the inner diameter of the containing tube, then the acoustic wave should start out as a highly directive beam.

For a delay time of 1msec the path length is approximately 5ft, so for long delays it is usual to use folded lines in order to reduce bulk. In these lines the delay path is folded once by a reflector block which presents two 45° reflecting surfaces to the path of the beam. Although the temperature coefficient of velocity of mercury is relatively low it becomes necessary when dealing with long delay lines to maintain the temperatures of the lines to close limits. Design considerations of various commercial delay lines are described in detail in the references[4,5,7].

Solid Delay Lines

Solid delay lines, except those of the wire-type, are of the wide class so that many of the factors affecting design and performance of liquid delay lines are still applicable. The efficiency of energy transfer is mainly dependent upon the closeness of matching of the acoustic impedance of the piezo-electric transducer with that of the delay medium, and the nature of the bonding between the two materials, Other points of major importance are the insertion loss, overall bandwidth and the degree of eradication of secondary pulses.

A wide range of materials has been experimented with for use as delay media, and these include fused quartz, fused silica, barium titanate, rochelle salt, glass, nickel, invar, magnesium alloys and steel. Bandwidth is highest with steel, and lowest with barium titanate, quartz or magnesium. Attenuation of the acoustic pulse per unit length varies with the particular delay medium, it is low for fused quartz and magnesium alloys[12], it is higher for glass and is very high for annealed nickel. Attenuation losses are generally high for coarse grained materials, but there does not appear to be any fixed relationship between these losses and grain size.

X-cut quartz crystals and also barium titanate ceramics can be used as transducers for longitudinal waves. Insertion loss is lowest with barium titanate transducers, but it is possible to obtain a good acoustic match by bonding an X-cut quartz crystal to a fused quartz delay line.

Y-cut quartz crystals, which are relatively more expensive, are required for shear wave propagation, and bandwidth is lower. It is difficult to design suitable transducers for this mode of propagation from barium titanate.

DELAY TIME

The velocity of propagation of sonic waves in any medium is dependent upon the inherent qualities of the substance used. The actual delay time is given by:

$$t = l/V$$

where t = delay time

l = effective length of line

V = velocity of propagation.

Now let

V_L = velocity of propagation of longitudinal waves.

V_s = velocity of propagation of shear waves.

E = Young's modulus.

C = shear modulus of rigidity.

K = bulk modulus.

ρ = density, g/cm³.

The relationship between the velocities of longitudinal and shear waves is then given by the following formulae:

$$V_L = (E/\rho)^{\frac{1}{2}} = \left(\frac{K+2C}{\rho}\right)^{\frac{1}{2}}$$

$$V_s = (C/\rho)^{\frac{1}{2}}$$

From which $t_s = (l/V_s) = l(\rho/C)^{\frac{1}{2}}$ for shear waves

and $t_L = (l/V_L) = l\left(\frac{\rho}{K+2C}\right)^{\frac{1}{2}}$ for longitudinal waves

and $V_s/V_L = (C/E)^{\frac{1}{2}} = \left(\frac{C}{K+2C}\right)^{\frac{1}{2}}$

so that a shorter path length is required for a given delay using shear waves.

ADVANTAGES OF THE SHEAR MODE OF PROPAGATION

Despite the difficulty inherent in transducer design shear wave propagation is preferable to the longitudinal mode for the following reasons:

(a) The relative velocity ratio of shear to longitudinal waves is approximately 1 : 1·6

The following figures have been quoted for fused silica of specific gravity 2·20.

Velocity of plain shear waves = 3·76 × 10⁵cm/sec.

Velocity of plain longitudinal waves = 5·96 × 10⁵cm/sec.

(b) Reflection of the incident wave from an interface can cause the effective mode of propagation to change from longitudinal to shear, this reflected pulse being delayed relative to the main pulse, with resultant distortion. Shear waves, however, are reflected from interfaces without effective change of mode provided that due care is paid to the geometry of the system and the shear wave is polarized perpendicular to the plane of incidence[11].

PARTICULAR TYPES OF SOLID DELAY LINE

The velocity of acoustic waves in solid media is about three times that in mercury, so that a 'straight-through' solid delay line would be cumbersome for delays greater than a few hundred microseconds. For example with the fused silica line previously mentioned, for a delay time of 100μsec the path length is 60cm using longitudinal waves and 37·5cm using shear waves.

Longer delays may be obtained by the use of multiple reflections in a solid quartz block (Fig. 5). The cross-beam type of fused quartz delay line was described by Arenberg at the 1954 I.R.E. convention[9,11]. He used a 17in diameter polygon stub in which the sonic wave was reflected between interfaces 31 times without interference. Delays of up to 3 or 4msec have been obtained by this method. The chief disadvantages of this system are that great care has to be taken in geometrical design to avoid multiple mode propagation, and in the machining of the block. It is difficult to design suitable transducers, and the overall system requiring a large fused quartz or vitreous silica block with a high degree of homogeneity is very costly.

Magnesium alloys, used as delay media, have given reasonably good results with shear waves. Unfortunately, the variation of delay time with temperature for these alloys cannot be neglected, and this factor severely limits their use. The difficulties entailed in bonding Y-cut quartz crystals to solid media are also quite pronounced.

The three main causes of attenuation of sonic waves within metal delay lines appear to be:

(a) The elastic hysteresis loss

(b) A scattering effect due to finite grain size, similar to the Rayleigh sound scattering effect

(c) The sound diffusion process.

These effects have been investigated by Mason and McSkimin[12] who have measured attenuation and velocity of both longitudinal and shear wave pulses in aluminium and glass rods over a wide frequency range. Their results indicate that glass and fused quartz are affected only by the hysteresis losses, while for aluminium the calculated scattering losses agree quite well with the measured values.

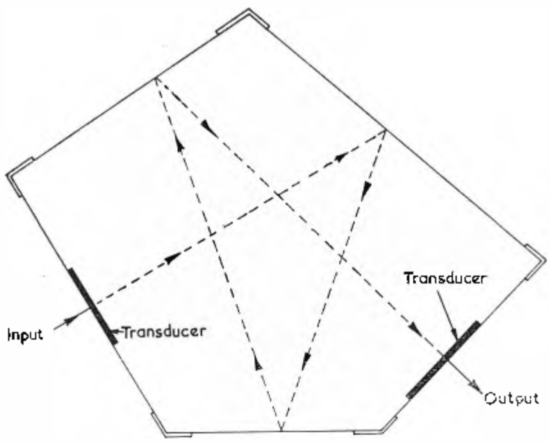

Fig. 5. Reflection from interfaces in solid lines

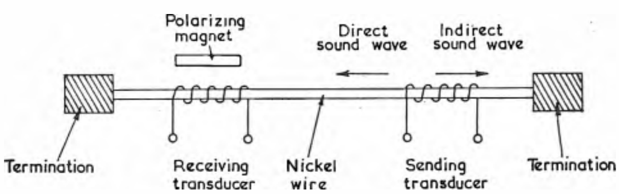

Fig. 6. Magneto-strictive delay line showing sending and receiving transducers and echo absorbing terminations at each end of the line

The applicability of various metals and alloys for thermally stable delay lines has been studied by Mebs, Darr and Grimsby[13] who have also investigated different types of pressure holders and adhesives for use in crystal transducer attachments. They have taken measurements of temperature variation of signal attenuation, distortion and delay time on a number of delay lines. Their results show that of the various metals and alloys tested, including nickel, magnesium alloys, invar and steel, two isoelastic nickel-chrome alloys possessed the smallest variation of delay time with temperature over the range $-50°C$ to $+200°C$.

Wire-Type Acoustic Delay Lines

These delay lines are of the narrow class, and usually employ magnetostrictive transducers for conversion of energy between electrical and sonic forms. The magnetostrictive effect may be described as the change in dimensions of a material brought about by the application of a magnetic field, and the reverse (or Villari) effect is a change in permeability of the material due to stress.

The transmitting and receiving transducers are coils through which the sonic conductor, consisting of a length of some magnetostrictive material, is threaded. The receiving transducer is subjected to a biasing field, and to reduce echoes the line is terminated by some form of damping pad at each end (see Fig. 6). The application of a current pulse to the transmitting transducer causes a magnetic flux to be created in its magnetostrictive core, producing a dimensional change in this section of the line. The result of this electromechanical action is to launch a stress wave along the line at the velocity of sound in the material used. Due to the Villari effect this stress wave in its passage through the receiving transducer produces a flux change so that a voltage is induced in the coil.

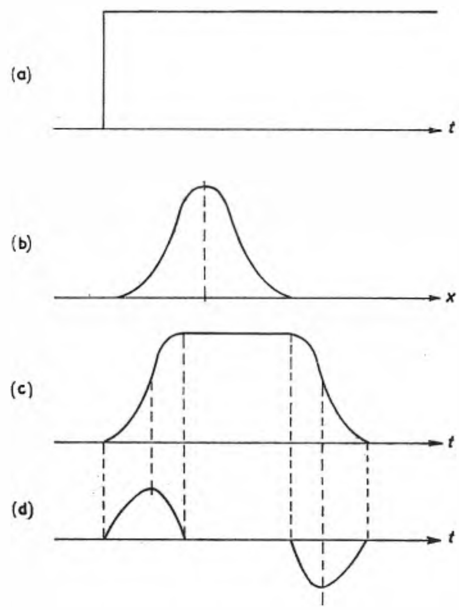

Fig. 7. Magneto-strictive delay line waveforms
(a) Input current pulse
(b) Propagated stress wave along delay medium
(c) Flux variation in core of output coil
(d) Output voltage

Terminations and Sonic Conductor Supports

Damping pads used to prevent reflection from the ends of the sonic conductor are usually of rubber or of some plastic material with similar absorbing properties.

The material to be used for wire supports must be carefully chosen in order to reduce to a minimum any effects of dispersion and attenuation of the sonic waves. Synthetic sponge[16] and expanded polythene tube[17] have been found to provide adequate support with negligible acoustic effect.

Pulse Response

From the simplified description of the magnetostrictive delay line it can be seen that the stress variations in the core material of the receiving transducer caused by the sonic pulse determine the voltage induced in the output coil. Hence the output voltage is proportional to the derivative of the sonic pulse. Similarly, the acoustic pulse produced by the input transducer is related to the differential of the applied signal. The output voltage is thus proportional to the second derivative of the input signal. The waveforms are illustrated in Fig. 7.

Investigation of the properties of the magnetostrictive line[15] has shown that for a particular acoustic medium the output waveform is dependent primarily upon the following factors: the effective length of the transducers, the number of turns on the coils, the time taken for the flux to penetrate the line material, and the strength of the applied magnetic fields.

By considering the resonant frequency of the core element[15] it can be seen that increase in axial length of the coil improves the low frequency response at the expense of the higher frequencies. The losses in the delay line are mainly due to the electromechanical coupling. For this to be increased it is essential to reduce stray magnetic fields to a minimum, and the transducer coils should be wound as closely as possible to the core element. The upper limit to the value of inductance, and hence to the number of turns on the coils, is determined by the frequency band to be transmitted. Bandwidth may be improved by introducing Ferroxcube cheeks at the ends of the coils[16].

The finite time taken for flux saturation has an adverse effect upon the resolution of the system[17]. This time can be minimized by using the delay medium in the form of fine wire, ribbons or tubing[18].

A magnetic bias field is necessary in order to operate the output transducer. The polarity and amplitude of the output pulse is dependent upon the direction and magnitude of this field.

Variability of Delay Time with Temperature

The delay time is dependent upon the path length of the sonic pulse and on its velocity. The effect of temperature changes upon a line using longitudinal waves is mainly determined by the variation of Young's Modulus for the material over the temperature range considered.

An expression for the delay time for a wire of length l has been already derived, and is given by:

$$t = l/V_L = \frac{l}{(E/\rho)^{\frac{1}{2}}} \text{ for longitudinal waves}$$

and it can be shown[16] that the variation of delay time with temperature is given by:

$$dt/t = -\tfrac{1}{2}\,((dl/l) + (dE/E))$$

where the thermoelastic coefficient is considerably larger than the coefficient of linear expansion.

The most suitable transducer core material on account of its high values both of magnetostriction and change of permeability with stress, is nickel and this has a temperature coefficient of velocity of about 140 parts in $10^6/{}^\circ$C. This is relatively small and can be easily compensated for in short delay lines. For long time delays it is usual to attach the magnetostrictive transducers to a sonic conductor of a different material chosen for its low temperature coefficient and low attenuation of sonic waves. Various media which have been used for this purpose include piano wire, R 31 steel, Nispan-C, and various nickel-iron alloys some of which can be constructed for almost negligible temperature coefficients. Details of a number of these materials are given in the references[8,16].

Modes of Propagation

Although the sonic pulses in the actual core of the magnetostrictive transducer must clearly be in the longitudinal mode, it is not essential to use this mode of propagation along the sonic conductor when this is of a different material. The torsional mode is preferable for long delays as it requires a shorter length of wire for a given delay. In addition to this, it is not subject to the effects of distortion caused by finite diameter of the wire, and less subject to distortion due to curvature of the wire and to parasitic transverse motion.

A comparison of the relative velocities of waves propagated by these modes[16] (similar to that previously derived for longitudinal and shear waves) shows that the ratio

$$V_T/V_L \text{ is approximately } 0{\cdot}6$$

where V_T = velocity of propagation of torsional waves

and V_L = velocity of propagation of longitudinal waves,

so that the path length required for a given delay time is shorter if torsional propagation is used.

With torsional delay lines it is difficult to design suitable transducers, and various types are in use, including:

(1) Piezo-electric, using split tube barium titanate

(2) Magnetostrictive, requiring two longitudinal transducers.

Torsional lines have been designed for delays of up to 6 to 7msec, and these may be coiled into compact units. With wire-type lines the delay time may easily be made variable by suitable positioning of transducers. A further interesting development may be the use of ferrite tube as the delay medium.

Special applications of these lines[15] include their use for static storage, as frequency dividers, and as serial word generators.

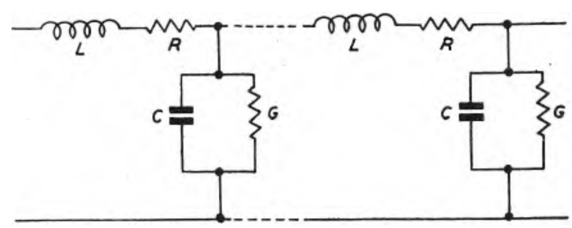

Fig. 8. Equivalent circuit of transmission line showing line constants

Electromagnetic Delay Lines

Unlike ultrasonic delay lines the electromagnetic type do not require any form of energy conversion as they utilize the delay incurred by the passage of the electromagnetic wave itself through specially designed transmission lines.

An transmission line has four primary constants (see Fig. 8):

L = distributed series inductance/unit length (in henries)

C = distributed shunt capacitance/unit length (in microfarads)

R = distributed series resistance/unit length (in ohms)

G = distributed shunt conductance/unit length (in mhos)

and the voltage and current distributions are given by the following equations:

(where x = path length, and t = time in seconds)

$$\partial^2 v/\partial x^2 = LC\,\partial^2 v/\partial t^2 + (CR + LG)\,\partial v/\partial t + RGv \quad \ldots (1)$$

$$\partial^2 i/\partial x^2 = LC\,\partial^2 i/\partial t^2 + (CR + LG)\,\partial i/\partial t + RGi \quad \ldots (2)$$

The solution of equations (1) and (2) can be shown to be

$$V = A \cosh Px + B \sinh Px \qquad (1)$$

$$\text{and } i = -B/Z_0 \cosh Px - A/Z_0 \sinh Px \qquad (2)$$

where Z_0, the characteristic impedance of the line, is given by the formula:

$$Z_0 = \sqrt{\left[\frac{R + j\omega L}{G + j\omega C}\right]} \quad \ldots\ldots\ldots\ldots\ldots (3)$$

and P, the propagation constant per unit length, is given by:

$$P = \alpha + j\beta$$

where α the attenuation constant, and β the phase constant, of the line are given by the following expressions:

$$\alpha = \sqrt{[\tfrac{1}{2}(R^2 + \omega^2 L^2)^{\frac{1}{2}}(G^2 + \omega^2 C^2)^{\frac{1}{2}} + \tfrac{1}{2}(RG - \omega^2 LC)]} \quad (4)$$

$$\beta = \sqrt{[\tfrac{1}{2}(R^2 + \omega^2 L^2)^{\frac{1}{2}}(G^2 + \omega^2 C^2)^{\frac{1}{2}} - \tfrac{1}{2}(RG - \omega^2 LC)]} \quad (5)$$

It can be shown that the condition for α to be a minimum is:

$$LG = RC$$

and in this case $\alpha = (RG)^{\frac{1}{2}}$

Two effects must now be considered

(1) In the case of a natural transmission line, e.g. a coaxial cable, the insulation resistance is very high, i.e. the leakage G is low.

Hence $RC > LG$

so that $\alpha \neq (RG)^{\frac{1}{2}}$

and will be dependent on frequency as shown in equation (4).

(2) The effects of increasing frequency is generally to increase R, due to skin effect, and to increase G, due to dielectric losses. Thus the expression: $\alpha = (RG)^{\frac{1}{2}}$ will increase with frequency.

From these considerations it can be seen that α will not be independent of frequency, and in general the bandwidth of such a line will be seriously limited by amplitude distortion. In addition, since the phase constant, β, is frequency dependent, phase distortion will be introduced as indicated by equation (5).

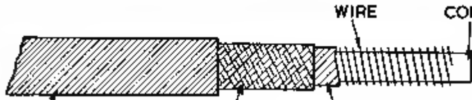

Fig. 9. Helically-wound delay cable

At high frequencies R is negligible compared with ωL, hence, as G is usually considerably smaller than ωC, the characteristic impedance is substantially a pure resistance, and is given by:

$$Z_0 = (L/C)^{\frac{1}{2}}\Omega$$

The velocity of propagation at high frequencies can also be expressed in terms of L and C, the time taken for a wave to travel along a cable being

$$T = (LC)^{\frac{1}{2}} \text{ sec/unit length.}$$

Distributed-Parameter Delay Lines

The simplest form of delay line is a coaxial cable. The inductance of a length l cm of coaxial cable is given by:

$$L = \frac{(\mu l)\, 2\ln r_2/r_1}{10^9} \text{ H}$$

where μ is the permeability of the medium

r_2 = inner radius of outer conductor

r_1 = outer radius of inner conductor

The capacitance is:

$$C = \frac{Kl}{2\ln r_2/r_1 \times 9 \times 10^{11}} \text{ F}$$

where K is the dielectric constant of the medium. Hence the time delay T per unit length of the cable is

$$T = (LC)^{\frac{1}{2}} = \frac{K^{\frac{1}{2}}}{3 \times 10^{10}} \text{ sec}$$

since for insulators μ may generally be taken as unity.

A special type of cable is the helically wound delay line (Fig. 9). These delay cables have very high inductance, obtained by winding the inner conductor of a coaxial line in the form of a cylindrical spiral. Capacitance may be increased by close spacing of the conductors. Commercial cables are available with delays of up to about 8μsec/100ft.

From factors already considered the use of this type of delay line is restricted due to the effects of attenuation and distortion on the applied signal. Also an inconveniently long length of cable is needed for comparatively short delay lines.

Lumped-Parameter Delay Lines

A four terminal network composed of inductive, capacitive and resistive elements can be considered to have properties equivalent to a transmission line. For simplicity of design it is easier to lump the shunt capacitances together rather than distribute them along the line. Also, attenuation of signal strength in delay cables is largely due to dielectric losses, so that this may be considerably reduced in these artificial transmission lines if care is taken in choosing capacitors.

Delay lines of this type are relatively easy to construct as, in the simplest cases, standard radio components may be used. The design is based upon that of low-pass filters, and it can be shown[7] that the time delay at a frequency ω for a network consisting entirely of series inductances and shunt capacitors is given by:

$$T = \frac{2}{1 - (\omega/\omega_c)^2}$$

where ω_c is the cut-off frequency. The delay clearly varies appreciably with frequency, except for $\omega \ll \omega_c$.

An investigation[7] of the delay characteristics of low-pass filters has shown that an improvement can be brought about by the use of m-derived sections. The time delay in this case becomes:

$$T = \frac{2m}{\sqrt{[1 - (\omega/\omega_c)^2]\,[1 - (1 - m^2)(\omega/\omega_c)^2]}}$$

and with $m = 1{\cdot}27$ the flattest possible delay characteristic up to about $0{\cdot}55\ \omega_c$ may be obtained.

Care has to be taken in the construction of delay networks of this type to ensure that the effect of coupling between sections is reduced to a minimum.

Practical Limitations of Electromagnetic Delay Lines

The effective delay time attainable by increasing the number of sections of an artificial transmission line of this type is limited only by the losses in the capacitive and inductive elements. A theoretical analysis[19] of the effect of losses on the rise-time of pulses emphasizes the difficulty of designing satisfactory electromagnetic lines with delay greater than about 15 digit periods, due mainly to the dissipation in the inductive elements. The use of low permeability high-Q nickel-zinc ferrites around straight single conductors for the inductive elements has enabled the storage capacity to be increased to about 32 pulses. This method also reduces the insertion loss and the volume of each section.

Lattice-type delay networks have been investigated[20], and the design of electromagnetic delay systems of this type has been based upon the Fourier transform of the required pulse response. A network of this type has been designed to store 40 digits, giving a total delay of 80μsec. This appears, however, to be near the ultimate limit obtainable by this method and a network of this nature must require great care in design and assembly if instability is to be avoided.

Conclusions

A parallel can be drawn between delay lines of all types and band-pass filters from considerations of attenuation bandwidth and insertion loss. It is difficult, however, to assign an actual 'figure of merit' to the various types of delay line for direct comparison, as added to the main considerations of capacity and cost must be such factors as reliability, bulk, complexity and temperature dependence.

(1) Electromagnetic lines are probably the most suitable for delays of up to a few microseconds, but beyond this they compare unfavourably with the acoustic delay lines.

(2) Mercury lines have been used for many computer applications and have been proved reliable, but they suffer from many disadvantages in comparison with magnetostrictive lines, mainly due to weight, size, complexity and temperature instability.

(3) Wire-type delay lines employing magnetostrictive transducers are simple to construct, cheap, robust, and may be designed to have a very small temperature variation. Bandwidth obtainable with these lines is restricted.

(4) Other forms of solid delay line tend to be very complex, although this field is still being investigated.

(5) For delays greater than a few microseconds it is felt that the wire-type acoustic delay lines, as described, have considerable advantages over other forms of delay line for use in digital computers, and it would appear most satisfactory and economical to use the longitudinal mode of propagation for shorter delays, and the torsional mode for delays of from say 0·5msec up to what appears to be the present limitation, due to temperature, of about 6 to 7msec.

Acknowledgments

The author's thanks are due to Powers-Samas Accounting Machines Ltd for permission to publish this article, and to his colleagues A. Foster, C. K. Burchell and N. Burgess for their interest and encouragement and to P. Lonsdale for his assistance in the preparation of the article.

BIBLIOGRAPHY

1. Fagan, M. D. Bibliography of Ultrasonic Delay Lines. *Bell Syst. Monogr.* No. 2317.
2. Mason, W. P. Electromechanical Transducers and Wave Filters. (D. Van Nostrand Co. Inc., New York).
3. Kolsky, H. Stress Waves in Solids. (Oxford University Press, 1953).
4. Newman, E. A., Claydon, D. O., Wright, M. A. The Mercury Delay-Line Storage Unit of the Ace Pilot Model Electronic Computer. *Proc. Instn. Elect. Engrs. 100*, Pt. 2, 445 (1953).
5. Ryan, R. D. A Mercury Delay-Line Storage Unit. *J. Brit. Instn. Radio Engrs. 15*, 419 (1955).
6. McSkimin, H. J. Theoretical Analysis of the Mercury Delay Line. *J. Acoust. Soc. Amer. 20*, 418 (1948).
7. Blackburn, J. F. Components Handbook M.I.T. Radiation Series. 17, Ch. 6 and 7, 191.
8. Chance, B. Waveforms. M.I.T. Radiation Laboratory Series. 19, 756.
9. Arenberg, D. L. Ultrasonic Delay Lines. I.R.E. Convention Record of 1954. Pt. 6. p. 63.
10. McSkimin, H. J. Propagation of Longitudinal Waves and Shear Waves in Cylindrical Rods at High Frequencies. *J. Acoust. Soc. Amer. 28*, 484 (1956).
11. May, J. E., Jr. Low Loss 1 000 Microsecond Ultrasonic Delay Lines. I.R.E. Trans. on Ultrasonic Engng. PGUE 4, 3 (Aug. 1956).
12. Mason, W. P., McSkimin, H. J. Attenuation and Scattering of H.F. Sound Waves in Metals and Glasses. *J. Acoust. Soc. Amer. 19*, 464 (1947).
13. Mebs, R. W., Darr, J. H., Grimsley, J. D. Metal Ultrasonic Delay Lines. *J. Res. Nat. Bur. Stand. Wash. 51*, 209 (1953).
14. Bradburd, E. M. Magnetostrictive Delay Lines. *Elect. Commun. 28*, 46 (March, 1951).
15. Robbins, R. C., Millership, R. Applications of Magnetostrictive Delay Lines. Automatic Digital Computation. Proc. of a Symposium held at the N.P.L. (1953).
16. Scarrott, G. G., Naylor, R. Wire-type acoustic delay lines for digital storage. *Proc. Instn. Elect. Engrs. 103B*, 497 (1956).
17. Fairclough, J. W. A Sonic Delay-line Storage Unit for a Digital Computer. *Proc. Instn. Elect. Engrs. 103B*, 491 (1956).
18. Thompson, T. B., Lyon, J. A. M. Analysis and Application of Magnetostriction Delay Lines. I.R.E. Trans. on Ultrasonic Engng. PGUE 4, 8 (Aug. 1956).
19. Anderson, J. R. Electrical Delay-Lines for Digital Computer Applications. Trans. Inst. Radio Engrs. Prof. Group on Electronic Comput. EC.2. 5 (June, 1953).
20. Scarrott, G. G., Harwood, W. J., Johnson, K. C. Electromagnetic Delay Networks for Digital Pattern Storage. *Proc. Instn. Elect. Engrs. 103B*, 476 (1956).

A Transfer Process for Printed Circuits

A method of manufacturing printed wiring boards by a transfer process has been developed by the Philips Laboratories in Holland. The method employed is briefly as follows.

The first step is to coat a metal carrier with a thin, non-adhesive layer of copper. By means of silk-screening this film of copper is entirely covered with paint, except for the pattern for the wiring ultimately required. By a galvano-plastic method the wiring-pattern thus formed is then thickened with copper, and as a result the actual wiring is obtained. Next a coating of glue is applied, to fix the boards to the impregnated paper. Afterwards the boards are compressed together with the impregnated paper. The final operations are removal of the metal carrier and—by means of a chemical process—the film of copper on the board, which was originally applied to the carrier.

Several considerations led to the development of the transfer process. In the first place the copper-clad laminate necessary for the etching-process, was difficult to obtain a few years ago, and in addition, it was fairly expensive. An important advantage of the transfer process, moreover, is the fact that where this system is employed hardly any copper in excess of that required for the wiring is used. Another consideration was that adoption of the transfer process eliminates dependence on suppliers of copper foil.

A detailed description of the process is as follows:—

The metal carrier constitutes the starting-point of the manufacturing-process. The metal to be used for the carrier can be chosen almost at will. Good results are obtained with stainless steel, for example, with nickel-plated iron and with pure nickel. It is important that the plates be non-rusting and that, after fulfilling their task as carriers, they be easy to clean so that they can be used again. The dimensions are determined solely on the basis of practical considerations. As large a size as possible was aimed at, since this offers the greatest appeal from the aspect of business economics, but at the same time the sheets had to be easy to handle. The choice fell on the size 650 × 450mm, which, dependent on the design, is large enough for 8 to 15 wiring-diagrams. Four such sheets can be laid side by side under the press. Both sides of the carrier are used.

The first operation following careful cleaning is application of an extremely thin layer of copper, which must be fairly easy to remove from the carrier at a later stage. This film of copper, which is 1/10 000in thick, is applied by a plating-process after the carrier has been dipped in a bichromate solution. The bichromate treatment ensures that later the film of copper can be separated from the carrier without causing any damage.

The next phase is silk-screening of those parts of the copper film to which no wiring is to be applied later on. That is why in this case, as opposed to that of the etching-process, the protective paint is applied to the negative of the desired wiring-pattern on the copper-plated carrier. It is important for the sheet to be kept as flat as possible during this operation; one of the methods employed to ensure that this requirement is met is the use of a vacuum under the sheet. To ensure accuracy of the pattern the screen must be kept as close to the sheet as possible.

The paint employed is a modified phenolic resin, which must conform to the requirements that on completion of the whole operation it will retain good electrical properties. To speed up drying of this paint the sheet subsequently passes through a drying tunnel, after which the opposite side of the sheet is silk-screened and dried.

Those parts of the sheet to which no paint has been applied, and which therefore form the pattern for the wiring, are next thickened with copper by a galvano-plastic method. This is done in the customary way, and the thickness required is determined by the designer of the set for which the printed wiring is intended. Current-intensity and duration of treatment of course govern the thickness. At Philips the lines of the wiring have, as a general rule, a minimum thickness of 1/1 000in and the thickness of the protective faces is 4/10 000in.

The next step is to bake the paint, for, to ensure that it has the right electrical and chemical properties, the paint has to polymerize. Then a coating of glue must be applied to the sheet, to affix the impregnated paper. This coating has to be applied very evenly, and the method employed is to dip the sheets in a solution of modified phenolic resin and subsequently to take them out of the solution slowly and smoothly. Following a short drying-process the sheets go to the press. The necessary sheets of impregnated paper are fitted on both sides of the carrier, and the press is then set in motion. Next the carrier, in between the two hard-paper boards, is removed.

The final operation is removal of the film of copper, which was first applied to the carrier and now—after the carrier has been taken away—remains on the hard paper. To remove this film, the sheet is dipped in a bath of chromic acid. The sheet is then dipped in an alkaline solution, to break down any chromic-acid remaining into chromates.

The Propagation of Slow Waves

By J. Dain*

This article discusses the fundamental properties of the field patterns of travelling electromagnetic waves as applied to particle accelerators and microwave electron tubes.

It includes remarks on characteristics peculiar to periodic guiding structures and on waves with group and phase velocities directed in opposite senses.

THE post-war developments in microwave tubes and particle accelerators has seen an ever increasing use of the interaction between beams of moving charged particles and travelling wave electromagnetic fields. This, in turn, has brought about a greater understanding of the principles underlying the propagation of waves at velocities substantially below the velocity of light in free space. The purpose of this article is to give a resumé of the knowledge gained. It is interesting, however, to start with a brief historical survey.

The cavity magnetron, developed in Britain during the last war, was the first r.f. generator to use interaction between electrons and a travelling wave. In this oscillator the space charge cloud exchanges energy with one of the rotating field components of the standing wave pattern set up in the anode cavities. The r.f. fields grow and are maintained provided the angular velocities of the electrons and the wave are roughly equal. The next phase of development came in 1947 with the introduction of the travelling wave tube in which a beam of electrons interacts with a travelling wave in a linear arrangement. The discovery of the Carcinotron or backward wave oscillator in 1951 led to an appreciation of the fact that a travelling wave may have its phase and energy velocities in opposite directions. Later developments in the sphere of low noise tubes have carried over some of the concepts of guided waves into the realm of space charge waves on beams. It now appears probable that the upper frequency limit of electron tubes will be raised most by the further development of tubes based on this principle of continuous interaction between beam and field.

List of Principal Symbols

E =	component of electric field	(V/m)
H =	component of magnetic field	(A/m)
Q =	quality factor of resonator	
V =	beam voltage	(V)
Z_0 =	impedance of free space = 120π	(Ω)
Z_1 =	beam coupling impedance	(Ω)
Z_2 =	shunt impedance	(Ω)
P =	power flow	(W)
W =	energy stored per unit length	(J/M)
c =	velocity of light	(m/sec)
d =	guide width	(m)
f =	frequency	(c/s)
j =	$\sqrt{-1}$	
l =	guide length	(m)
p =	pitch of periodic structure	(m)
s =	slot height	(m)
t =	time	(sec)
v_g =	group velocity	(m/sec)
v_p =	phase velocity	(m/sec)
x, y, z =	co-ordinates of position	
α =	attenuation constant	(N/m)
β =	phase constant	(m^{-1})
β' =	$\sqrt{\beta^2 - \omega^2\mu\epsilon}$	(m^{-1})
β_n =	$\sqrt{\omega^2\mu\epsilon} = 2\pi/\lambda$	(m^{-1})
γ =	propagation constant = $\alpha + j\beta$	
ϵ =	dielectric constant of free space	(F/m)
λ =	free space wavelength	(m)
λ_G =	guide wavelength	(m)
θ =	phase change/pitch	(Rad)
ψ =	angle of developed helix	(Rad)
μ =	permeability of free space	(H/m)
ω =	$2\pi f$	(Rad/sec)

The history of linear accelerator development is similar. Prior to the war there were but few schemes using travelling waves and these were very restricted mainly due to the lack of suitable sources of r.f. power. The wartime development of pulsed microwave oscillators paved the way for intensive work on electron accelerators. Meanwhile the general development of tubes for lower frequencies encouraged work on linear accelerators for protons and heavier particles. In this field the search is always for more energy or more beam current with a given input to the machine and the waveguide development has been directed with one or other of these aims in view.

With so much at stake in the form of bandwidth or tuning range or output energy it is not surprising that the problem of guiding slow-waves claims a great deal of attention. Proposals for new guiding structures are made almost more rapidly than their properties can be analysed, but despite this there are still many gaps to be bridged between that which is theoretically possible and that which has been accomplished in practice.

Basic Parameters of Travelling Waves

With a wave propagating in the positive Z-direction the field components may be supposed to vary as

$$\exp(j\omega t - \gamma z) \qquad (1)$$

where $j = \sqrt{-1}$

$$\lambda = \alpha + j\beta$$

The real part of the propagation constant, α, is a measure of the attenuation in the wave. Specifically the power loss per unit length is $2\alpha P$, where P is the power flowing in the wave. The imaginary part of the propagation constant yields the phase velocity according to the relation

$$v_p = \omega/\beta \qquad (2)$$

The phase velocity is, by definition, the velocity with which the equiphase surfaces move. It is well known that this velocity may exceed the velocity of light without violation of the Special Theory of Relativity. However, on this occasion the interest is within the range of about $0{\cdot}02c$ up to nearly $1{\cdot}0c$.

The electric and magnetic fields composing the wave store energy in equal amounts for a given length of a lossless system. This result has been shown valid for a periodic structure provided the energy storage is averaged out taking an integral number of pitches of the structure[1]. This principle of the equipartition of the energy may be used in the calculation of the phase constant β and variational methods have been established for determining upper and lower limits for it in certain cases when an exact analysis is too cumbersome.

The group velocity of the wave is perhaps most con-

* *The English Electric Valve Co., Ltd.*

veniently defined by the relation

$$v_g = 1/\partial\beta/\partial\omega \quad \ldots\ldots\ldots\ldots\ldots\ldots (3)$$

It has also been established[1,2] that the group velocity is equal to the energy velocity. Hence if P is the power flow and W is the total average stored energy per unit length

$$v_g = P/W \quad \ldots\ldots\ldots\ldots\ldots\ldots (4)$$

As before, for periodic structures the average value of W must be based on an integration extending over an integral number of pitches of the structure. The significance of group velocity in a periodic guiding system will be considered in greater detail in a later section.

Two further parameters of interest need introduction. The first concerns the coupling between the wave and a beam and is usually termed the series or beam coupling impedance. It is defined by the relation

$$Z_1 = E^2/2\beta^2 P \quad \ldots\ldots\ldots\ldots\ldots\ldots (5)$$

where E, the relevant component of the electric field, is usually assigned a root mean square value to compensate for its possible variation in amplitude over the cross-section of the beam.

The second parameter, the shunt impedance, is defined as

$$Z_2 = E^2/2\alpha P \quad \ldots\ldots\ldots\ldots\ldots\ldots (6)$$

and is related to the losses of the system.

The significance of these parameters in electron tube or particle accelerator design will now be examined in turn.

Since both devices rely on an approximate equality of beam and phase velocities the beam energy or voltage is related to the phase velocity of the wave, i.e.

$$-eV = m_0c^2\left\{(1 - v_p^2/c^2)^{-1/2} - 1\right\}\ldots\ldots (7)$$

where e is the (algebraic) charge of the particle and m_0 is its rest mass. For non- relativistic electrons this reduces to the well-known equation

$$v_p/c = 1{\cdot}98 \times 10^{-3}\sqrt{V} \quad \ldots\ldots\ldots\ldots (8)$$

Thus for an electron tube a knowledge of the required operating voltage determines the phase velocity for which the guiding system must be designed.

In a travelling wave amplifier the bandwidth is determined by the rate of variation of phase velocity with frequency. From the definitions (2) and (3)

$$\partial v_p/\partial\omega = (v_p/\omega)\,.\,(1 - v_p/v_g) \quad \ldots\ldots\ldots (9)$$

so that a low group velocity implies a rapid variation of phase velocity with frequency and a narrow band of amplification. The bandwidth is greatest for equal group and phase velocities, i.e. in a non-dispersive system.

Similar remarks apply to the backward wave oscillator. This tube oscillates at the frequency where the phase velocity is nearly the beam velocity. From this it follows that the tuning rate of the tube is given by

$$\partial f/\partial V = \tfrac{1}{2}(f/V)\,.\,(1 - v_p/v_g)^{-1} \quad \ldots\ldots\ldots (10)$$

where f and V are the operating frequency and voltage respectively. Since the phase and group velocities are of opposite sign the r.h.s. of equation (10) is always positive and an increase of operating voltage always raises the frequency. For a wide tuning range a high group velocity is required, but for a reduced sensitivity to inadvertent changes of voltage the group velocity should be low.

For particle accelerators it is desirable to have as high a group velocity as other considerations, such as efficiency, will allow. High group velocity implies greater tolerance on the frequency of excitation and on the fabrication of the accelerating guide. However, from equation (4) it can be seen that a high group velocity is to be obtained with a high power flux or low stored energy. It is often found that the problems of beam focusing set a lower limit to beam size and consequently to the stored energy. In these circumstances the high group velocity that is desired may not be obtained without the creation of huge power fluxes and a sacrifice has to be made.

The beam coupling impedance is of major concern in the design of travelling wave amplifiers and oscillators. It is combined with the beam admittance into the familiar Pierce Gain Parameter[3] C. High coupling impedance improves the gain per unit length of an amplifier and leads to greater conversion efficiencies. In the backward wave oscillator high C reduces either the starting current for a given length or, conversely, the length for a given starting current. Again efficiency is improved as the coupling between the beam and the circuit increases. In accelerators the coupling impedance is not of such immediate importance.

The situation is reversed when the shunt impedance of a guiding system is considered. An accelerator is usually designed to give as high an output energy as possible consistent with other practical considerations. Now for an accelerator of length l such that $\frac{1}{2}\alpha l$ is less than unity, the peak output voltage V_0 is given approximately by the formula

$$V_0^2 = lP'Z_2 \quad \ldots\ldots\ldots\ldots\ldots\ldots (11)$$

where P' is the power dissipated in the accelerator. Consequently the shunt impedance, which has the dimensions of resistance per unit length, is directly related to the output voltage obtainable in a given length with a given power loss.

Techniques of Measurement

The previous section has indicated the significance of the main parameters of a guiding system. The intention now is briefly to mention some of the methods used for measuring them.

The most direct method for measuring the phase velocity is to set up a standing wave in the guide and investigate this with a moving search probe. In the simplest case the distance between the adjacent peaks or troughs of the pattern is one half of a guide wavelength and the phase velocity is then derived from the relation

$$v_p/c = \lambda_G/\lambda \quad \ldots\ldots\ldots\ldots\ldots\ldots (12)$$

with λ_G the measured guide wavelength and λ the free space wavelength. In practice the presence of a fast mode of propagation may cause irregularities in the pattern[4] and with periodic structures the presence of the space harmonics also may give rise to distortion and cyclic shifts of the minima and maxima[5]. The interpretation of the measurements must then be made with greater care.

If these measurements of phase velocity are extended over a band of frequencies the group velocity can be calculated using, for example, a re-arrangement of equation (9). The attenuation constant, however, is not usually determined with any accuracy from standing wave patterns. An accepted procedure is to set up an isolated section of the guide as a resonant cavity and measure the Q's and resonant frequencies of this cavity. The attenuation constant is determined from the definition of Q:

$$Q = \omega \times \text{Energy stored/Power dissipated}$$

or in the present notation

$$Q = \omega Wl/2\alpha Pl \quad \ldots\ldots\ldots\ldots\ldots (13)$$

l being the length of the resonator, which in fact cancels out and is irrelevant to the calculation. Using expression (4) for the group velocity it follows that

$$\alpha = \omega/2Qv_g \quad \ldots\ldots\ldots\ldots\ldots\ldots (14)$$

Thus, with a previous determination of the group velocity the attenuation factor is known. It should be remarked that this resonance technique also will yield the phase velocity and hence the group velocity if the mode numbers, that is to say the number of half-wavelengths in the length of the resonator, can be found for the various resonances.

The coupling impedance and shunt impedance of a guiding structure are usually determined by perturbation techniques[6,7,8,9]. The fields in the resonant cavity are perturbed by the introduction of small metal or dielectric bodies. The perturbation causes a shift in the resonant frequency of the cavity and the calculations follow from a measurement of this shift. It has been shown[10] that the frequency shift is related to the perturbing body and the original field strengths in the following way.

$$\delta f/f = -(E_o \cdot P + H_o \cdot M)/4W_o \quad \ldots\ldots (15)$$

where E_o and H_o are the unperturbed fields, supposed uniform in the vicinity of the perturbation and W_o is the total energy stored in the resonator by the field. P and M are respectively the electric and magnetic dipole moments of the body and are proportional to the fields, that is to say

$$P = pE_o$$
$$M = mH_o$$

where p and m are constants determined by the geometry and inductive capacitances of the perturbing body.

Suppose now two dissimilar bodies are introduced in turn into the same position in the resonator. Two shifts in frequency are produced and from the two simultaneous equations of the form of (15) either the magnetic or electric field may be eliminated. For example with suffixes 1 and 2 denoting the first and second experiments

$$E_o^2/4W_o = (m_1\delta f_2/f - m_2\delta f_1/f)/(m_2p_1 - m_1p_2) \quad \ldots\ldots\ldots\ldots (16)$$

If the bodies are placed at a point of maximum electric field in the standing wave pattern of the resonator $E_o = 2E$, where E is the amplitude of one of the travelling waves. Furthermore W_o, the total energy stored, is equal to $2Wl$, where W is the energy per unit length stored by one of the travelling waves. With these two relations and the expression (4) for the group velocity equation (16) can be put in the form

$$E^2/2P = (l/v_g) \cdot (m_1\delta f_2/f - m_2\delta f_1/f)/(m_2p_1 - m_1p_2) \quad \ldots (17)$$

This result, coupled with previously determined values of α and β yields the values of the coupling impedance (equation (5)) and the shunt impedance (equation (6)). As a final observation on this method it should be noted that if the magnetic field is zero at the position of the perturbation then only one disturbance need be introduced and this is conveniently a metal body. The relevant equation now becomes

$$E^2/2P = -(l/v_g) \cdot (1/p) \cdot \delta f/f \quad \ldots\ldots (17a)$$

This completes the present discussion of the basic parameters and methods used for measuring them. The following sections will be devoted to a treatment of topics selected for their interest in various aspects of the subject.

On Anomalous Dispersion

The interest in systems in which the energy velocity is oppositely directed to the phase velocity makes it pertinent to inquire in what circumstances such waves may or may not be obtained. As will be mentioned later a periodic guiding structure always supports these waves; for a guide with an invariant cross-section it is often impossible to obtain anomalous dispersion.

Consider first a single E-wave in a lossless system. From Maxwell's equations it may be shown that

$$\left.\begin{aligned} E_x &= (\beta/\omega\epsilon) \cdot H_y \\ E_y &= -(\beta/\omega\epsilon) \cdot H_x \end{aligned}\right\} \quad \ldots\ldots\ldots\ldots (18)$$

Since the power flow is given by a surface integral of the form

$$P = \tfrac{1}{2} R_e \int (E_x \cdot H_y^* - E_y \cdot H_x^*)\, dS$$

where the asterisk denotes the complex conjugate, it follows that the power flow may be expressed as

$$P = \tfrac{1}{2}(\beta/\omega\epsilon) \cdot \int (H_xH_x^* + H_yH_y^*)\, dS \quad \ldots (19)$$

Similarly for a single H-wave the expression for the power flow can be reduced to

$$P = \tfrac{1}{2}(\omega\mu/\beta) \cdot \int (H_xH_x^* + H_yH_y^*)\, dS \quad \ldots (20)$$

Now the integrand in equations (19) and (20) is always positive and consequently the power flow is always directed in the same sense as the phase velocity.

For a hybrid wave where the guiding structure causes coupling between an E-wave and an H-wave this result is not necessarily applicable. Suffice it to say that most hybrid waves have their phase and energy velocities in the same direction.

Simply Periodic Structures

It has been demonstrated that the travelling wave field guided by a periodic structure may be considered as built up from an infinite set of waves termed space harmonics[9,11] The amplitude and phase of these harmonics depends on the geometry of the structure and on the frequency of excitation. The phase constants are related by the equation

$$\beta_m p = \theta + 2m\pi;\ m = 0, \pm 1, \pm 2 \quad \ldots\ldots (21)$$

where p is the pitch of the structure and θ is the phase change per pitch in the field pattern.

It is conventional to restrict θ to the range 0 to π radians since values outside this range do not yield any new values for the magnitudes of the propagation constants as given by equation (21) In making this statement it is assumed that no essential distinction is to be made between complete wave patterns travelling with the same velocity in the positive or negative Z-direction. It is to be noted in this respect also that a helical waveguide system is an exceptional case of a periodic structure in that it appears as a continuous system in a set of rotating co-ordinates. In this case the above restriction on θ does not apply; however, it has been shown that forbidden zones do exist[12] and that these are given by the condition

$$\beta_m^2 > \omega^2\mu\epsilon$$

for any value of m. In other words no space harmonic may propagate with a velocity greater than the free space velocity.

The approximate pitch of the structure appropriate to a given voltage of operation is readily calculated. At the mid-band point it is usually to be recommended that θ has the value $\pi/2$. In this case

$$\beta_m p = 2\pi(m + \tfrac{1}{4}) \quad \ldots\ldots\ldots\ldots (22)$$

so that

$$|v_p/c| = \omega/c \cdot \gamma\, |\beta_m| = (p/\lambda) \cdot |m + \tfrac{1}{4}| \quad \ldots (23)$$

Combining this with the expression (8) relating voltage and phase velocity gives

$$p = 1{\cdot}98 \times 10^{-3}\, \sqrt{V} \cdot \lambda \cdot |m + \tfrac{1}{4}| \quad \ldots\ldots (24)$$

With the sign convention allotted to θ the harmonics defined by m zero or positive have phase velocities in the positive Z-direction; the harmonics defined by m negative have phase velocities in the opposite sense. All waves, however, have the same group velocity

$$v_g = p/\partial\theta/\partial\omega \quad \ldots\ldots\ldots\ldots (25)$$

so that one set of harmonics may be regarded as having anomalous dispersion.

This does not mean that the individual harmonics carry power in the opposite sense to their phase velocity. Suppose the pattern is composed of E-waves and evaluate the power carried by any two harmonics. It is sufficient to consider two harmonics only since the expression for the power flow is of the second degree in the field components. For the m^{th} and n^{th} harmonics:

$$P_{nm} = \tfrac{1}{2} R_e \int \Big\{ (E_{xm} + E_{xn})(H_{ym}^* + H_{yn}^*) - (E_{ym} + E_{yn})(H_{xm}^* + H_{xn}^*) \Big\} dS \quad \ldots\ldots (26)$$

and by the use of equation (18) this may be reduced to the form

$$P_{nm} = \tfrac{1}{2}(1/\omega\epsilon)\int \Big\{ \beta_m (H_{xm}H_{xm}^* + H_{ym}H_{ym}^*) + \beta_m(H_{xn}H_{xn}^* + H_{yn}H_{yn}^*) + (\beta_m + \beta_n)\, R_e\, (H_{xm}H_{xn}^* + H_{ym}H_{yn}^*) \Big\} dS \quad \ldots\ldots\ldots (27)$$

The first term of the integrand represents the power carried by the m^{th} harmonic alone, the second term that carried by the n^{th} alone and the last term is the cross-product power. If n and m are of opposite signs one of the waves carries power in the opposite direction to the pattern as a whole. As a particular case in point at the π-mode cut-off with m positive and n negative and equal to $-(m+1)$

$$\beta_n = -\beta_m$$
$$|H_{xn}| = |H_{xm}|$$
$$|H_{yn}| = |H_{ym}|$$

The cross-product power is zero and so is the total power since the two waves carry equal powers but in opposite directions.

There arises therefore an apparent paradox. The combination of two space harmonics, which necessarily have the same group velocity, causes a reduction in the power flow. In other words one harmonic behaves as though its group and energy velocities are directed in opposite senses in contradiction to the result previously established. It is important to remember that energy velocity and energy storage must be referred to the pattern as a whole and not to the individual space harmonics.

Multiply Periodic Structures

For definiteness consider a multiply periodic structure with only two differing cells in one pitch such as that shown in Fig. 1. To obtain some comparison with the singly periodic systems the pitch will be given the value $2p$.

As before the field pattern is built of an infinite set of harmonics with propagation constants given by an equation of the form

$$\beta_{m'}2p = 2\theta + 2m'\pi;\ m' = 0, \pm 1, \pm 2 \quad \ldots\ldots (28)$$

In this form 2θ is the phase change for a complete pitch of $2p$ and once again is restricted to the range 0 to π radians.

For the harmonics m' even and equal to $2m$ equation (28) reduces to the form

$$\beta_{m'}p = \theta + 2m\pi;\ m = 0, \pm 1, \pm 2 \quad \ldots\ldots (29)$$

which compares directly with equation (21).

For the harmonics with m' odd and equal to $(2n-1)$ equation (28) becomes

$$\beta_{m'}p = (\theta - \pi) + 2n\pi;\ n = 0, \pm 1, \pm 2 \quad \ldots\ldots (30)$$

which is similar to the original form of equation (21).

It is evident that the increase in geometrical complexity has increased the number of space harmonics. However, θ is to lie between 0 and $\pi/2$ radians so that the range of variation of the individual phase constants is reduced.

The zero-mode contamination in the rising-sun magnetron is apparent. When θ, m and n are all zero

$$\left.\begin{array}{l} \beta_0 p = 0 \\ |\beta_{-1} p| = \pi \end{array}\right\} \quad \ldots\ldots\ldots\ldots\ldots (31)$$

corresponding to the zero and π-modes of the anode.

A singly periodic structure may be considered as a limiting case of a multiply periodic system in which the individual cells of a pitch are all identical. How then are the two apparently different spectral distributions of the harmonics to be reconciled? If the analysis is carried out starting from the above example of the multiply periodic structure with two cells per pitch then the following results will be found on passing to the limit of identical cells. Over one part of the pass band of the guide the harmonics with m' odd have zero amplitude and the phase constants are given by equation (29) in agreement with equation (21) for values of θ between 0 and $\pi/2$ radians. Over the remainder of the pass-band the harmonics with m' even vanish and the propagation constants are given by equation (30). This is to be compared with equation (21) by the substitution

$$(\theta - \pi) = \theta'$$

so that:

$$\beta_{m'}\, p = \theta' + 2n\pi \quad \ldots\ldots\ldots\ldots\ldots (30a)$$

with:

$$-\pi \leqslant \theta' \leqslant -\pi/2$$

and thus the phase constants have equal magnitude but

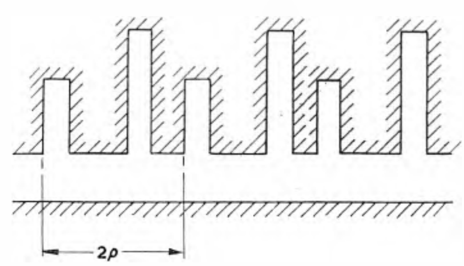

Fig. 1. Multiply periodic structure

opposite sign to those given by equation (21) for the range of $\pi/2$ to π radians. The change of sign is of no significance; the relevant parameter is the relation between the phase and group velocities and this is the same for either analytical approach.

Reverting now to the structure with two unequal cells per pitch the previous argument suggests and calculations verify, that circumstances will arise where the harmonics with m' even will have substantially larger or smaller amplitude than those with m' odd. In the interaction with charged particles only one harmonic couples strongly with the beam. It is a feature of good design therefore to try to ensure that this harmonic belongs to the predominant set of the field pattern.

Multiply periodic structures have found their main application in the rising-sun magnetron to give greater mode separation. They have also been considered as an alternative to the helix to give a phase velocity constant over a wide frequency band[13]. In this application the prime disadvantage is that the harmonic with the most nearly constant phase velocity is not the lowest order harmonic and it is difficult therefore to obtain a high coupling impedance.

Much physical insight into the general behaviour of slow waves can be gained from the study of a few simple cases. Since both electron wave tubes and particle accelerators require an axial component of electric field it is natural to start the discussion within an E-wave which has, by definition, no axial magnetic field. For the first example the wave is supposed to be travelling above the $y=0$ plane with components independent of the x co-ordinate. The fields of this wave may be put in the form

$$\left.\begin{aligned} E_z &= E \\ E_y &= -\mathrm{j}\,(\beta/\beta')E \\ H_x &= \mathrm{j}\,(\omega\epsilon/\beta')E \end{aligned}\right\} \exp(-\beta' y)\exp \mathrm{j}(\omega t - \beta z) \quad \ldots\ldots (32)$$

with the subsidiary relation

$$\beta' = \sqrt{(\beta^2 - \omega^2\mu\epsilon)}$$

Since the interest is with waves of low velocities

$$\beta^2 \gg \omega^2\mu\epsilon$$

and as an approximation therefore

$$\beta' \simeq |\beta| \quad \ldots\ldots\ldots\ldots\ldots\ldots (33)$$

For a wave travelling below the plane $y = 0$ the sign of β' is reversed in the expressions (32) for the three field components.

The exponential decay with distance from the guiding plane $y=0$ shows that the fields are confined closely to this surface. This is a characteristic feature of all slow waves in that the amplitude of the field decays rapidly away from the surface guiding the propagation; moreover, the slower the wave the more rapid is the fall in amplitude with distance. To a good approximation the fields have decreased by the factor $1/e$ in a distance given by

$$3{\cdot}12 \times 10^{-4}\lambda\sqrt{V} \quad \ldots\ldots\ldots\ldots\ldots (34)$$

where V is the beam voltage and λ the operating wavelength. Thus for a 1·6kV beam and 3cm wavelength this distance is roughly 0·4mm. It is evident, for example, that a travelling wave tube built to operate under these conditions must have the beam kept within a distance of this order of magnitude from the helix or the coupling between the beam and the circuit will be greatly reduced.

To return now to the simple E-waves travelling above and below the plane $y = 0$. If these have equal amplitudes the Z-component of electric field is continuous across the surface but the component of magnetic field is not. This discontinuity may be accounted for by a current flowing in the surface with a density given by

$$J_z = -2\mathrm{j}\,(\omega\epsilon/\beta')\,.\,E\exp \mathrm{j}(\omega t - \beta z) \quad \ldots\ldots (35)$$

in other words the plane $y = 0$ should be given an intrinsic reactance

$$Z = \tfrac{1}{2}\mathrm{j}\,(\beta'/\omega\epsilon) \quad \ldots\ldots\ldots\ldots\ldots\ldots (36)$$

This relation is perhaps more comprehensible using the approximation (33) and the relations

$$Z_0 = \sqrt{(\mu/\epsilon)}$$

$$|\beta| = (c/v_p)\,.\,\sqrt{(\omega^2\mu\epsilon)}$$

which yields the result

$$Z = \tfrac{1}{2}\mathrm{j}(c/v_p)\,.\,Z_0 \quad \ldots\ldots\ldots\ldots\ldots (37)$$

and this demonstrates that the slower the wave the higher must be the reactance of the surface.

The need for reactance in the surface may be appreciated from another viewpoint. If the energy stored in the fields is evaluated it will be found that there is an excess of electric energy in these fields. The inductive reactance of the surface $y = 0$ makes good the deficit of magnetic energy and restores the balance required in the complete system. By integration it can be shown that the power flow and the total energy stored per unit length in the Z-direction and for a width d in the x-direction are given by

$$\left.\begin{aligned} P &= \tfrac{1}{2}\epsilon d\,.\,E^2\,\omega\beta/\beta'^3 \\ W &= \tfrac{1}{2}\epsilon d\,.\,E^2\,(\beta^2 + \beta'^2)/\beta'^3 \end{aligned}\right\} \quad \ldots\ldots\ldots (38)$$

From these relations the group velocity and the coupling impedance referred to the electric field at $y = 0$ may be calculated as

$$\left.\begin{aligned} v_g &= \omega\beta/(\beta^2 + \beta'^2) \\ Z_1 &= (\lambda/2\pi d)\,.\,(\beta'/\beta)^3\,.\,Z_0 \end{aligned}\right\} \quad \ldots\ldots\ldots (39)$$

where λ is the free space wavelength.

For slow waves where the approximation (33) is valid it will be seen that the group velocity is one half the phase velocity.

The simulation of the inductive surface will be considered later; as a final comment on this example it should be mentioned that conducting sheets placed above and below the inductive surface raise the group velocity but reduce the coupling impedance. The effect is negligible, however, if the spacing of the sheets from the surface exceeds roughly one guide wavelength.

H-waves may be supported by a surface with a capacitive reactance and the field in this instance takes the form (for y positive):

$$\left.\begin{aligned} H_z &= H \\ H_y &= \mathrm{j}\,(\beta/\beta')\,H \\ E_x &= \mathrm{j}(\omega\mu/\beta')\,H \end{aligned}\right\} \exp(-\beta' y)\exp \mathrm{j}\,(\omega t - \beta z) \quad \ldots\ldots (40)$$

This leads directly to the second example chosen for discussion, the developed sheath helix[14]. In this system the plane $y = 0$ is considered to be fully conducting in a direction making an angle ψ with the x-axis and to have zero conductance normal to this direction. To meet these boundary conditions it is necessary to have both E and H waves above and below the surface and the field for y positive takes the form

$$\left.\begin{aligned} E_x &= \mathrm{j}\,(\omega\mu/\beta')\,H \\ E_y &= -\,\mathrm{j}\,(\beta/\beta')\,E \\ E_z &= E \\ H_x &= \mathrm{j}\,(\omega\epsilon/\beta')\,E \\ H_y &= \mathrm{j}\,(\beta/\beta')\,H \\ H_z &= H \end{aligned}\right\} \exp(-\beta' y)\exp \mathrm{j}\,(\omega t - \beta z) \quad \ldots\ldots (41)$$

The boundary conditions impose the restrictions

$$\beta^2 = \omega^2\mu\epsilon\,\mathrm{cosec}^2\,\psi$$

that is to say

$$|v_p/c| = |\sin\psi| \quad \ldots\ldots\ldots\ldots\ldots\ldots (42)$$

and

$$E = \mathrm{j}\,Z_0\,H \quad \ldots\ldots\ldots\ldots\ldots\ldots (43)$$

Once again the power flow and the energy storage can be evaluated for a width d in the x-direction. It is found that

$$\left.\begin{aligned} P &= \epsilon\,d\,.\,E^2\,.\,\omega\beta/\beta'^3 \\ W &= \epsilon\,d\,.\,E^2\,.\,\beta^2/\beta'^3 \end{aligned}\right\} \quad \ldots\ldots\ldots\ldots\ldots (44)$$

so that the power flow is twice that for the E-wave alone (equation (35)) whereas the stored energy is virtually the same. The interpretation of this is as follows. The surface $y = 0$ is no longer inductive but couples the E-wave to the H-wave which then makes good the deficit of stored magnetic energy. This H-wave however produces the same power flux as the E-wave with a consequent raising of the group velocity but a reduction of the coupling impedance. The group velocity is in fact equal to the phase-velocity, i.e. a non-dispersive guide and the coupling impedance is

$$Z_1 = \tfrac{1}{2}\,(\lambda/2\pi d).(\beta'/\beta)^3.\,Z_0 \quad \ldots\ldots\ldots\ldots (45)$$

It was from considerations such as these that the cross-wound helix[15] was evolved. Superpose two waves of the form of equation (41) subject to the condition that one is supported by a surface conducting at an angle ψ with the x-axis, the other by a surface conducting at $-\psi$. Two modes are possible; one is an H-wave with no axial electric field corresponding to in-phase excitation of the currents in the helices and the other is an E-wave corresponding to out-of-phase excitation. This mode has field components given by equation (32) and the velocity of propagation by equation (42). The results of equations (38) and (39) are applicable hence the cross-wound helix has a coupling impedance about twice that of a single helix but is necessarily more dispersive.

The helix waveguide has played a dominant part in electron wave tubes, but its coupling impedance tends to zero as the phase velocity tends to the velocity of light. Thus it is found that the vane type or corrugated waveguide has been used extensively in linear accelerators for electrons since the beam velocity is greater than $0{\cdot}99c$ for only moderate energies. The final example will be this structure in its developed form as shown in Fig. 2. The corrugations extend indefinitely in the x-direction and the slots between them are open in the plane $y = 0$ and shorted in the plane $y = -l$; the pitch of the structure is p and the slot height is s.

Since this is a periodic structure an accurate solution should take account of the space harmonics. For the present analysis only the fundamental component will be taken and an approximate solution will be obtained based on a method suggested by Cutler[16].

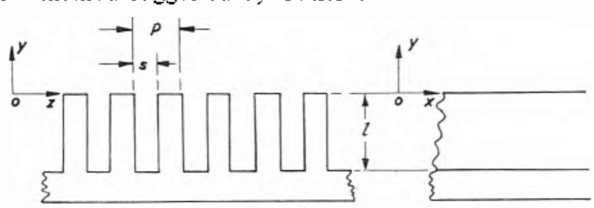

Fig. 2. Details of corrugated waveguide

Above the slots the field takes the form of equation (32) and within the slots it is given by

$$\left.\begin{aligned} E_z &= E' \sin \beta_a (l + y) \\ H_x &= \mathrm{j}\,(E'/Z_0) \cos \beta_a (l + y) \end{aligned}\right\} \exp \mathrm{j}(\omega t - \beta z_0) \quad \ldots\ldots \ (46)$$

where z_0 is the mean value of z for the slot in question. These two fields are matched by equalizing the voltage per pitch above and below the slot mouth giving

$$E\,.\,p = E'\,.\,s \sin \beta_a l$$

and by equating the x-component of magnetic field across the same boundary yielding

$$(\omega\epsilon/\beta')\,.\,E = (E'/Z_0) \cos \beta_a l$$

Solving these equations subject to the slow wave approximation, equation (33) shows that

$$|c/v_p| = (s/p)\,.\,\tan \beta_a l \quad \ldots\ldots\ldots\ldots \ (47)$$

So that a slow wave requires the slot to be almost one-quarter of a wavelength long.

The weakness of the corrugated waveguide as a structure is readily demonstrated. In the first example of two waves supported by an inductive surface this surface served to compensate for the unbalance between the energy stored by the electric and magnetic fields of the waves. Consider now the corrugated structure and evaluate the electric energy stored in the wave above the corrugations. For a width d and unit axial length this is

$$W_1 = \tfrac{1}{8}\epsilon d\,.\,E^2 (\beta^2 + \beta'^2)/\beta'^3 \quad \ldots\ldots\ldots\ldots \ (48)$$

whereas the energy stored by the electric fields within the slots for the same width and length is

$$W_2 = \tfrac{1}{8}\epsilon d\,.\,E'^2\,.\,(p/s)\,.\,\mathrm{cosec}^2 \beta_a l \ \ [l - (1/\beta_a) \sin 2\beta_a l] \quad \ldots\ldots\ldots\ldots \ (49)$$

Since the slots are almost a quarter of a wavelength deep

$$W_2 \simeq (\pi/16)\,\epsilon d\,.\,E^2\,.\,(p/s)\,.\,(1/\beta_a) \ldots\ldots\ldots \ (50)$$

so that putting $(p/s) = 2$ and using the slow-wave approximation (33) in the expression for W:

$$W_2/W_1 \simeq |c/v_p| \quad \ldots\ldots\ldots\ldots\ldots \ (51)$$

This shows that the slots store far more electric energy than the wave above them and in most cases no practical use can be made of the field associated with it.

The external field of this corrugated structure has the same form as that for the cross-wound helix, but lies on one side only of the surface. Thus it has a coupling impedance about twice that of the cross-wound helix and four times that of the single helix. However, the energy stored in the slots reduces the group velocity by a factor of roughly $4(1 + c/v_p)$ down on that for the single helix. As a numerical example a corrugated guide designed for use with a 1kV beam will have a group velocity about one-seventieth of its phase velocity.

This example illustrates a misconception that sometimes arises. Casual thought may lead to the conclusion that a guiding system giving very low group velocity has, in consequence, a high coupling impedance. At a given phase velocity a high coupling impedance occurs only if the power flux is small, whereas a low group velocity obtains if either the power flux is small or the stored energy is high. The corrugated guide fulfils the second condition and does not have usually a very high coupling impedance[17,18]. However, it does possess a high series impedance, figures of 40MΩ per metre have been quoted[19] and it is a relatively efficient structure for accelerating electrons.

Conclusions

This article has touched briefly on several topics in the subject of the propagation of slow waves and its particular application to electron wave tubes and particle accelerators. The purpose has been to underline in a direct fashion features that are not always appreciated and to back this exposition with examples illustrating the shortcomings of existing guiding systems.

It is to be hoped that enough has been said to show that there is more to the design of a slow wave circuit than setting the wave velocity to some prescribed value. Since at least three parameters need consideration it is usual to find that a new application calls for the development of a circuit suited as nearly as can be to the particular requirement.

REFERENCES

1. Bell, J. S. Group velocity and energy velocity in periodic waveguides. A.E.R.E. Rep. No. T/R 858 (1952).
2. Slater, J. C. Microwave Electronics. p.41 (D. Van Nostrand, New York, (1950).
3. Pierce, J. R. Travelling Wave Tubes. (D. Van Nostrand, New York, 1950).
4. Epsztein, B., Mourier, G. Definition, mesure et caracteres des Vitesses de phase dans les systemes a structure periodique. *Ann. de Rad. 10*, 62, (1955).
5. Allen, C. P., Clarke, G. M. Interpretation of wavelength measurements on tape helices. *Instn. Elect. Engrs. Monograph* No. 151R. (1955).
6. Hansen, W. W., Post, R. F. On the measurement of cavity impedance. *App. Phys. 19*, 1059, (1948).
7. Mullett, L. B. Perturbation of a cavity resonator. A.E.R.E. Rep. No. G/R 853, (1952).
8. Nalos, E. J. Measurement of circuit impedance of periodically-loaded structures by frequency perturbation. *Proc. Inst. Rad. Engrs. 42*, 1508, (1954).
9. Kitchen, S. W., Schelburg, D. Resonant cavity field measurements. *App. Phys. 26*, 618, (1955).
10. Casimir, H. B. G. On the theory of electromagnetic waves in resonant cavities. *Phillips Res. Rep. 6*, 162, (1951).
11. Millman, S. A spatial harmonic travelling wave amplifier for 6 mms. wavelength. *Proc. Inst. Rad. Engrs., 39*, 1035, (1951).
12. Sensiper, S. Electromagnetic wave propagation on helical structures. *Proc. Inst. Rad. Engrs. 43*, 149, (1955).
13. Lines, A. W., Nicoll, G. R., Woodward, A. M. (Mrs.) Some properties of waveguides with periodic structures. *Proc. Inst. Elect. Engrs. Pt. 3*, 263, (1950).
14. Brossart, J., Doehler, O. Sur les proprietes des tubes a champ magnetique constant. *Ann. de Rad. 3*, 328, (1948).
15. Chodorow, M., Chu, E. L. Cross-wound twin helices for travelling wave tubes. *App. Phys. 26*, 33, (1955).
16. Cutler, C. C. Electromagnetic waves guided by corrugated conducting surfaces. B.T.L. Rep. No. MM-44-160-218.
17. Pierce, J. R. Circuits for travelling wave tubes. *Proc. Inst. Rad. Engrs. 37*, 510, (1949).
18. Field, L. M. Some slow-wave structures for travelling wave tubes. *Proc. Inst. Rad. Engrs. 37*, 34, (1949).
19. Harvie, R. B. R-S. Travelling wave linear accelerators. *Proc. Phys. Soc. 61*, 225, (1948).

A Multi-channel Dekatron Scaling Unit

By F. W. Lovick*

The scaling equipment described in this article is suitable for counting simultaneously in up to six channels, by means of plug-in units, each recording on a Dekatron cold-cathode counter tube and mechanical register. The apparatus, while being simple, inexpensive and compact, can be adapted to accommodate a variety of counting rates, and contains its own power supplies.

INVESTIGATIONS such as the simultaneous study of the activity of several fission or spallation products usually require, in addition to Geiger-Müller or proportional counters, a large number of scaling units. In many cases the activities concerned are not large, and the short resolving times of commercial scalers are unnecessary. The multi-channel scaling unit described in the present note was developed for such applications; it is simple, cheap and compact, and has proved reliable in service.

The unit was designed to provide six separate scalers for counting rates up to 100 per second, with easy adaptation to higher counting rates with a reduction in the number of channels available. The basic unit is a 'scale of ten' comprising an input pulse shaping stage, a Dekatron cold cathode counting tube, and a mechanical register circuit. Power supplies for six of these units and for six quenching probe units are contained in the main framework of the apparatus, the separate scaling units being constructed as 'plug-in' sections, so that any faulty scaler can be readily replaced.

The mechanical register restricts the counting rate of a single scaling unit to 100 counts per second, however, by using two units in series, with the register of the first inoperative, a counting rate of 1 000 per second is available in up to three channels. By using three units in series, the counting rate can be increased to the maximum quoted by the manufacturers of the Dekatron tube, namely 4 000 per second, and two channels are then available. The Dekatron tube was chosen for this application because of its simplicity, compact size and reliability, and while its maximum counting rate is not particularly high, it was deemed adequate, as for the most part quenching probe units with a dead time of 500μsec would be used to operate the scalers.

The compact form of the equipment lends itself to the photographic recording of all channels simultaneously; the register valves may alternatively be used to actuate a tape recording system.

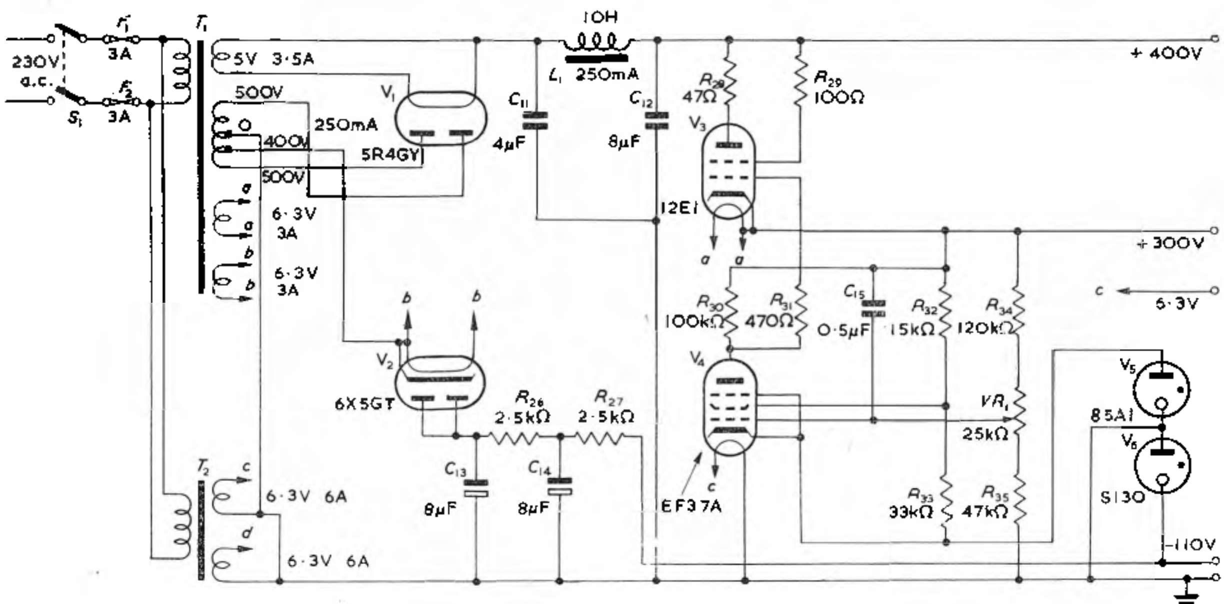

Fig. 1. Stabilized power supply for Dekatron scalers
(Heater winding "d" used for quench probe valves)

General Description

A conventional stabilized power supply is used (Fig. 1), consisting of a pentode valve V_4 (CV358), controlling a series valve V_3 (CV345), the reference tube V_5, being a Mullard 85A1. This circuit provides a 300V positive supply of 250mA, to operate the Dekatron units and quenching probe units. A negative line of 110V is also obtained from the transformer through a rectifier V_2 (CV574) smoothing circuit, and stabilizer valve V_6 (CV1110). The unstabilized 400V positive supply from the filter network is used for the Dekatron tube anode supply, and for the mechanical register valves.

Each scaling unit (Fig. 2) consists of the following circuits, a pulse shaper, followed by a Dekatron scaling

* *University of Birmingham*

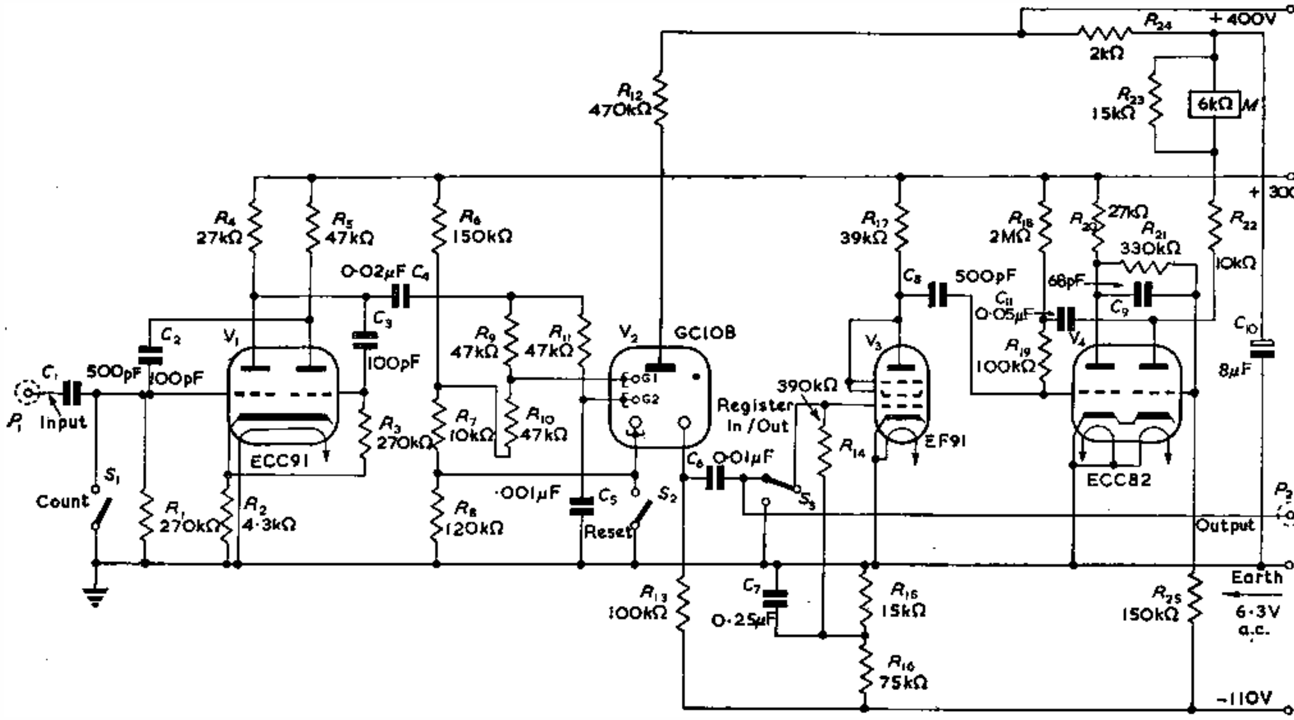

Fig. 2. Dekatron scale of ten and register unit

tube, feeding a pulse invertor, and finally a register valve.

The pulse shaper V_1 (CV858) is a double triode valve, acting as a monostable multivibrator, and when triggered by a positive pulse of 8 to 10V amplitude, it delivers to the Dekatron guide network a negative pulse of 150V amplitude and 50μsec duration. The sensitivity of the stage is adjusted by a potentiometer forming the cathode bias resistor.

The Dekatron tube V_2 is operated by the negative pulse, which is phased by the guide network, the components of which are those recommended by the manufacturers of the tube. Every tenth pulse causes the glow to dwell on the output cathode, and the pulse thus produced can be used either to drive a second scaling unit, or to feed the pulse invertor.

The pulse invertor V_3 (CV138) is a triode connected pentode valve, normally biased beyond cut-off. The positive output pulse from the Dekatron tube, of about 50V amplitude, causes the valve to conduct, producing at its anode a negative pulse.

This negative pulse is used to operate V_4 (CV491) which is a monostable multivibrator having the mechanical register of 6kΩ resistance as the anode load of the triode valve, which is normally non-conducting. The arrival of a negative pulse initiates the flip-flop action of the circuit, and causes a pulse of current of duration about 40msec to flow through the register coil thus recording a count.

The Dekatron tubes are reset to zero in the normal manner, by momentarily disconnecting all cathodes and guide potentiometers from earth, but excluding the Dekatron output cathodes. The potential of the disconnected electrodes rises about 100V positive to earth, thus causing the glow to rest on the output cathodes ('0'), of each tube.

When scaling units are used in series, each Dekatron tube has to be reset separately, but the counting switch of the first unit controls the series, providing succeeding count switches are left on.

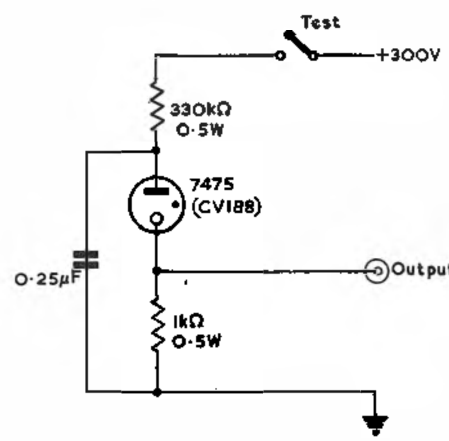

Fig. 3. A simple neon test pulse generator

Constructional Notes

The scaling units are constructed on the 'plug-in' principle. Each unit is a complete chassis, with front panel, and has a 6-pin miniature Jones type plug at the rear, which transmits all the necessary power supplies to the unit, and locates with a socket on the main framework.

This main framework carries the stabilized power supply, and allows a ventilating current of air to flow upwards by convection to cool the respective units. If necessary, the top of the cabinet can be fitted with an exhaust fan, if over-heating is experienced.

Fig. 3, shows a simple neon test pulse generator which can be incorporated in one of the front panels to test individual scaling units.

The main framework has at the rear a row of six 6-pin sockets, which supply power to any quenching probe units, or cathode-followers, if required.

MARINE RADAR SIMULATORS

Marine navigational training undertaken at sea under watchkeeping conditions is invariably prolonged, and, in consequence, expensive. Many problems of navigation arise only very occasionally, so that a navigating officer, despite lengthy experience, may find himself faced by a situation with which he is totally unacquainted. These conditions apply particularly in darkness or fog, when normal navigational hazards are multiplied and when safe navigation is dependent upon rapid interpretation of radar information.

Such situations are often difficult, possibly dangerous, to simulate at sea—and certainly very costly. To overcome the many obstacles involved, Marine Radar Simulation is now being introduced.

This simulation equipment, under the direction of a controller, allows a student navigator to perform tactical and collision-avoidance exercises, entirely by radar, within a training school. The results of such exercises can be rapidly analysed upon completion without setting into motion any operational radar organization, and can be watched throughout every stage by a controller, classes of students, or examining officers.

In operation, radar evidence of various types of ships, aircraft, coastlines and fixed objects can be presented by artificially-generated radar signals controlled by an instructor, who may impose a continually changing series of navigational situations which must be interpreted by the student operator. In turn, the operator will call for the necessary alterations of course and speed, behaving in all respects as if he stood before the radar screen of a seaborne vessel. On his display screen he will see the results of his calculations, assisted by compass and speed indications repeated from the controller's console. The alterations demanded by the operator will not be realized immediately; an inertia period is imposed to simulate the inherent delay in achieving changes of speed or heading, but his repeater-indicators will keep him informed of his own vessel's actual speed or course at any specific moment.

The controller, who accepts the student operator's directives, may be similarly equipped with a display screen, although if he is situated in close proximity to the operator this additional screen may be deemed unnecessary. The controller also commands facilities for displaying the normal echoes of coastlines, estuaries and other static geographical characteristics, and may apply up to six additional vessels, with which the parent ship—controlled by the student operator—may enter into evasion or interception exercises.

Further monitor screens can be remotely sited to provide a display identical to that of the operator's, allowing an audience of other students or examiners to follow and analyse each exercise as it progresses.

A marine simulator embodying these features has recently been introduced by the Special Products Division of Ultra Electric Ltd and comprises the following units.

Realistic Motion Computer Unit (Parent Vessel)

This computer is intended for use as the radar parent ship and is provided with simulated inertia to impart realistic delay and overshoot in response to helm and engine. Manual controls are provided for

(a) Rate of turn: Calibrated Port and Starboard 0 to 90°/minute or any other desired rate.

(b) Speed: Calibrated Ahead 0 to 25 knots, and Astern 0 to 5 knots.

(c) Set tonnage: Calibrated 2 000 to 50 000 tons. This introduces the realistic delay and overshoot to changes in (a) and (b).

The unit computes northing and easting velocity vectors of the chosen speed and rate of turn, while provision is made for ship's head to north stabilized axis transformation. A heading indicator (angle of ship's head to compass) and a speed indicator are also incorporated in this unit.

Simple Motion Computer Unit (Ship-Target Echoes)

This unit is designed for use in radar target ship simulation and is identical in all respects to the Realistic Motion Computer except that the simulated inertia and axis transformation elements are omitted. It is possible with this computer to rapidly set the course of the target to any direction, straight or turning, and to select a speed within the specified range. The northing and easting velocity vectors for this course and speed are then computed.

Relative Position Data Computer Unit

Northing and easting velocity vectors of the parent ship and the target ship are fed into this unit, which computes the difference velocity vectors, integrates to find the

The Ultra marine radar simulation equipment showing (left) a true motion unit, (centre) a p.p.i. display and (right) a control console

northing and easting difference distance vectors relating to the initial target positioning of the p.p.i., and then determines the bearing and range of the target-ship from the parent ship. The computed range and bearing information, together with the radar set trigger pulse, are used to operate bearing and range gates and effect the generation of a suitably delayed target pulse for display on the p.p.i. A relative bearing indicator and a relative range indicator, together with their manual setting-up controls, are provided on the front panel of this unit. The operation of these indicators and controls enables the target ship to be imposed in any position on the p.p.i. within a radius of 24 nautical miles from the parent ship.

Electronic Unit

This section houses all electronic circuits responsible for the simulation or facsimile of echoes and effects, including sea clutter and earth-curvature impression, which are applied to the p.p.i.

True Motion Unit

From the instant of switching to True Motion presentation, this unit integrates the northing and easting velocity vectors of the parent ship, to determine course and speed, and generates off-setting signals to move the origin of the p.p.i. time-base to reproduce this course and speed.

Coastal Mapping Unit

A flying spot scanner c.r.t., optical system, position-following mechanism, a photo-electric device and photographic transparency are used to generate realistic ground return radar signals. Any desired operational area can be selected and prepared on a photographic transparency for presentation on the p.p.i. A manoeuvring area of 525 square miles is provided while the picture element discrimination is better than 100 yards. This unit is particularly valuable for the training of operators in the use of radar for coastal, estuary, harbour and river navigation.

P.P.I. Display Unit

Two types of p.p.i. display units can be supplied, one for use as a picture-display repeater and the other being a complete p.p.i. display unit as used in a radar set to effect complete simulation for training purposes. The picture-display repeater may be employed in enabling groups of pupils or examiners to study the radar display during the progress of the exercise. The complete p.p.i. display unit embodies all the major features of existing marine radar equipments. It enables pupils to receive a comprehensive radar training, after which they should rapidly adapt themselves to the operation of any marine system.

A marine simulator equipment has also been produced by Redifon which provides similar facilities. The radar display unit is a standard equipment such as is carried operationally. The one used at present is a Decca type 45, a typical shipborne navigation radar, but other makes and types can be accommodated. The unit is employed without modification and the usual controls such as focus, brilliance, range-change, gain, anti-clutter, function in the same way as those on live radar. Two targets are provided as standard, but more can be added, six being a convenient optimum in terms of power requirement and ease of handling. Up to six display units can be provided for if required. By fitting a True Motion Display unit and associated control units, this aspect of training can also be covered. This permits the parent ship to be viewed as moving in accordance with the controls while the coastline remains stationary. A coastline generator unit is supplied as an integral part of the equipment. The coastline to be presented is reproduced as a photographic sheet which is scanned by a moving head actuated by the parent ship controls. This sheet may be withdrawn and replaced by a different one in a matter of a few seconds. The instructor can set in tide strength and direction to affect the parent ship only, causing appropriate drift. This facility which functions only with the relative motion display is useful in estuary navigation against fixed objects.

A New Submarine Cable to Belgium

A new submarine cable equipped with three submerged repeaters is being laid between Dumpton Gap in Kent and Middelkerke, a point on the Belgian coast about six miles from Ostend. The cable system will provide 120 telephone circuits between Canterbury and Ostend and will interconnect at these points with the national networks to provide two supergroups each of 60 telephone circuits between London and Brussels.

The submarine cable is coaxial with Polythene insulation 0·935in in diameter and 55 nautical miles in length. The inner conductor consists of a centre core of 7 copper strands with an overall longitudinally-folded copper tape of external diameter 0·26in. The Polythene insulation has a diameter of 0·935in over which the outer conductor consisting of 6 copper tapes is applied helically with an overall copper binding tape.

The three submerged repeaters will be spaced at intervals of about 19 nautical miles. Housed in cylindrical steel containers of a type similar to those used in the Newfoundland to Canada section of the Transatlantic cable, they will amplify the signals in both directions of transmission over the cable.

The submerged repeaters are energized at each end of the system by d.c. fed over the centre conductor of the cable from power units providing a closely regulated constant current supply. Normally both units are in operation giving double end feeding, but either unit is capable of running the whole system in the event of failure of the other unit.

Special terminal equipment for the submarine cable system is installed in the repeater stations at Canterbury and Ostend. In the Canterbury to Ostend direction the 120 telephone channels are transmitted in the frequency range 60 to 522kc/s and in the reverse direction transmission is in the range 672 to 164kc/s. Pilot frequencies 4kc/s from the edge of each band are permanently transmitted over the system to provide continuous monitoring and control of the performance of the system.

The submerged repeaters have been manufactured by Standard Telephones and Cables at their Woolwich factory and the submarine cable by the same company at their new cable factory at Southampton.

LETTERS TO THE EDITOR

(We do not hold ourselves responsible for the opinions of our correspondents)

Oscilloscope Pre-amplifier

DEAR SIR,—The transistor amplifier shown in Fig. 1 is a convenient pre-amplifier (gain $\times 20$) for use with oscilloscopes. The feedback pair[1] can be designed to be insensitive to variation in transistor parameters, supply voltage, and temperature, to within the accuracy necessary for oscilloscope use ($\sim$2 per cent). The switch S_1 connects input A directly to output B in the off position, and inserts the amplifier in the on position.

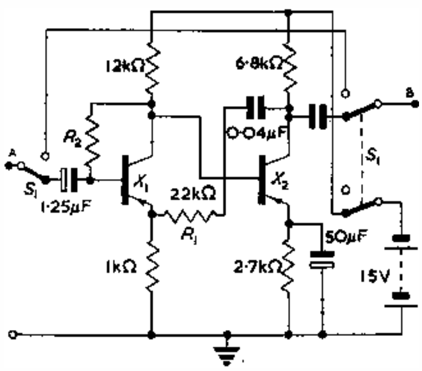

Fig. 1. The transistor amplifier circuit

The use of a relatively high supply voltage ($\sim$15V) and a high gain without feedback (>1 000) ensures that the only critical components are the two resistors R_1 and R_2.

The divider consisting of R_1 and the 1kΩ emitter resistance of X_1 fixes the overall gain. With R_1 a 10 per cent tolerance 22kΩ resistor, trimmed with a second 10 per cent resistor in parallel, the overall gain can be set accurately at 20. R_2 fixes the d.c. levels through the amplifier. Provided X_1 has a high current gain (>40), R_2 is not critical, and one fixed value (220kΩ) will serve for a range of transistors, giving approximately 1mA collector current in each transistor and voltage levels which are insensitive to supply voltage charges and temperature.

In a particular example (overall size 1¼in × 2in × 2½in), the performance for various types of transistor (with no change of component values) is shown in Table 1.

For various transistors of the same type, slight variations can be expected in the high frequency 3dB point. The noise level referred to the input is approximately 0·1mV peak-to-peak. The low frequency 3dB point can be reduced at the expense of higher noise level.

This amplifier is a useful accessory when measuring transistor parameters, particularly h_{12e}, by the voltmeter-ammeter method using an oscilloscope[2].

Yours faithfully,

R. E. AITCHISON,
Electrical Engineering Department,
University of Sydney.

REFERENCES

1. SCHENKERMAN, S. Feedback simplifies transistor amplifiers. *Electronics.* 27, 129 (1954).
2. IRE Standards on Solid-State Devices, Methods of Testing Transistors. *Proc. Instn. Radio Engrs.* 44, 1542 (1956).

TABLE 1

Gain = × 20

TRANSISTOR TYPE	INPUT IMPEDANCE at 1kc/s	3dB POINTS	FREQUENCY FOR AN INPUT IMPEDANCE OF 10kΩ
0C71	100kΩ	10c/s—95kc/s	75kc/s
0C45	100kΩ	10c/s—500kc/s	250kc/s
0C44	100kΩ	10c/s—600kc/s	280kc/s

A Simple Shaft Digitizer and Store

DEAR SIR,—In an article in the December 1957 issue, Mr. Tiffany attributes to the writer an empirical expression relating the apparent length of electrical contact in a ball-contact type of shaft digitizer to the mechanical length of the contact (p. 572, "Wear Testing").

In point of fact, the writer merely communicated the result to Mr. Tiffany. The expression was derived by Mr. E. R. Dymott of this establishment who noted that a series of results from experiments he was conducting could be usefully approximated over a reasonable range by the expression quoted.

Mr. Tiffany does not quote the constants of the expression; Mr. Dymott's complete expression is as follows:

$$\Delta L = 1{\cdot}4 + 0{\cdot}06P + 0{\cdot}014V - 0{\cdot}04i$$

Where P is the load on the ball contact (grams)

V is the voltage (volts)

i is the current taken (mA)

ΔL is the apparent increase in the total length of the contact (in units of 0·001in).

The expression applies to a 1/16in diameter stainless-steel ball contact working over a solid brass coded plate filled with Araldite 103. It was found to be valid for voltages up to 80V and for currents in the range 5 to 12mA. The valid range probably extends above 12mA. and possibly below 5. It is certainly incorrect for a current of 1mA.

As Mr. Tiffany so rightly points out, this effect sets an absolute lower limit to the length of electrical contact.

Yours faithfully,

W. T. BANE,
Control Mechanisms and Electronics Division,
National Physical Laboratory.

The author replies:

DEAR SIR,—I am most grateful to Mr. Bane for correctly attributing this most useful and interesting result, which is I believe, published fully for the first time here—hence my reluctance to quote more detail. The result shows clearly an ultimate limitation to the resolution of contact digitizers and confirms the view taken by Colvile in a recent correspondence[1], that optical and other non-contact types are more apt for very high resolution developments.

Yours faithfully,

A. TIFFANY,
Aircraft Research Association,
Bedford.

REFERENCE

1. COLVILE, R. F. Binary Coded Digitizers. *Electronic Engng.*, 30, 99 (1958).

The Reactance Valve at Audio Frequencies

DEAR SIR.—With regard to Dr. Alcock's useful article in the February issue, I should like to draw his attention to what appear to be minor misprints towards the end. Immediately under Equation (7), the expression should **read:**

$$d(1/Q)/dC = -(1/\omega C^2R) - (1/\omega C^2R_1) + (\omega R/g_m R_a)$$

and this leads to

$$\omega C = \sqrt{\left[\left(\frac{R+R_1}{R^2R_1}\right)g_m R_a\right]}$$

Finally, the expression for the mutual conductance should surely omit the factor 10^{-3}.

Yours faithfully,

J. E. ROBSON,
Cranleigh.
Surrey.

The author replies:

DEAR SIR,—I wish to express my thanks to Mr. Robson in pointing out the misprints in my recent article, for which I must apologize. The expression for $d(1/Q)/dC$ is as he has stated, as is that for ωC; though the form I have found most useful is:—

$$C = \sqrt{\left[\left(\frac{R+R_1}{R_1}\right)g_m R_a\right]}\Big/\omega R$$

In the expression for the mutual conductance it might perhaps be more consistent, in view of the arithmetic computation to write :—

$g_m = 9{\cdot}3 \times 10^{-3} \times 0{\cdot}94$ mhos.

Yours faithfully,
B. J. ALCOCK,
Bangor,
North Wales.

Pascal's Triangle and L-Type Ladder Lines

DEAR SIR,—In view of the interest shown recently in Mr. J. Forejt's table of coefficients[1,2,3] it may be of some use to point out that this table is just the table of binomial coefficients (n/r), usually known as Pascal's Triangle, as may be seen by reading the table diagonally.

Mr. Forejt's results is that:

$$\begin{bmatrix} 1+YZ & Z \\ Y & 1 \end{bmatrix}^n = \begin{bmatrix} C_{11}^{(n)} & C_{12}^{(n)} \\ C_{21}^{(n)} & C_{22}^{(n)} \end{bmatrix}$$

$$C_{11}^{(n)} = C_{22}^{(n+1)} = \sum_{r=0}^{n} \binom{n+r}{2r} Y^r Z^r$$

$$C_{12}^{(n)}/Z = C_{21}^{(n)}/Y = \sum_{r=0}^{n-1} \binom{n+r}{2r+1} Y^r Z^r$$

and this may most easily be proved by induction.

The coefficients which one picks from Pascal's Triangle, in the manner given by Mr. Forejt, are simply

$$\binom{n+r}{2r} \text{ and } \binom{n+r}{2r+1}$$

Yours faithfully,
D. T. SWIFT-HOOK,
Research Laboratories,
The General Electric Co. Ltd.

REFERENCES

1. FOREJT, J. Jednoduchy vypocet nekterych matic ctyrpolu. *Slabopr. Obz.* 155, 8 (1947).
2. FOREJT, J. L-Type Iterated Networks. *Electronic Engng.* 29, 455 (1957).
3. ROBSON, J. E. L-Type Iterated Networks. *Electronic Engng.* 29, 558 (1957).

The correspondent replies :

DEAR SIR,—The relationship of my scheme to the Pascal's triangle is evident and already known. The advantage of my inductive derivation is in easier application of columns for evaluating the coefficients for single terms of matrixes and the scheme is for this purpose mnemotechnically preferable. The general form of coefficients, as stated by Mr. Swift-Hook may be of use for simple expressions without complete evaluation of my scheme. It can lead to further theoretical conclusions too.

Yours faithfully,
JINDRICH FOREJT,
Faculty of Radiotechnics,
Podebrady,
Czechoslovakia.

Measurements of the Characteristic Impedance of a Coaxial Cable

DEAR SIR,—Mr. L. B. D'Alton's article in the January issue, has prompted me to send you a description of an even simpler method for the same kind of measurement, which I developed a year ago. In this method, I measure the characteristic impedance and the velocity of propagation in cables by means of a grid dip meter and a small capacitor of known value, as may be seen from the theory described below.

The input impedance Z_s of an open-circuited low loss transmission line having a length d is $Z_s = -\mathrm{j}.R_c.\cot\beta d$ where R_c is its characteristic impedance, and $\beta = 2\omega f/cp$ f is the frequency, c the velocity of light in vacuum, and p the retardation in the line.

With a grid dip meter loosely coupled to a small loop soldered to the input of the line, there is a dip every time Z_s passes through zero. Let f_0 be the frequency when the first zero of Z_s occurs.

Then $\quad Z_s = -\mathrm{j}.R_c.\cot\beta_0 d = 0$

$$\beta_0 d = \pi/2$$

$$2\pi f_0 d/\mathrm{pc} = \pi/2$$

$$p = 4f_0 d/cp$$

Terminating now the same length d of the same line with a small known capacitance C, we determine the frequency f_1 when the first zero of Z_s occurs. So

$$Z_s R_c.\frac{1/\mathrm{j}.\omega_1.C + \mathrm{j}.R_c.\tan\beta_1 d}{R_c \mathrm{j}.\tan\beta_1 d/\mathrm{j}.\omega_1.C} = 0$$

$$\therefore 1/\mathrm{j}.\omega_1.C\mathrm{j}.R_c.\tan\beta_1 d = 0$$

$$\therefore R_c = \cot\beta_1 d/\omega_1.C$$

where $\omega_1 = 2\pi f_1$ and $\beta_1 = 2\pi f_1/pc$. or

$$R_c \frac{\cot 2\pi f_1 d/pc}{2\pi f_1 C}$$

The precision of these measurements depends on the determination of the frequencies f_0 and f_1. Good grid dip meters permit measurements with errors of the order of 1 per cent. Besides, it is always possible to verify f_0 and f_1 with a wavemeter of a better class, or a good communications receiver.

The arrangement of Mr. D'Alton (Fig. 1, *art.cit.*) also permits the measurements of frequencies when zeros of Z_s occur. So, it could be used in a determination of R_c and p by the method explained. In this case, it is more convenient to use an r.f. voltmeter in place of the receiver.

The grid dip meter has the advantage of permitting measurements in balanced lines.

In the following example, a sample of coaxial cable with $d = 4{\cdot}35$m was measured. The first zero was found at $f_0 = \ldots$ 11·2Mc/s (open-circuited cable). Thus

$$p = 4f_0 d/pc \ 0{\cdot}65 \text{ (nominal: } 0{\cdot}66).$$

Terminating the cable by $C = 150$pF the first zero was found at f_1 7·7c/s. Thus

$$R_c = \frac{\cot 2\pi f_1 d/pc}{2\pi f_1 C} \ 73{\cdot}6\Omega \text{ (nominal : } 75\Omega).$$

Yours faithfully,
A. H. GUERRA VIEIRA.
Depart. de fisica, Escola Politechnica,
Sao Paulo, Brazil.

The author replies :

DEAR SIR,—I was interested to read Mr. A. H. Guerra Vieira's description of his cable-measuring technique and was impressed by its simplicity. There appears, however, to be a small but significant error inherent in the system.

If L_2 is the inductance of the loop soldered to the cable and R_2 its effective resistance and if M is the mutual inductance between the grid dip oscillator's coil L_1 and the loop then the coupling transfers into the primary side a resistance $R_T = \omega^2 M^2/Z_2^2$ and an inductance $L_T = -\omega M^2/Z_2^2 X_2$ where $Z_2^2 = R_2^2 + X_2^2$ and $X_2 = \omega L_2 - R_c \cot\beta d$. Now if $L_2 = {\cdot}01$ μH (which is approximately the inductance of a ½in loop) and if $Q_2 = \omega L_2/R_2 = 100$ and $L_1 = 15\mu H$ (which are representative values) then for the 4·35m 75Ω cable in question for which $p = {\cdot}65$ the table shown below may be compiled.

The first case above is interesting in that the primary inductance is effectively halved. Admittedly the coupling factor k is rather too high to be representative but the looser coupling $k = {\cdot}007$ gives the same relative effects and it is quite clear that the dip occurs not at $\beta d = 90°$ but at $\beta d = 89{\cdot}48°$ (i.e., 0·6 per cent low.)

Further, because of L_T the actual frequency is higher than the indicated frequency by about ·02 per cent in the third case above. This error though small adds to the error in βd in making the indicated value of p about ·62 per cent too low.

The same arguments apply but the errors which are cumulative with one another and with the error in p above become more serious. The dip occurs not when Z_S (with the 150pF termination) becomes nearly equal to ωL_2 and by graphical methods I find that this occurs for the 75Ω cable when the frequency is 7·73Mc/s.

But if R_c is actually 75Ω the frequency which makes Z_S zero is 7·68Mc/s. Therefore, the value assigned to f_1 in your correspondent's final formula would be 0·7 per cent high which with the error in p makes cot $\beta_1 d$ 3·8 per cent low and produces an error in R_c of −4·5 per cent. Frequency 'pulling' will reduce this error but the reduction will be slight.

I appreciate Mr. Vieira's suggestion for using the circuit of Fig. 1 (*art.cit*) for the determination of the condition $Z_s = 0$ and I believe such an arrangement would, given a sensitive r.f. voltmeter, yield very accurate results.

Yours faithfully,
L. B. D'ALTON,
Department of Electrical Engineering,
University College,
Dublin.

βd	$M(\mu H)$	k	$R_T(\Omega)$	$L_T(\mu H)$
89·48°	40×10^{-3}	0·1	365	−7·5
90°	40×10^{-3}	0·1	0·112	−0·16
89·48°	$2{\cdot}74 \times 10^{-3}$	0·007	1·7	$-0{\cdot}35 \times 10^{-3}$
90°	$2{\cdot}74 \times 10^{-3}$	0·007	$0{\cdot}53 \times 10^{-3}$	$-0{\cdot}75 \times 10^{-3}$

BOOK REVIEWS

Synthesis of Passive Networks

By E. A. Guillemin. 741 pp. 462 figs. Medium 8vo. John Wiley & Sons Inc., New York. Chapman & Hall Ltd, London. 1957. Price 120s.

SIX years ago, Professor E. A. Guillemin of the Massachusetts Institute of Technology published the first of a series of volumes on the modern theory of electric networks. With the title *Introductory Circuit Theory*, the first volume provided a complete course of instruction in the fundamentals of linear network analysis from the modern point of view. This was to be followed by a volume dealing with Fourier and Laplace transformation theory and network synthesis at an introductory level, but work on this volume was interrupted in order to accelerate the publication of the third volume, *Synthesis of Passive Networks*, which, the author believed, was more urgently needed.

Network synthesis is network design by a process which is the reverse of network analysis. In the latter we proceed from the network (a mathematical structure abstracted from the physical system) to a statement about its behaviour. In synthesis this procedure is reversed; the datum is a statement about behaviour from which we proceed to a network. The process involves the solution of two separate problems; the first is the analytical characterization of the desired network behaviour in the form of a rational function of complex frequency (the approximation problem) and the second is the determination of the topology and constituent elements of a network whose behaviour corresponds exactly to the selected function (the realization problem). The term synthesis is reserved for the design of networks in this way. The old-established technique of constructing a network according to remembered and recorded information and subsequently developing the arrangement until satisfactory agreement with the specification is obtained is not network synthesis. Once an acceptable rational approximation of the required behaviour is established, the methods of synthesis lead to a design that is complete and unalterable.

Professor Guillemin's book presents the fundamental theory and describes the methods appropriate to the approximation and realization problems of network synthesis. It opens with a preface which, like that of *Introductory Circuit Theory*, reflects the author's thirty years of experience in the teaching of electrical engineering science—both prefaces should be read by every educator in the scientific field. Of the book's fifteen chapters, the first thirteen deal with the realization problem. Chapter I is concerned with the properties of driving-point and transfer impedance functions. It was Dr. Otto Brune, to whom the book is dedicated, who first examined the properties of physically realizable driving-point functions. He called such functions 'positive real'. The greater part of the first chapter of the book is devoted to a study of these functions and to methods of testing a given function for positive real character. In Chapter II the detailed characteristics of driving-point and transfer immittances of networks containing only two kinds of elements are considered. Driving-point reactance and susceptance synthesis by the methods of Foster and Cauer is introduced in the following chapter which concludes with an interesting discussion of normal co-ordinates and of particular network configurations for which these have a direct physical interpretation. Methods analogous to those of Foster and Cauer for the synthesis of dissipative single-energy driving-point immittances are developed in Chapter IV. Equivalent and reciprocal networks are the subjects of the next chapter which contains a critical examination of the transformation theory of Cauer, Howitt, and Burington which has turned out to be of less value than was supposed by its proponents.

Before proceeding to the synthesis of the general driving-point immittance the author prepares the way by devoting three chapters to two terminal-pair network theory, the synthesis of non-dissipative two terminal-pair networks, and certain relevant aspects of function theory. The last of these chapters contains a wealth of information of vital importance in network theory. Among the topics discussed is the construction of an immittance function from its real part by algebraic methods and by the use of Hilbert transforms. The synthesis of the general driving-point immittance function by the methods of Brune and Darlington are introduced in Chapter IX and in Chapter X the techniques due to Bott, Duffin, and Miyata for avoiding the appearance of mutual inductance are presented. Transfer immittance synthesis is the topic of the next three chapters. The treatment is thorough and includes an account of the realization of transfer immittances without the use of inductance.

The last two chapters deal with the approximation problem. Although the solution of this problem precedes that of the realization problem in the design of a network the author considers that familiarity with the methods of realization is necessary for a true appreciation of the problem of approximation. Chapter XIV is concerned with the rational function representation of the required network performance when this is prescribed in terms of frequency response. Approximation in terms of Butterworth, Chebyshev, and Jacobian elliptic functions is considered together with the use of Fourier methods and a method based on semi-infinite slopes. The potential analogue and linear phase approximation are also discussed. The final chapter deals with approximation when the behaviour of the network is prescribed in terms of time response.

Professor Guillemin has been closely associated with the development of network synthesis since its possibilities came to light in 1924. He has played a prominent part in bringing the subject to its present state of evolution and has at last set down the essence of the subject in a book that has been eagerly awaited in engineering circles. A further volume is promised in the preface; perhaps it will tell us something of the recent work of such contributors as Fialkow and Gerst. It is true that the methods of synthesis, in its present phase of development, are not always as convenient nor as effective as the less refined techniques in common use, nevertheless a study of the theory is worthwhile because, as the author has stated elsewhere, not only does it "broaden one's horizon with regard to the whole picture of network, but it eliminates much aimless searching for the unattainable, and sharpens the focus of our attention upon the truly relevant features of our problem."

S. R. DEARDS

The Exploration of Space by Radio

By R. Harbury Brown and A. C. B. Lovell 207 pp. 132 figs. Demy 8vo. Chapman & Hall Ltd. 1957. Price 35s.

THE authors and publishers are to be congratulated on publishing this interesting book to coincide with the completion of the Jodrell Bank radio telescope, and at a time when our interests in space are stimulated by perhaps the most exciting aspect of the International Geophysical Year, the earth satellites. The role of the Jodrell Bank telescope in tracking, by radar, the Russian earth satellites is already well known, and *The Exploration of Space by Radio* provides an up to date account of the science of radio astronomy, for the study of which the radio telescope was built.

The authors have devoted very nearly all their energies, since the war, to researches in radio astronomy, and are very competent to write this book, which they have accomplished in a clear and lucid style. The book, which is written for scientists rather than for the layman, has three introductory chapters to familiarize the reader with the relevant aspects of astronomy, radio waves, and the techniques of radio astronomy respectively. Then follow chapters, listed here in order of length, on the following subjects; meteors; galactic and extragalactic radio emissions; solar radio waves; radar investigations of the moon, planets and earth satellites; the 21cm hydrogen line; the scintillation of radio stars; the Jodrell Bank radio telescope; and the Aurora Borealis.

The chapter on solar emission of radio waves is not as comprehensive nor as up to date as the rest of the book, and it might have been an advantage to devote a larger proportion of the text to this, and to galactic and extragalactic emissions rather than to meteors. It is also unfortunate that no photograph of the Cambridge interferometer aerial, which has already located nearly 2 000 radio stars, is included, when there are ten photographs of the Jodrell Bank telescope.

Apart from the minor lapse of figure 33 on page 48, *The Exploration of Space by Radio Waves,* is an excellent book and is to be recommended.

B. ELSMORE

Dictionary of Electronics and Waveguides

By W. E. Clason. 600 pp. Demy 8vo. Elsevier publishing Co., New York, Princeton, Amsterdam. Cleaver-Hume Press Ltd. 1957. Price 90s.

THE dictionary contains over 2 000 words in its basic list. This list, in which terms are defined in English, clearly distinguishes between American and British usages. Each term is set in its proper subject field and defined according to the most precise international standard available. Corresponding terms in French, Spanish, Italian, Dutch and German then appear, arranged horizontally across the facing page. At the end of the book an alphabetical list for each of the other languages gives numerical keys to the basic English word list. In order to assure maximum usefulness for this dictionary, certain principles proposed by UNESCO have been used as a guide so that this volume will fit into a pattern which will ultimately cover all interrelated fields and all necessary languages.

The BEAMA Catalogue

962 pp. Large Demy 4to. 4th Edition. Published for The British Electrical & Allied Manufacturers' Association, Inc., by Iliffe & Sons Ltd. 1958. Price £6.

THIS edition has been produced earlier than usual so that copies will be available for distribution at the Brussels Universal and International Exhibition where the British Electrical and Allied Industry have a large collective exhibit in the British Industries Pavilion.

The descriptive catalogue pages have been designed throughout to a standard format, each division being printed in a distinctive second colour. The profusely illustrated announcements display the products manufactured by member firms. The divisions are classified as (A) Electrical Power Plant (blue); (B) Electrical Equipment in Industry, Transport and Communications (maroon) and (C) Domestic and Commercial Electrical Appliances, Lighting, Accessories and Installation Material (orange).

In addition to the comprehensive catalogue, separate supplementary volumes of Divisions A, B and C, including the complete trade directory of all member firms, have been made available for special use at the Brussels Exhibition.

A five language glossary of technical terms used in the Buyers' Guide is included to help overseas buyers not fully conversant with English terminology. Product headings are listed in English, French, German, Portuguese and Spanish, thus providing a comprehensive cross-reference in five languages.

The Classified Buyers' Guide lists under more than 1 300 headings the comprehensive range of electrical and allied equipment manufactured by BEAMA firms.

The Trade Directory gives the principal addresses of all BEAMA member firms in the United Kingdom, subsidiary or branch offices, etc., and over 4 780 names and addresses, grouped territorially, of member firms' overseas branches, representatives and agents. A list of addresses of the BEAMA overseas committees is also given.

Wireless and Electrical Trader Year Book 1958

372 pp. Demy 8vo. 29th Edition. Trader Publishing Co. Ltd. 1958. Price 12s. 6d.

THIS Year Book was first published in 1925 and is the standard guide for all connected with sales or services, and of great assistance to overseas buyers wanting to contact British sources of supply.

Features of the new edition include condensed specifications of nearly 250 current commercial television receivers, and information on valve and cathode ray tube base connexions, with over 300 valve base diagrams.

New features are a section giving brief specification details of tape recorders and information on Band 3 convertors. The special section giving both alphabetical and territorial lists of radio and electrical wholesalers, in which association members are indicated, is again included, as also is the comprehensive table of television tuning frequencies of superhet receivers and sideband characteristics of superhet and t.r.f. models.

Telecommunication Economics

By T. J. Morgan. 452 pp. 50 figs. Demy 8vo. Macdonald & Co. (Publishers) Ltd. 1958. Price 50s.

CERTAIN aspects of the economics involved in the engineering of public utility plant, such as the provision of external line plant for the telephone service, have been covered in various technical journals. This book attempts an application of the general principles to investigate the economic merits of alternative engineering schemes, particularly those arising when planning large utility schemes. Although the work is addressed mainly to telecommunications engineers, it is felt that the methods suggested are applicable to other utility organizations. There is a foreword by Brigadier Sir Lionel H. Harris, K.B.E., T.D., M.Sc., M.I.E.E., Engineer-in-Chief, General Post Office.

CHAPMAN & HALL

Ready 17 June

TELEVISION IN SCIENCE AND INDUSTRY

by

V. K. Zworykin
E. G. Ramberg
L. E. Flory

A JOHN WILEY BOOK

312 pages *Illustrated* *80s. net*

CONFORMAL TRANSFORMATIONS IN ELECTRICAL ENGINEERING

by

W. J. Gibbs
D.Sc., M.I.E.E.

227 pages *Illustrated* *45s. net*

37 ESSEX STREET, LONDON, W.C.2

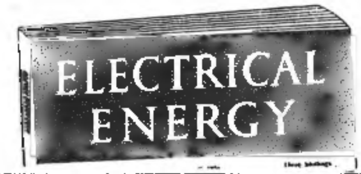

For the Advancement of Electrical Science

ELECTRICAL ENERGY is a monthly technical journal for electrical engineers having a scientific turn of mind. Its articles are designed to bridge the gulf between research and the practical application of the knowledge so gained to industry. Bringing up-to-date information about new theories, methods and materials, it is of inestimable value to electrical designers.

Annual subscription £1 . 16 . 0d.
Single copies 3s. 0d.

Order from your newsagent or direct from—

MORGAN BROTHERS (Publishers) LTD.,
28 Essex St., Strand, London, W.C.2

ELECTRONIC EQUIPMENT

A description, compiled from information supplied by the manufacturers, of new components, accessories and test instruments.

UNIVERSAL COUNTER

(Illustrated below)

Racal Engineering Ltd, Western Road, Bracknell, Berkshire

The computing counter controller type SA.501 uses only ferrite core and transistor techniques in the counting circuits and has an easy to read in-line display. It may be used for the measurement of frequency or time intervals or for batch counting and control.

It will count random pulses at up to 50kc/s with an accuracy of $\pm$ 1 count $\pm$ crystal stability, maximum registration being 9999. The time-base is variable from 1msec to 10sec in 1msec intervals. Both mains operated and battery operated versions of the counter are available.

In addition to its uses as a counter, frequency meter or chronometer the instrument can be used as a pulse frequency divider whereby it will divide

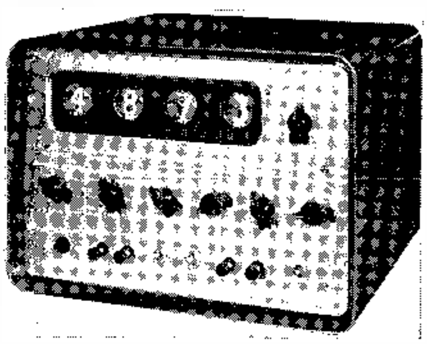

any input frequency up to 10kc/s by any factor from 2 to 10 000 according to the setting of the selector switches. It may also be used as a pulse delay generator: the desired delay is set up on the time-base selectors, the initial pulse is applied to the 'start' terminal and, after the desired delay, an output pulse is produced.

A.M. SIGNAL GENERATOR

(Illustrated above right)

Marconi Instruments Ltd, St. Albans, Hertfordshire

The TF 801C is the latest in the range of precision a.m. generators produced by Marconi Instruments. Its salient features include a frequency cover of 10 to 500Mc/s with 0·5 per cent tuning accuracy, a built-in crystal calibrator, exceptionally low spurious f.m. and a high-quality 50Ω output with a v.s.w.r. of less than 1·2.

Its carrier level is continuously variable from 0·1μV to 0·5V, and 1kc/s sine-wave a.m. may be applied internally at any depth up to a maximum which is at least 30 per cent and, at most carrier frequencies, is 90 per cent. An alternative 'high' output condition yields a maximum of 1V modulated or 2V unmodulated at most frequencies.

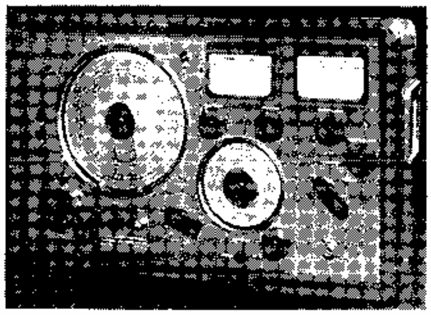

Modulation may also be applied externally. For sine-wave inputs, the modulation frequency range is 30c/s to 20kc/s and the modulation depth is monitored up to 90 per cent. For pulse inputs, the modulating circuit is d.c. coupled and will accept p.r.f.'s up to at least 50kc/s.

The main tuning dial, with its approximately 75in of scale, allows fast and accurate reading; the auxiliary incremental dial—driven from the single tuning control—allows precise and easy interpolation for bandwidth measurements. Output stability during tuning is ensured by an automatic level control system.

The circuit includes a tuned power amplifier and gives an r.f. output of unusual purity. Modulation is applied to the power amplifier without disturbance to the operating parameter of the master oscillator—the low incidental f.m. and good response to pulse modulation are due to this arrangement.

CABLE FAULT LOCATOR

(Illustrated below)

H. Tinsley & Co. Ltd, Werndee Hall, South Norwood, London, S.E.25

This instrument, type 5335, utilizes a conventional Wheatstone bridge circuit in which the two sections of the faulted conductor, one on each side of the fault, comprise the two external arms of the bridge. The other two arms are contained within the instrument. By use of a detector circuit of extremely high input resistance, it is possible to locate high resistance faults without loss of sensitivity. With this bridge arrangement faults having resistance from zero up to

at least 200MΩ in dielectrics such as rubber, and much higher in the case of polyethylene, can be located with an accuracy well within $\pm$ 0·5 per cent a typical error being 6in in 500ft or $\pm$0·1 per cent.

A guard terminal is provided so that the effect of surface leakage on accuracy may be eliminated and in extreme cases corrections for internal cable leakage may easily be applied.

Coarse and fine controls are provided for initially balancing the bridge under shorted input conditions. The bridge is balanced under measuring conditions by adjustments of a precision potentiometer having ten rotations for full travel. A robust pointer meter is used as the null indicator.

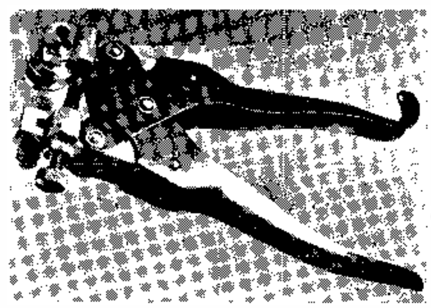

CABLE STRIPPING PLIERS

(Illustrated above)

Creators Ltd, Plansel Works, Sheerwater, Woking, Surrey

These new roller type cable stripping pliers have been designed to remove the insulation from cables of $\frac{1}{8}$in to $\frac{3}{4}$in diameter.

The cable passes over an aluminium V-pulley in one of the jaws and is guided in a straight line along the inside of a shaped handle. The other jaw carries a replaceable steel stripping blade and an adjustable and lockable stop-screw which prevents the blade from cutting into the cable core.

Three blade positions and two roller positions are provided to accommodate cables of different diameters, and the blade clamping plate can be adjusted to limit the depth of the cut. Two sizes of roller are available, the smaller for cable diameters from $\frac{1}{8}$in to $\frac{3}{8}$in and the larger for diameters from $\frac{3}{8}$in to about $\frac{3}{4}$in; rollers for special cable sections can be made up as required.

GENERAL PURPOSE COUNTER

(Illustrated above right)

Airmec Ltd, High Wycombe, Buckinghamshire

General purpose counting equipment type 1339A has been designed and developed in conjunction with the United Kingdom Atomic Energy Research Establishment to provide comprehensive scaling facilities for geiger and scintillation counters used for the

accurate assay of alpha, beta and gamma active samples.

Two main units form the basic equipment and these may be supplemented by suitable accessory sub-units for beta, gamma counting to serve any of the alcohol quenched types of counter and most types of halogen quenched counters, or for alpha counting and scintillation type probes.

Of the two main units, the power unit provides all the power supplies, including stabilized e.h.t. for the basic equipment and all necessary equipment. The scaling unit, which is the second of the two units referred to, consists of a slow scaler sub-unit and a paralysis/timing sub-unit. It also has incorporated a dummy panel and adaptor panel which are replaced by the accessory units when required. Essential features of the basic equipment include facilities for slow speed scaling and a choice of paralysis times, together with an automatic timing control.

Accessory equipments include a quenching sub-unit for use with geiger counters for beta gamma counting, and an amplifier/discriminator sub-unit for alpha counting with scintillation type probes. A fast scaler sub-unit may also be provided where the sample disintegration rate is high.

Adequate reliability of all the scaler sub-units is ensured by the periodic operation of a built-in test facility in the scaling unit to check the performance under marginal circuit conditions. A meter system is provided in the power unit for routine checking of supply voltages.

WAFER SWITCH

(Illustrated below)

Walter Instruments Ltd, Garth Road, Morden, Surrey

The new type G.E. switch has been designed for radio band-change and instrument circuit switching where space is restricted.

This switch occupies a space of less than $1\frac{1}{2}$in diameter to a depth ranging from $\frac{1}{2}$in for a single wafer to a maximum determined by the number of wafers and spacings. Constructed on a contact clip and knife action rotor blade principle, special measures are incorporated to ensure rigid contact fixing and positive indexing. Both sides of the wafer may carry completely insulated contacts, and 22 contact positions are available.

Indexed at 30°, the following switching combinations can be provided on each wafer: 1 pole, up to 12 positions; 2 poles, up to 9 positions; 3 poles, up to 5 positions; 4 poles, up to 4 positions; 5 poles, up to 3 positions. The contact rating is 250mA at 100V r.m.s.

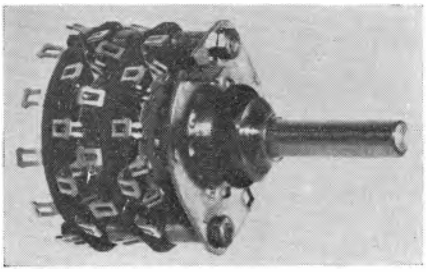

A.C. VALVE-VOLTMETER

(Illustrated below)

Advance Components Ltd, Roebuck Road, Hainault, Ilford, Essex

This valve-voltmeter is a compact and portable instrument of high performance. It incorporates a four-stage amplifier with bridge rectification to the meter. There are twelve ranges covering from 0·001V to 300V a.c. and measurements are possible down to 100μV. A very low capacitance screened lead is

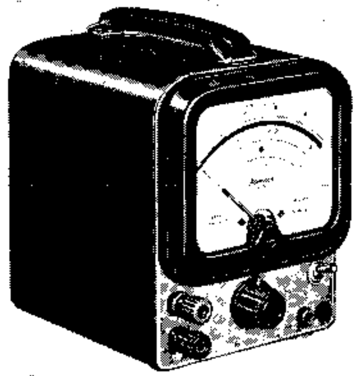

provided for use on the more sensitive ranges. The scale is calibrated in r.m.s. volts and also dB referred to 0dBm (1mW/600Ω). Measurements may be made between 10c/s and 5Mc/s and, having a high input impedance (10MΩ), it is useful for all amplifier measurements and voltage measurements generally. It can also be used as a null detector, indicator or amplifier for frequencies between 10c/s and 10Mc/s. Calibration from 15c/s to 2Mc/s is ±3 per cent ±3 per cent f.s.d. From 2Mc/s to 4·5Mc/s the meter reads within ±2dB. The Type 77 can also be used as an amplifier with a gain of 1000, adjustable in 10dB steps, up to 5Mc/s.

RADIATION WARNING INSTRUMENT

(Illustrated above right)

Radiation, 7 Sheen Park, Richmond, Surrey

A new warning device of the ionization chamber type which gives a loud warning on receiving a gamma dose of 30 milliroentgens is now available in portable form. It is a battery operated pocket type unit weighing $12\frac{1}{2}$oz. It also responds to beta rays. Headphones may also be plugged into the Monitor.

The instrument uses transistors and is also suitable for outdoor operation in

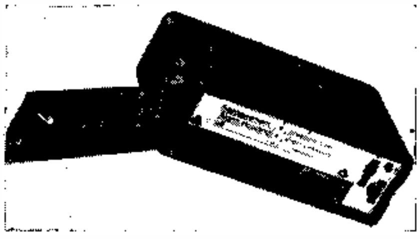

temperate climates. The batteries have a capacity of 220mAh and as they are discharged only during the emission of the signal and no current is drawn during measurement, they provide for 2 to 3 months' operation under normal conditions.

The Monitor has a flat response to radiation energies ranging from under 100kV to 3MV, an important consideration as in most cases the radiation is composed of various energies owing to Compton scatter. It is a useful supplement to the pen type dosemeter which measures the cumulative dose received by the worker, as it gives early warning of a rise in the dose rate.

U.H.F. COMMUNICATIONS RECEIVER

(Illustrated below)

Stratton & Co. Ltd, Alvechurch Road, Birmingham, 31

THE Eddystone "770U" receiver is primarily intended for communications services on frequencies between 150Mc/s and 500Mc/s.

The heart of the receiver is a specially designed miniature turret housing the inductances, and the associated ganged capacitor. Both are of course physically small, yet of robust construction and well able to stand up to the continuous usage for which the receiver as a whole is designed. The valve sockets form an integral part of the tuning assembly and, as a result, good performance is secured throughout the range of the receiver.

The first stage is an r.f. amplifier, using a 6AJ4 in a grounded grid circuit and contributing useful gain on all frequencies. The oscillator valve is a special type for u.h.f. work and operates efficiently and with excellent stability in the fundamental mode up to the highest frequency covered.

A germanium diode acts as mixer and feeds into a low noise amplifier of the cascode type, using a double triode valve This first intermediate frequency is 50Mc/s. Further amplification at 50Mc/s is provided by a pentode stage.

A double triode valve again changes the frequency to 5·2Mc/s and there are two i.f. stages operating on this fre-

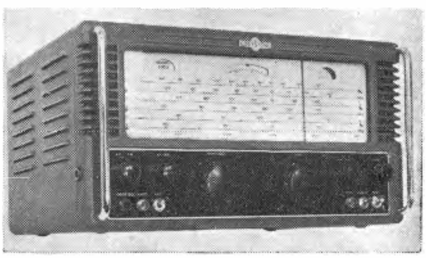

quency. Hence ample overall gain is provided.

The later stages follow conventional practice. With the switch in the 'a.m.' position, the signal is rectified by a germanium diode and then passes to the audio amplifying and output stages.

In the f.m. position of the switch, the signal is applied to a limiter valve, thence to a discriminator and finally to the audio stages. Automatic gain control can be operative at all times, while the noise limiter (switched from the panel) is effective, on a.m. in reducing noise of a pulse type.

The versatility of the "77OU" is increased by two features. One is the inclusion of an additional winding on the first i.f. transformer, so enabling a signal (at 50Mc/s) to be fed into the i.f. stages from an auxiliary r.f. head. The impedance at this point is approximately 75Ω.

The other special feature is the fitment of a cathode follower valve after the second i.f. chain. The output, at low impedance, is brought out to a coaxial socket and enables the characteristics of a signal to be examined on an oscilloscope.

SERVO-DRIVEN POSITION INDICATOR

(Illustrated above)

Sperry Gyroscope Co. Ltd. Great West Road, Brentford, Middlesex

This instrument is a self-contained unit for presenting the information obtained by a remote transmitter in a clear and unambiguous manner to a high degree of accuracy.

A fine indication is provided by means of a clear-reading centrally-positioned digital counter. Five-digit presentation is standard, but smaller maximum counts can be arranged. The relationship between the value indicated on the counter and movement of the transmitter can be arranged to suit a wide range of applications.

In order that the proportionate position of the transmitter can be seen instantaneously and without the need for interpretation a proportionate band indicator is included, consisting of a variable-length orange arc framed in the black background of the dial. This presentation is particularly valuable when the full-scale reading is less than 99 999 on the counter.

The slow-motion tell-tale consists of a disk rotating behind a window in the lower part of the dial. It indicates movements whose rates are too slow to be immediately noticeable on the counter. Lines engraved on the disk can be arranged to give the correct sense of 'up and down' or 'left and right' movement if desired.

The three presentations, together with the synchro receiver, are geared together and driven by a two-phase servomotor. An error signal caused by misalignments between the transmitter and receiving synchro is amplified in the transistor amplifier incorporated in the indicator and energizes the servomotor, which drives the indicator until alignment is obtained. A velocity-stabilizing term to prevent hunting is obtained from a tachogenerator built into the servomotor.

The cylindrical case is arranged for panel mounting with connexions at the rear by two Plessey 6-way plugs and sockets. The zero-setting control is also at the rear and therefore cannot be tampered with once the instrument is mounted.

AUTOMATIC COIL WINDING MACHINE

(Illustrated below)

Distributed by R. H. Cole (Overseas) Ltd. 2 Caxton Street, London, S.W.1

The Aumann automatic coil winding machine WPA has been developed for mass producing coils on which auxiliary operations have to be performed. Considerable reductions in winding times are achieved by the sequential winding arrangement, which enables the operator to carry out all manual operations as well as the removal of the completed coils without stopping the machine. It is also suitable for winding unsupported coils e.g. field coils, and for flanged formers, provided the same gauge of wire is used throughout and paper-interleaving and intermediate tappings are not required.

A solid base plate carries a 6 or 8 position indexing table and a headstock with a wire guide pulley on a rotating faceplate. The wire from the take-off stand is led through the hollow drive

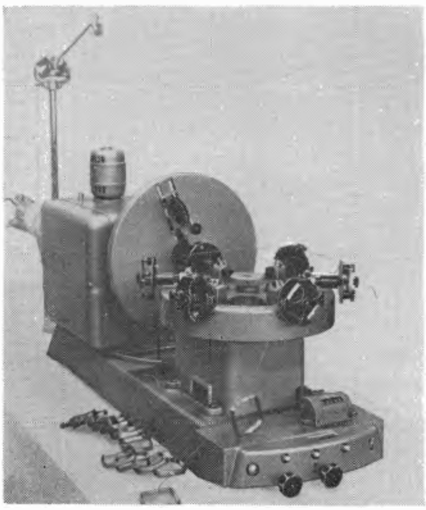

spindle, around the pulleys and is then attached to the coil former on the indexing table. The final pulley rotates around the jig and serves as wire guide to produce the coil. A to and fro motion of the wire guide relative to the indexing table gives the necessary layer winding action. On reaching the preset number of turns the machine switches off automatically. After the counter has been reset the indexing table automatically moves to the next station, the wire takes up its initial position on the former and a new winding is produced as before. This cycle of operations is continuously repeated and the operator has only to remove the completed coils and replace the formers. As the machine cannot restart before the counter is reset, it is possible for the indexing table to move while the operator is handling a coil.

HIGH SPEED COUNTER

(Illustrated below)

Electronic Machine Co. Ltd. Mayday Road, Thornton Heath, Surrey.

This recently introduced high speed counter is capable of counting articles passing between the photocell and light-heads at a rate of up to 3000 per minute.

Designated the 'D.I.' it employs a Dekatron counting tube and cold-cathode valves.

As will be seen in the illustration, the Dekatron counting tube is on the right and this records the count in units. On the left is an electromagnetic counter which records counts of ten, the total number which the counter will accept before resetting to zero being 9 999 999. A reset device is fitted so that a new count can be commenced at any given time. To the left of the illustration is seen the photocell and lightheads which are usually easily fixed in the path of the objects to be counted.

MINIATURE SEALED RELAY

Engel & Gibbs Ltd, Warwick Road, Boreham Wood, Elstree, Hertfordshire

Engel and Gibbs announce that a hermetically sealed version of their miniature relay series 'G' is now available. These relays, which are a miniature version of the P.O. 3000 relay, can be supplied with operating coils wound for 6, 12, 24, or 48V d.c. The connexions are made via metal to glass seals, eight connexion pins are incorporated and the relay can be supplied with any contact combination within this limitation.

Short News Items

The Television Society has awarded the following premiums for outstanding papers read before the London meetings in 1956/57.

The Wireless World Premium to Dr. D. Gabor, F.R.S. (Imperial College), for his paper on "A New Picture Tube."

The Mervyn Premium to Dr. E. L. C. White, M.A., (E.M.I. Research Department) for his paper on "Alternatives to the N.T.S.C. Colour System."

The Mullard Premium to Mr. S. N. F. Doherty, B.Sc., and Mr. P. L. Mothersole (Mullard Research Laboratories) for their paper on "Automatic Gain Control Circuits in Television Receivers.

The E.M.I. Premium to Dr. J. A. Saxton, M.I.E.E. (D.S.I.R. Radio Research Station) for his paper on "Scatter Propagation and its Application to Television."

The Electronic Engineering Premium to Dr. R. Pearce, B.Sc., A.M.I.E.E., (E.M.I. Research Department) for his paper on "The Return of Electrostatic Focusing."

The Pye Premium to Mr. Ian Atkins (Senior Dramatic Producer, B.B.C. Television) for his paper on "Studio Production Techniques."

Automatic Telephone & Electric Co Ltd, The English Electric Co Ltd, and Ericsson Telephones Ltd announce the formation by them of a jointly owned company for the development and manufacture of transistors and other semiconductor devices. The company, to be known as Associated Transistors Ltd, has an authorized capital of £750 000 and is constructing a factory at Ruislip, Middlesex, of some 55 200 ft². While the primary purpose of the company is to manufacture switching transistors for the telecommunications requirements of the sponsor companies, it will also manufacture semiconductor devices of more general application.

The G.P.O. has awarded a contract to Marconi's Wireless Telegraph Co Ltd for the radio equipment for five stations of the new v.h.f. Public Correspondence Maritime Telephone Service. This is the service by means of which passengers and others on suitably equipped vessels approaching or leaving the shores of this country will be able to call any subscriber on the G.P.O. telephone system. The first of the new stations, at North Foreland, Kent, is due to come into service in August, for vessels in the Straits of Dover and within 40-50 miles of North Foreland. Additional stations at Niton, Isle of Wight, and Land's End should be ready for service in the summer of 1959. The site of the fifth station has not yet been determined. Marconi Type HX86B transmitters and HR86B receivers will be used at all stations. The equipment will be mounted in special racks, and to simplify monitoring and testing procedure specially designed test gear will be mounted in the same racks. Each station will have two complete radio channels, one of which will be simplex and used exclusively for calling, and in cases of emergency. This will operate on the internationally agreed frequency of 156·8Mc/s. When contact is established the call will be switched to a duplex working channel, which will operate on one of the internationally agreed channels for public correspondence.

Decca Radar equipment has been ordered by the Hamburg Harbour Commission for equipping Hamburg Harbour and the adjacent stretch of the River Elbe with four land-based radar stations. The contract has been awarded to Telefunken GMBH in collaboration with Decca Radar Ltd. The radar equipment to be installed comprises the Decca Harbour Radar Type 32 and Decca Interscan Display system. This equipment is of the same type as that recently installed by Decca at the Port of Southampton and shortly to be fitted at the Liverpool Docks. It is also being installed at Khandla in India.

The Plessey Co Ltd and Brayhead (Ascot) Ltd have entered into a joint development and manufacturing agreement covering television tuners and f.m. permeability tuners. It is understood that the agreement provides for the complete interchange of tooling, and technical and manufacturing processes covering radio and television tuners. Although independent laboratories are being maintained, the two companies will co-operate closely in all forward development.

The Radio and Electronic Component Manufacturers' Federation, whose exhibition at Grosvenor House and Park Lane House, London, W.1, was held in April, announces that it is organizing an exhibition of British electronic components to be held in the Ostermans Marmorhallen, Stockholm, from 29 September to 3 October next. This will be the third exhibition since the war to be held in Stockholm by the British component manufacturers, the previous ones being in 1953 and 1948. The London exhibition was visited by representatives from 29 countries abroad. France led with 78 visitors and Holland was second with 53. Other countries sending more than 20 experts specially to see the show were Belgium, Denmark, Sweden and the U.S.A. Russia, with 11 signing in, China and Japan were among other countries represented.

The General Post Office announces that candidates who intend this year to take the competition for some 30 appointments in the Post Office basic professional grade of Executive Engineer, will be eligible if they possess the Diploma of Technology. In previous years, the entry qualification has been possession of a degree in engineering or physics, but a Diploma of Technology has now been included.

The Air Transportation Committee of the American Institute of Electrical Engineers has been sponsoring annual technical conferences for more than ten years. The activity of these conferences has steadily grown and at last year's conference in Dayton, 60 technical papers were presented and over 400 engineers attended the conference. The Air Transportation Conference for 1958 has been scheduled for 25-27 June during the Summer General Meeting of the A.I.E.E. at the Statler Hotel, Buffalo, New York. Over 70 technical papers are under preparation by leading engineers in the aircraft industry and the Armed Forces.

An International Symposium on Nuclear Electronics will be held from 16-20 September at the UNESCO building, Paris. Further information may be obtained from Colloque International Electronique Nucleaire, Societé des Radioelectriciens, 10 Avenue Pierre-Larousse, Malakoff (Seine), France.

The Societé des Radioelectriciens which organized a Congress on Ultra-High Frequency Circuits in October 1957 will publish the Proceedings in July. The texts will be published in English and in French. Further information may be obtained from the Congres Circuits et Antennes Hyperfrequences Ste des Radioelectriciens, 10 Av. P. Larousse, Malakoff (Seine).

Mullard Ltd have announced that at the recent Instruments, Electronics and Automation Exhibition they received orders totalling £70 000 for ultrasonic equipment.

Copies of the Annual Report of the Council of the Institution of Electrical Engineers for the session 1957/58 and of the accounts for the year ended 31 December 1957 are now obtainable by members of the Institution on application to the Secretary.

Erratum. Equation (1) on page 210 of the April issue (letter from M. Pacak of the Czechoslovak Academy of Science) should read

$$G' = G\,\frac{1-G_k}{1-G_k-G_d}$$

Notes from ———

NORTH AMERICA

New Measuring Instruments

Several new instruments have been announced recently by Millivac Instruments of Schenectady. These are as follows.

PRECISION D.C. VALVE-VOLTMETER

The MV-57A sensitive precision d.c. valve-voltmeter fills the gap between ordinary valve-voltmeters, having 2 or 3 per cent accuracy, and extremely accurate but expensive digital voltmeters. Accuracy is $\frac{1}{4}$ per cent absolute (not full scale), the measuring range 100μV to 1kV and the input impedance 6MΩ on low ranges and 60MΩ from 1V upwards. Precision measurements are made through automatic comparison of accurate calibration signals, taken from a standard cell-controlled 1kV d.c. supply, with the unknown voltage. If signals differ the needle pulses, but ceases pulsation as soon as the calibrator signal is completely balanced against the unknown voltage, which is then read on a 4-digit precision Dekapot, having better than 0·01 per cent linearity.

PRECISION A.C. VALVE-VOLTMETER

The MV-32A precision a.c. valve-voltmeter uses an electronically protected vacuum thermo-couple as its r.m.s.—responsive meter - rectifier. Accurate measurements are made by comparing the unknown voltage with an accurately calibrated 1kc/s signal and adjusting the calibrator-attenuator until both the unknown voltage and the calibrator signal produce exactly identical needle deflexions. Five 'transfer points' are available for this comparison to accommodate signal waveforms having maximum permissible crest factors between 2 and 10. Accuracy within the 'basic' frequency range of the instrument (50c/s to 5kc/s) is better than $\frac{1}{2}$ per cent, at other frequencies 2 per cent. Total frequency range is 10c/s to 500kc/s and total voltage range 300μV to 1kV. Calibrator accuracy is 0·1 per cent.

DIFFERENTIAL-INPUT D.C. VOLTMETER

The MV-37A differential-input d.c. millivoltmeter has a high common mode rejection ratio (1000:1), not only on its sensitive 'direct' ranges but also on its non-sensitive range where the input-signal is being attenuated. Attenuator errors between the two input channels are eliminated by a switching relay which inserts the same input attenuator alternatively in either channel. Storage capacitor, in the meantime, maintain the input potential of the other channel.

POLARIZED D.C. VOLTMETER

The MV-27D DC microvoltmeter has 250μV full scale sensitivity, its highest range being 0 to 1kV. In its three lowest ranges, 250μV, 1mV and 2·5mV, it uses mid-zero scales to facilitate null-indicator operation in bridge circuits. All other ranges are left-zero for maximum scale length and highest reading accuracy and convenience. The instrument is housed in a modernized cabinet with recessed front panel, has a larger indicating meter and is polarized, thereby eliminating 'needle fold-over' under negative overloads on the mid-zero ranges, as did occur in earlier models.

WIDEBAND AMPLIFIER

The VS-102A post-amplifier has a gain of 300, a frequency response of 20c/s to 10Mc/s and a maximum output of 28V peak-to-peak. Its output impedance is adjustable between 35 and 130Ω, to match various transmission lines. It is used to increase the output voltage and output power of continuous wave generators and sweep generators, to make possible alignment of amplifier output stages at their true high operating signal level. Capacitive loads as high as 100pF have practically no influence on the output voltage of this amplifier at its upper 10Mc/s frequency limit.

Torsional Wave Delay Lines

A delay line capable of providing a long delay in a small space was described at the Institute of Radio Engineers Annual Convention in a paper prepared by R. N. Thurston and L. M. Tornillo of Bell Telephone Laboratories. Known as a spiral coiled wire torsional wave delay line, it permits the clear resolution of 10μsec pulses spaced 20μsec apart.

Delay lines are useful in many applications such as computer memories, trigger delay circuits, range-measurement circuits in radar installations, and in pulse decoding systems for electronic switching. The packaging of these delay lines in a small volume is important.

The delay line consists essentially of a length of 0·038in diameter wire made of alloy called Vibralloy which has been coiled into a flat spiral to conserve space. Vibralloy, a ferromagnetic alloy developed at Bell Laboratories, is used as it has a high mechanical Q and low temperature coefficient of delay.

Torsional waves are transmitted through the Vibralloy wire at about $2{\cdot}68 \times 10^5$cm/sec, making the theoretical delay about 3·72μsec/cm. In one experimental line, a 15ft length of wire exhibited a delay of 1·65msec at 840kc/s. The wire was coiled into a spiral about 4in in diameter and then heat treated at 500°C for $1\frac{1}{2}$ hours.

Specially designed ceramic torsional transducers are used to inject and detect the torsional waves. These transducers limit the bandwidth of the system to about 11·5 per cent. Total insertion loss for the 1·65msec line was 9dB, of which 6dB was line loss and 3dB represented conversion loss in the transducers. Bandwidth was about 100kc/s.

A number of experimental delay lines have been built using this technique. Results indicate that such delay lines are small in size, rugged, reliable, and relatively insensitive to moderate changes in temperature.

Electronic Abstracting

An electronic machine that will read an article and then write an abstract of it was described at a recent convention of the Institute of Radio Engineers in New York.

H.P. Luhn of the IBM Corporation stated that the complete text of an article is first transcribed on to a magnetic or punched tape in a code that can be understood by an electronic data processing machine, such as the IBM 704 computer. The machine then analyses the text word by word to derive statistical information concerning the frequency and distribution of the words in the text.

From this, the machine determines the relative degree of significance of the words and then grades each sentence as to its importance. Sentences scoring highest in significance are automatically extracted from the text and printed out by the machine to form the "Auto-Abstract."

I.R.E. Canadian Convention

The third annual I.R.E. Canadian Convention and Exposition will be held from 8 to 10 October in the Automotive Building, Exhibition Park, Toronto, Canada.

Last year's Convention included electronic and nucleonic exhibits by 166 Canadian, United States and overseas companies. The technical programme of 25 sessions, at which 115 papers by leading experts were read covered a wide range of subjects.

The increasing importance being assumed by the electronic and nucleonic industries in the Canadian economy would indicate that the 1958 I.R.E. Canadian Convention will surpass in size and importance any previous scientific convention and exposition held in that country.

Exhibition participation by overseas manufacturers is welcomed.

Conference on Magnetism and Magnetic Materials

The fourth Conference on Magnetism and Magnetic Materials will be held in Philadelphia, 17-20 November, 1958, at the Sheraton Hotel. This conference is sponsored by the American Institute of Electrical Engineers in co-operation with the American Physical Society, the Institute of Radio Engineers, the Metallurgical Society of A.I.M.E., and the Office of Naval Research. Authors should submit titles of proposed papers by 1 August and abstracts by 1 September to the Programme Chairman, H. B. Callen, Department of Physics, University of Pennsylvania, Philadelphia, Pa. Further details may be obtained from C. J. Kriessman, Local Chairman, Remington Rand Univac, 1900 W. Allegheny Avenue, Philadelphia.